

# **NIRIM**

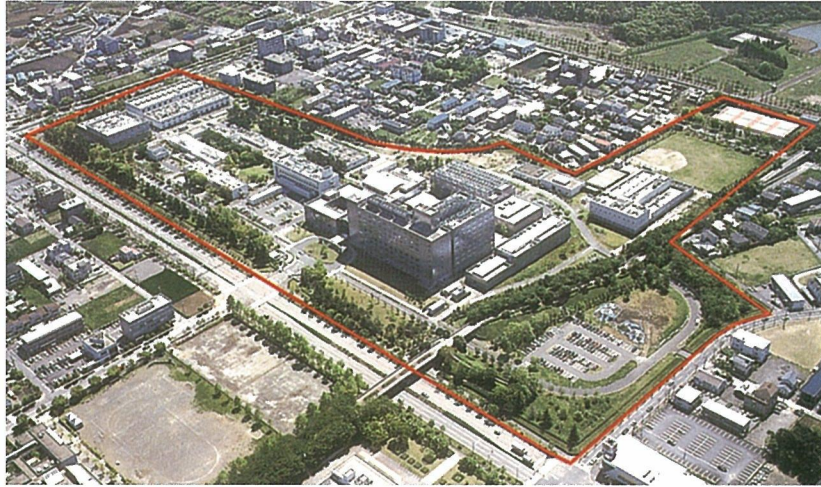
## **Research Activities**

**2000**

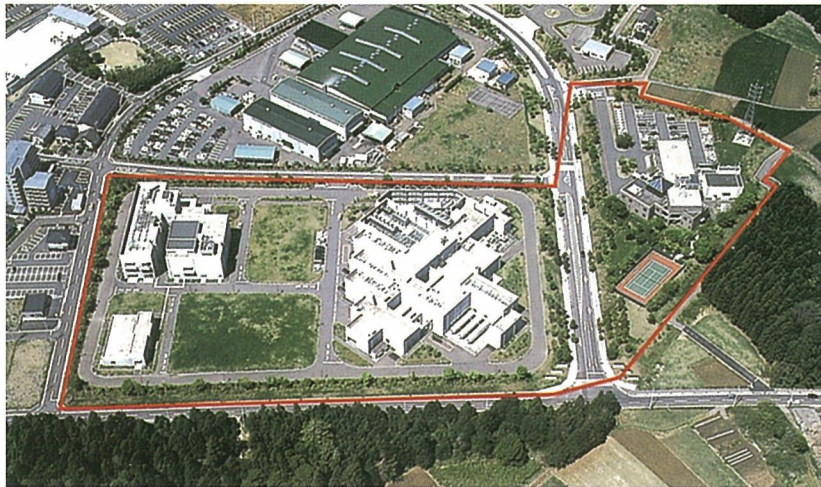
**National Research Institute for Metals**

**Japan**





Sengen Site



Sakura Site



Meguro Site

## Preface

I am pleased to present herewith the "NRIM Research Activities 1999". This report is intended to describe the annual activities at National Research Institute for Metals (NRIM), focusing on our research programs and the progress we have made in FY 1999.

As from Jan 2001, the Science and Technology Agency (STA) and the Ministry of Education, Science and Culture were integrated into the Ministry of Education, Culture, Sports, Science and Technology (MEXT). Following on April 1 2001, NRIM and National Institute for Research in Inorganic Materials (NIRIM), both attached to the MEXT, are merged into one organization and started as the National Institute for Materials Science (NIMS), which is operated as an Independent Administrative Institution (IAI). In preparation for the drastic administrative reform, lots of discussion was made in NRIM how to administrate the institution and how to direct the research subjects in FY 1999.

In terms of research direction, STA launched the "Leading Research Program for IAIs" in FY 1999 in order to endeavor the new research management system for IAIs. "High Temperature Materials Project for the 21<sup>st</sup> Century", proposed by NRIM, was selected as one of the test cases in which various attempts have been made for the more flexible research management.

On the other hand, we carried out the mid-point external assessment for the "New Century Structural Materials Project" in January 2000, which is one of the core projects for the 5<sup>th</sup> long-term research plan. In the 4<sup>th</sup> Ultra-steel Workshop, held simultaneously with the assessment, we obtained excellent evaluation and encouragement from industry and other institutions.

In addition, we conducted the Institute Evaluation in March 2000 where we received encouraging comments from the External Evaluation Committee. The results of this evaluation are to be reflected to the establishment of the new institution.



Through these activities described, I believe that we shall make every effort to render our institute to be the Center Of Excellence in materials science. To all of you, who have supported NRIM, we greatly appreciate your continued understanding and encouragement for the new organization "NIMS"

*Masatoshi Okada*

March 2001  
Dr. Masatoshi Okada

# NRIM Research Activities 2000

## Contents

<b>Research in Progress 1999–2000</b> .....	1
A List of Research Program .....	1
Research Programme .....	3
<b>Publications</b> .....	68
Papers Published in 1999 .....	68
<b>International Cooperation</b> .....	76
International Collaboration Research .....	76
List of Visiting Foreign Researchers .....	79
Brief Introduction of STA Fellowship Program .....	87
<b>Organization of NRIM</b> .....	88
Organization .....	88
Budget and Personnel in Fiscal Year of 2000 .....	88
<b>How to get to NRIM</b> .....	89
<b>List of Keywords</b> .....	91

## Research in Progress 1999-2000

### □ A List of Research Program

1. Composition, Temperature and Pressure-Induced Structural Changes and Physical Properties of Material
2. Angle-resolved Photoelectron Spectroscopy Study on Surface Structures and Electronic Properties
3. Coating of Photocathode and Fundamental Investigation of Photoelectron Emission from Laser illuminated Photocathode for TEM
4. Development of New High Pressure Techniques and its Application to the Investigation in Newly Synthesized Compounds
5. Atom Probe Microanalysis of Advanced Metallic Materials
6. Improvement of the Accuracy of Inductively Coupled Plasma-Mass Spectrometry through Sample Preparation and Isotope Dilution Analysis
7. Study on the Unusual Metallic State and Electronic Structure of Magnetic Materials
8. Optical Studies on Intra-4f-shell Photoluminescence in Bulk Growth Yb Doped InP
9. Transport and Optical Properties of a Salmon-Sperm-DNA Film in High Magnetic Fields
10. Theoretical Study on Atomic Diffusion and Electronic State in Metal Oxides
11. Computer Simulation on the Vortex States and Phase Transitions of High-T<sub>c</sub> Superconductors under an External Magnetic Field
12. Design Factors of Heat Resistant Ferritic Steels
13. First-Principles Theory of Dislocations in Solid
14. NRI Long-Term Fatigue Data Sheet Project-I
15. NRI Creep Data Sheet Project-V
16. Fatigue Behavior and Microstructure of Metals
17. Dynamic Microstructural Change and Mechanical Properties in Ceramics at High Temperatures
18. Fracture Mechanism of Welded Structure of Stainless Steel at Cryogenic Temperature
19. Search for Group IV Elements Compounds Including Alkaline-earth-metal Elements
20. Characterization and Evaluation of Cryogenic Structural Materials
21. Microstructural Control for High Performance Refractory Metals
22. Crystal Growth and Dissolution Mechanisms in Peritectic System
23. Application of Ionization Separation Technique to Gaseous Process
24. Fabrication and Characterization of Nano-Structured Materials
25. Diffusion Bonding between Transition Metals (Cr, Fe, and Ni) and Metals of Group IV~VI
26. Cladding or Coating Processes by Utilizing Semi-Solid Processing
27. Effect of Interface Damage on Fatigue Crack Growth for Fiber-Reinforced Titanium Alloy Matrix Composite
28. Fabrication and Characterization of Nano-Structured Materials
29. Evaluation of Mechanical Properties for Metal Matrix Composites
30. The Development of High Strength High Conductive Cu Base In-Situ Composite
31. Development of Brazing Technique for the Fabrication of Rocket Engine
32. Preparation of Ionic Conductors by Pressurization
33. High Temperature Materials 21 Project
34. Control of the In-plane Texture of High-T<sub>c</sub> Superconducting Thin Films for Microwave Applications
35. High-Resolution Real-Time Investigation on Defect Formation under Surface and Interface-reactions
36. Understanding and Improvement of Radiation-Induced Degradation in the Advanced Nuclear Materials
37. Influence of Nuclear Transmutations on Low Activation Structural Materials for Fusion Reactor Application
38. Isotope Separation and Its Application to Materials
39. Development of Light Weight High Strength Ti<sub>2</sub>AlNb Titanium Intermetallic Alloy
40. Improvement of Thermal and Mechanical Properties of LI<sub>2</sub>-type titanium trialuminide
41. Functions of Hydrogen in Environmental Degradation of Structural Materials (Environmental embrittlement behavior and hydride formation of intermetallic compounds)
42. Development of Basic Superconducting Technology for High Field Micro-SMES
43. Investigation of New Nonlinear Optical Crystals for Wavelength Modulation, Single Crystal Growth and Principle Technology Development for Optical Devices
44. Surface Modification by Plasma Source Ion

- Implantation
45. Research and Development of High-Performance Light Alloys for Hydrogen Storage
  46. Designing of Function and Structure for Functionally Graded System
  47. Development of Essential Technique for Improving Coil Current Density in Superconducting Magnet
  48. Creation of Multi-functional Materials by Assemblage of Primitive Functions
  49. Development of Advanced Shape Memory Thin Films by Sputtering
  50. Study on the Processing and Assessment of Ecomaterials
  51. Materials Efficiency Accounting based on MLCA
  52. Fabrication of Quasicrystals and Investigations of Their Properties
  53. Study on Combustion Synthesis of Useful Intermetallic Compounds
  54. Promotion of Collaborative Studies Using User Facilities of Center for Advanced Physical Fields
  55. Development of New Superconductors for Nuclear Fusion Use
  56. Development of 1 GHz NMR Spectrometer
  57. Fundamental Studies on Very High Magnetic Field Generation
  58. Development of Magnetic Separation System
  59. Materials Development through Control of Phase Transformations by High Magnetic Field
  60. Advanced Cryogenic System for Ultra Low Temperature
  61. Test Methods of Superconductors
  62. Measurement Technologies and Reference Materials for Low Temperature Thermophysical Properties of Solids
  63. Measurement Technologies and Reference Materials for Low Temperature Thermal Expansion of Solids
  64. Development of Superconductors for Ultrahigh field Uses
  65. Development of Fundamental Technologies for Excited Neutral Beams
  66. Advanced Characterization of Micro and Nanometer Scale Structure of Materials by Brilliant Synchrotron x-rays at the SPring-8
  67. Surface Chemical Analysis
  68. Development of Low Frictional Vacuum Materials with Strain Energy by Supersaturation as Trigger for Self-organization
  69. The Chamber Material for Standard Vacuum Pressure Measurement
  70. Combinatorial Study on Interface and Surface of Functional Materials
  71. Study on Strengthening of Ferrite Matrix Steels for Welded Structures
  72. Advanced Ultra-High-Strength Steels (1500-MPa-plus class)
  73. Strategic Research on Advanced Ferritic Steels for 650 °C USC Boilers (R&D of Structural Materials for 21<sup>st</sup> Century)
  74. Enhanced Durability of Structural Steels in Marine Environment
  75. Manufacture Processing of Recyclable Simple-System Alloys
  76. Regenerative Manufacturing Process by Utilizing Impurities in Materials
  77. Effect of Aging Degradation on Localized Corrosion of Structural Materials for Light Water Reactors
  78. Computational Simulation of Mechanical Properties and Behavior of Materials for Atomic Power Plants by Taking Microstructures into Account
  79. Mechanical Properties of Thin Films and Coatings
  80. Toughness Evaluation of Structural Steels
  81. Evaluation Method of High Temperature Fracture Property for Creep Brittle Materials
  82. Development of Analysis Method for Dynamic Dislocation Motion at High Temperature and Study on Controlling Process of High Temperature Deformation

## □ Research Programme

### Characterization / Properties

#### 1 Composition, Temperature and Pressure-Induced Structural Changes and Physical Properties of Material

*T. Hirata, Materials Physics Div.*

[April 1998 to March 2001]

When pressure is applied to materials or their composition and/or temperature are changed, any structural change(s) are induced, affecting the physical and electronic properties of materials. The current research subject covers the following content.

A: Oxygen position, octahedral distortion, and bond-valence parameter from bond lengths in  $Ti_{1-x}Sn_xO_2$  ( $0 \leq x \leq 1$ ), which are deduced based on the virtual crystal approximation, or Vegard's law, from the bond lengths of  $TiO_2$  and  $SnO_2$ .

B: Temperature dependence of the Raman spectra of  $1T-TaS_2$ . This topic reveals that the three broad Raman bands observed above  $220\text{ cm}^{-1}$  exhibit noticeable changes of the frequency toward the low wavenumbers in the vicinity of 200 K, where  $1T-TaS_2$  undergoes a first-order transition of the charge density wave (CDW).

C: Raman and infrared spectra of  $Ce_{1-x}M_xO_{4-0.5x}$  ( $M=Pb, Sr$  and  $Ca$ ) and  $Ce_{1-x}Bi_xVO_4$  as a function of  $x$ , which exhibit noticeable differences between  $Ce_{1-x}M_xVO_{4-0.5x}$  and  $Ce_{1-x}Bi_xVO_4$ , and among  $Ce_{1-x}M_xVO_{4-0.5x}$ . The  $x$ -dependence of position, linewidth and intensity of the Raman/infrared modes is presented and discussed, to substantiate distinctive spectral features.

**Keywords:** lattice distortion, phase transitions, phonons, infrared and Raman spectra.

#### 2 Angle-resolved Photoelectron Spectroscopy Study on Surface Structures and Electronic Properties

*M. Shimoda, J.Q. Guo\*<sup>†</sup>, T.J. Sato\*, A.-P. Tsai\*, Materials Physics Division*

(\*: Aperiodic Solids Research Team, <sup>†</sup>: CREST, Japan Science and Technology Corporation, Japan)

[April 1998 to March 2001]

We have performed X-ray photoelectron diffraction (XPD) and reflection high-energy electron diffraction (RHEED) measurements to investigate the surface structure of the decagonal  $Al_{72}Ni_{12}Co_{16}$  quasicrystal, which is known as a two-dimensional

quasicrystal. RHEED patterns for the surface parallel to the quasiperiodic planes are almost identical to the selected-area electron diffraction (SAD) patterns taken along the twofold axes of the bulk sample. The XPD images show clear tenfold-symmetric patterns, which is consistent with the long-range orientational order of the decagonal quasicrystal. These facts suggest that the surface has the same quasiperiodic structure as in the bulk. We have also found that  $Ar^+$ -ion bombardment to the quasiperiodic surface induces a surface phase transition; Al atoms near the surface are selectively sputtered and a crystalline layer of Al-Co(Ni) alloys with bcc-like structure is formed. The crystalline layer consists of multiply-twinned grains which expose the (110) surface with ten different orientations corresponding to the tenfold-symmetry of the substrate. The quasicrystalline structure are restored by annealing, which means the quasiperiodic structure is stable even at the surface<sup>1)</sup>.

**Keywords:** photoelectron diffraction, reflection high-energy electron diffraction, surface structure, quasicrystal

- 1) Surface structure and structural transition of decagonal Al-Ni-Co quasicrystal, M. Shimoda, J.Q. Guo, T.J. Sato, A.-P. Tsai, *Surface Science* **454-456** (2000) 11

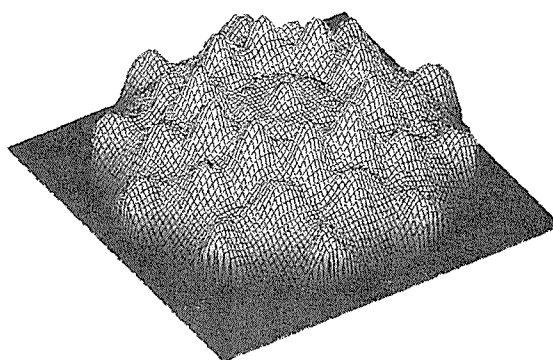


Fig. Co 2p XPD image from the quasicrystalline surface of the decagonal  $Al_{72}Ni_{12}Co_{16}$  quasicrystal

#### 3 Coating of photocathode and fundamental investigation of photoelectron emission from laser illuminated photocathode for TEM

*T. Kimoto and M. Amano, Materials Physics Division*

[April 1999 to March 2002]

The higher brightness electron source improves high resolution microscopy, electron holograph, microscopic ultimate analysis, coherent electron micro-diffraction and so on in a transmission electron microscope (TEM). For this reason a Lanthanum hexaboride (LaB<sub>6</sub>) tip whose brightness is about 10 times higher than a conventional Tungsten hair-pin tip, was developed for a thermal emission type electron source in the 1980's. In the 1990's a field emission type electron source whose brightness is about 10 - 100 times higher than LaB<sub>6</sub> tip source was developed for practical use, which enables us to perform electron holography.

It is estimated that a photocathode of high quantum efficiency illuminated by a laser beam could be an electron source for TEM whose brightness is 100-1000 times higher than a field emission type electron source. A few purely fundamental researches have been performed on the characteristics of laser illuminated photocathode so far, but few fundamental researches on the practical laser illuminated photocathode for TEM or other instruments have been carried out. It is necessary for the development of the practical photocathode to devise a special method to coat photocathodes such as Cs<sub>3</sub>Sb onto the top of a cathode tip, because their quantum efficiency decrease rapidly just as they react chemically to small amount of oxygen<sup>1)</sup>. It is also necessary to cool effectively the laser illuminated photocathode in the high vacuum and high voltage.

In the present research the fundamental experiment is aimed in order to get data for the development of a practical photocathode type electron source, a new type high brightness electron source for TEM. For this purpose, we verify the effectiveness of the devised method of coating Cs<sub>3</sub>Sb photocathode by vacuum evaporation and find the best coating condition. We measure the temperature of laser illuminated photocathode which is cooled with a specially devised method for many experimental conditions.

The effect of temperature of the photocathode, shape of the top of the photocathode tip, environmental vacuum and cathod voltage on the beam current of the photoelectron from the laser illuminated photocathode was examined. To perform our research we use the Argon ion laser and the specially designed devices which were already made to carry out the present fundamental research. The development of a special cathod tip which is cooled by Peltier effect was also carried out besides development of coating method.

**Keywords:** high brightness electron source, transmission electron microscope (TEM), coating of Cs<sub>3</sub>Sb on cathod tip, quantum efficiency for photoelectric effect, laser illumination, Argon ion laser, vacuum evaporation, cooling of laser illuminated photocathode

## Reference

Laser Illuminated High Current Photocathodes, L. R. Danielson, C. Lee and P. E. Oettinger, Applications of Surface Science 16 (1983) 257-267.

## 4 Development of New High Pressure Techniques and its Application to the Investigation in Newly Synthesized Compounds

*A. Matsushita, J. Tang, J. Ye, T. Naka, H. Abe, S. Ishida and K. Maruyama, Materials Physics Division*

[April 1999 to March 2001]

We have pursued for a number of years a research project in high pressure physics, centering around the physical properties of magnetic intermetallic compounds. One of the recent objects is Fe<sub>3-x</sub>V<sub>x</sub>Al compounds. We have investigated the effect of pressure on the temperature dependence of resistivity in Fe<sub>2</sub>VAl Heusler compound. We found that this compound has a pseudo energy gap of a few hundreds Kelvin at Fermi level. At ambient pressure the electrical resistivity of this compound exhibits a monotonic behavior with a negative temperature coefficient below room temperature. The origin of this temperature dependence has been attributed to the energy gap, but we found with high pressure experiments that this interpretation is not true. At higher pressures the monotonic behavior changes and a plateau appears around 100K. After detailed studies we have reached a conclusion that we must consider three temperature dependent factors which affect the electrical resistivity. One is the variation of charge carrier density owing to the pseudo energy gap, the second one is the phonon scattering and the third one is the magnetic scattering. Especially the magnetic scattering seems to dominate at low temperatures; interestingly it is increasing as decreasing temperature.

In these research projects we mainly used a piston-cylinder type pressure cell and a cubic anvil for generating high pressure. The maximum pressure obtained with these high pressure techniques is 9GPa. In this new research project we will develop a new high pressure technique using a dia-

mond anvil cell aiming at higher pressures. We are planning two programs. One is a program to develop a technique of electrical resistivity measurement in a diamond anvil cell. Another is a X-ray diffraction measurement at low temperatures using a diamond anvil cell.

In this project we pursue another research that is to explore new compounds containing non-metallic elements or compounds formed with only non-metallic elements. Previously the research objects were mainly intermetallic compounds. But we will explore interdisciplinary fields in this project.

**Keywords:** high pressure, magnetic materials

### Recent Publications

Specific heat of the spin density wave state in  $\text{Ce}(\text{Ru}_{0.85}\text{Rh}_{0.15})_2\text{Si}_2$  under pressure. J. Tang, T. Matsumoto, H. Abe and A. Matsushita, *Solid State communications*, **109**(1999), 445.

Effects of Pressure on the Electrical Resistivity of  $\text{Pr}_1\text{Ba}_2(\text{Cu}_{1-x}\text{M}_x)_4\text{O}_8$  with  $\text{M}=\text{Zn}, \text{Ni}$  and  $x=0, 0.01, 0.02$ . A. Matsushita, S. Horii and Y. Yamada, *Physica C* **331**(2000), 195.

### 5 Atom probe microanalysis of advanced metallic materials

*K. Hono, Materials Physics Division*  
[April 1996 to March 2001]

Properties of metallic materials are controlled by microstructures. Conventional structural materials such as steels, aluminum alloys, intermetallics and superalloys are all strengthened by controlling their microstructures. The microstructural scale of metallic materials are becoming smaller and smaller, and many microstructures in the modern industrial materials are in a subnanometer scale. Magnetic properties and other functional properties of metallic materials are sensitive to their nanoscale microstructures and interfacial structures. Thus, microstructural characterizations of metallic materials in less than a nanometer scale resolution is essential for understanding the mechanisms of various novel properties in materials.

This project aims to obtain better understandings of the underlying mechanisms of mechanical and magnetic properties of metallic materials by characterizing microstructures of advanced materials. For this purpose, we employ the atom probe field ion microscope (APFIM) technique which is capable of analyzing local chemical compositions with an atomic resolution. Unlike other analytical tech-

niques, it can detect all alloying elements including light atoms such as Li, Be, B, C, N and O which often make key roles in controlling materials properties. By making use of a three dimensional atom probe (3DAP), it is possible to map out elemental distributions in alloys in a three dimensional real space with a near-atomic resolution. During the last fiscal year, we have installed an energy compensated three-dimensional atom probe, by which it became possible to map out alloying elements with close mass-to-charge ratios. Fig. 1 shows 3DAP elemental maps of Al, Ti, Ni, Co, and Fe atoms near a  $\gamma'/\gamma$  interface of Inconel X-750 alloy. In the  $\gamma'$  precipitate, (002) atomic layers are resolved corresponding to the internal  $\text{L1}_2$  ordering of the  $\text{L1}_2$  phase. For complementary microstructural characterization, conventional transmission electron microscopy (TEM) and high resolution electron microscopy (HREM) techniques are also employed. Our research interests include nanocrystalline magnetic materials, magnetic thin films, amorphous and nanocomposite alloys, microstructures and phase transformations in steels and aluminum alloys and other industrial metallic materials.

Part of this project is conducted in collaboration with the Frontier Research Center for Structural Materials. The most up-to-date reports of this project can be found in the following WWW site:  
<http://www.nrim.go.jp/open/usr/apfim>

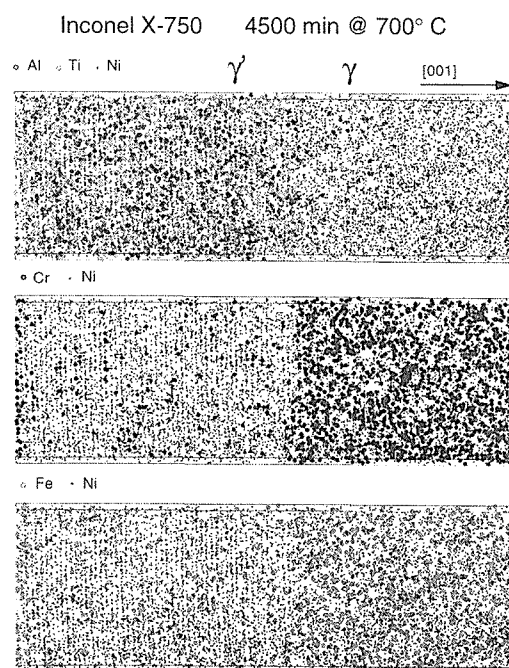


Fig. 1 3DAP elemental maps of  $\gamma'/\gamma$  interface of Inconel X-750 alloy aged for 75 h at 700 °C.

**Keywords:** atom probe, APFIM, transmission electron microscopy, TEM, nanostructure, microstructure, phase transformation

### Related Papers

K. Hono, "Atom probe microanalysis and nanoscale microstructures in metallic materials" (OVERVIEW), *Acta mater.*, 47, 3127 (1999).

### 6 Improvement of the Accuracy of Inductively Coupled Plasma-Mass Spectrometry through Sample Preparation and Isotope Dilution Analysis

*K. Sato, K. Ide, T. Kobayashi and M. Amano, Materials Physics Division*  
[April 1997 to March 2001]

The latest trend of the international coordination for standard materials and chemical analysis requires the establishment of standard analytical methods which are traceable to the SI-unit. Following such a trend, we have studied for establishing the Inductively Coupled-Mass Spectrometry (ICP-MS) with a matrix separation method and the Isotope Dilution-Mass Spectrometry (ID-MS).

For the quantitative analysis of trace elements in iron standard materials, it is important to eliminate the ion scattering effect caused by the matrix, the effect of space charge and the memory effect. In this study, the application of metal chelate/solid phase extraction (SPE) has been examined for the separation of matrix. Sodium N,N-diethyl dithiocarbamate trihydrate (DDTC) was used as the chelating reagent, and the reversed-phase system solid phase Bond Elute C18 was used for SPE. The assay elements were 7 elements of Ni, Co, Cu, Cd, In, Pb and Bi. The ID-MS was applied for the quantitative analysis of Ni.

The optimum condition has been investigated for the matrix separation using the metal chelate/SPE. It is necessary to mask  $\text{Fe}^{3+}$ , because DDTC reacts with  $\text{Fe}^{3+}$  and forms Fe chelate which is insoluble in water. Tartaric acid, ammonium oxalate and citric acid ammonium were examined as the masking reagent. The tartaric acid of  $15.0 \text{ g } 100 \text{ ml}^{-1}$  was necessary for masking the solution containing  $1.0 \text{ g}$  of  $\text{Fe}^{3+}$ , which is less than the amount of other organic acids. The formation of metal chelate depends on pH. In the solution below pH5.0, the DDTC decomposed to  $(\text{C}_2\text{H}_5)_2\text{NH}^{2+}$  and  $\text{CS}_2$ , and in the solution pH 5.0 ~ 9.9, all metal ions formed the metal chelates. In the presence of tartaric acid, the Fe chelate decreased with increasing pH from 9.9 to 10.6 due

to the masking effect against  $\text{Fe}^{3+}$ . The Fe chelate did not formed above pH10.6. While the formation of Fe chelate was accelerated with increasing the amount of DDTC. The maximum recovery rate was obtained at 0.1 M 4.0 ml of DDTC without the iron chelate formation.

The amount of the solid phase Bond Elute C18 affects the retention ability of metal chelates and the time of treatment. The Bond Elute C18 has a large specific surface area, so it was considered only a small amount of it was necessary for the SPE. However 0.25 g of it was not enough for the perfect retention of metal chelates, and 0.75 ~ 1.0 g of it took a lot of time ( $>10 \text{ ml min}^{-1}$ ) for the treatment due to the impingement on the solution flow. The optimum amount of the solid phase was 0.5 g for the high recovery rate and the short time treatment.

The elution of metal chelates from the solid phase must be carried out by using a least amount of eluate to increase the concentration effect. As the suitable eluate, 6 M hydrochloric acid, 6 M Hydrochloric acid + 0.1% hydrogen peroxide, 6 M nitric acid and 6 M nitric acid + 0.1% hydrogen peroxide were examined. The 6 M nitric acid + 0.1% hydrogen peroxide was found to be best eluate from the point of recovery rate and reproducibility. The least amount of the eluate was 5 ml.

In order to select the enriched isotope material for Ni analysis using the ID-MS, the effect of isobar elements was examined. The isotopes of Ni are  $^{58}\text{Ni}$  (68.07%),  $^{60}\text{Ni}$  (26.22%),  $^{61}\text{Ni}$  (1.13%),  $^{62}\text{Ni}$  (3.63%),  $^{64}\text{Ni}$  (0.92%). There are the effects of isobar elements between  $^{58}\text{Ni}$  and  $^{58}\text{Fe}$ , and between  $^{64}\text{Ni}$  and  $^{64}\text{Zn}$ . Thus  $^{60}\text{Ni}$  was selected as an enriched isotope material and the calculation was carried out by using the value of  $^{62}\text{Ni} / ^{60}\text{Ni}$ .

The precision of analysis (RSD) of each assay element obtained by using the metal chelate/SPE separation ICP-MS method was Co: 0.36, Ni: 0.32, Cu: 0.51, In: 1.66, Pd: 0.97 and Bi: 1.06 (%), respectively. The RSD of each element was less than 2%. The detection limit ( $3\sigma$ ) of each element was Co: 0.38, Ni: 0.43, Cu: 2.90, Cd: 0.93, In: 0.23 and Bi: 0.42 ppb (m/m), respectively. The result shows that the quantitative analyses of sub ppm (m/m) is possible by this method.

The result of quantitative analysis of Ni in the iron and steel standard material JSS 001-4 (information value:  $<0.3 \text{ ppm}$  (m/m)) obtained by using the metal chelate/ SPE separation ID-MS was  $0.057 \pm 0.005 \text{ ppm}$  (m/m). This value has no significant difference compared with the values  $0.033 \pm 0.004 \text{ ppm}$  (m/m),  $0.037 \pm 0.017 \text{ ppm}$  (m/m) (the non-matrix separation method / ID-MS) and  $0.074 \pm 0.028 \text{ ppm}$  (m/m) (the matrix separation

method / ID-MS), which were obtained by the collaboration with the national Institute of Materials and Chemical Research.

The value obtained by using the metal chelate / SPE separation ICP-MS) of each assay element in the iron and steel standard material JSS 001-4 was Co:  $0.32 \pm 0.05$  ppm (m/m) (certified value: 0.3 ppm (m/m), Cu:  $0.54 \pm 0.09$  ppm (m/m) (certified value: 0.5 ppm(m/m), Pb:  $0.16 \pm 0.03$  ppm (m/m) (certified value:0.2 ppm), Cd:  $0.15 \pm 0.05$  (information value: <0.3 ppm (m/m), In:  $0.019 \pm 0.008$  (information value: 0.019  $\pm$  0.008 ppm (m/m) and Bi:  $0.3 \pm 0.01$  ppm (m/m) (no-information value). The result shows that the analytical values are in good agreement with the certified values.

We have proved that the quantitative analysis of trace elements in iron and steel standard materials can be carried out with high accuracy and with high sensitivity by using the metal chelate/SPE separation ICP-MS / ID-MS method without any complicated and time-consuming pretreatment.

**Keywords:** ID-MS, solid phase extraction, DDTC, high-purity iron.

## 7 Study on the Unusual Metallic State and Electronic Structure of Magnetic Materials

*H. Kitazawa, Physical Properties Division*  
[April 1998 to March 2001]

The discovery of high  $T_c$  superconductive cuprates has stimulated much interest on the physics and chemistry of various oxides and chalcogenides, which exhibit superconductivity, colossal magnetoresistance, metal-insulator (M-I) transition, etc. One of the interesting problems of these materials is that the electronic state differs from the conventional Fermi liquid. It is obvious that the electron correlation should play an important role in the anomalous metallic state. So far, much work has been focused on the 3d transition-element oxides, while 4d or 5d transition-element compounds have not been paid much attention because of the weaker electron correlation. Recently, it was found that the spinel-type chalcogenide  $\text{CuIr}_2\text{S}_4$  exhibits the M-I transition at about 230 K. More interestingly, the external pressure stabilizes the insulating phase, while the general band theory expects that the external pressure enhances the overlap of the related orbitals and leads to a tendency of metallization. Our aim is to clarify the origin of anomalous physical properties of  $\text{CuIr}_2\text{S}_4$  and understand the electron correlation extensively by detailed ex-

perimental research.

We have investigated the M-I transition by the chemical substitution method. Single-phase polycrystalline samples of  $\text{Cu}_{1-x}\text{Zn}_x\text{Ir}_2\text{S}_4$  ( $0 \leq x \leq 0.9$ ) have been successfully prepared. The Zn substitution drastically suppresses the M-I transition. The detailed structural, electrical resistivity and magnetic susceptibility measurements show some important clues to the mechanism. A model involving charge ordering and the dimerization of  $\text{Ir}^{4+}$  has been proposed to elucidate the main experimental results. Superconductivity has been found in  $\text{Cu}_{1-x}\text{Zn}_x\text{Ir}_2\text{S}_4$  ( $0.25 \leq x \leq 0.7$ ) with  $T_c$  below 3.4 K. The normal-state resistivity shows anomalous behavior, suggesting that the superconductivity may have some exotic aspect.

**Keywords:** metal-insulator transition, electron correlation, 5d transition element, chalcogenides

## Related Papers

Metal-Insulator Transition and Superconductivity in Spinel-Type System  $\text{Cu}_{1-x}\text{Zn}_x\text{Ir}_2\text{S}_4$ , H. Suzuki, T. Furubayashi, G. Cao, H. Kitazawa, A. Kamimura, K. Hirata and T. Matsumoto, *J. Phys. Soc. Jpn* 68 (1999) 2495-2497.

## 8 Optical Studies on Intra-4f-shell Photoluminescence in Bulk Growth Yb Doped InP

*T. Takamasu, H. Suzuki, Y. Imanaka and G. Kido*  
[April 1999 to March 2003]

## Introduction

Intra-4f-shell photoluminescence of rare-earth doped semiconductor system attracts great attention because of its high efficiency and suitable PL energy for fiber optics[1]. Many different combinations of rare-earth materials and semiconductors have been extensively studied, however, photoluminescence mechanism is still unclear so far. The difficulty in studying such system exists partly in the absence of good bulk samples. Recently, we have succeeded in growing good bulk samples of Yb doped InP crystal which shows very high efficiency of 4f-shell PL below 140K[2]. Here, we report optical properties of this bulk Yb doped InP under strong magnetic fields.

## Experimental

InP:Yb bulk single crystal was grown by the modified Bridgman method with W crucibles sealed in a high vacuum. The initial loaded Yb

concentration is between 0.25% and 5.2%. which corresponds to  $5 \times 10^{19} \text{cm}^{-3}$  and  $1 \times 10^{21} \text{cm}^{-3}$ [3]. From the temperature dependence of magnetization, we have confirmed that the Yb has only one crystallographic site and estimated Yb concentration is ranging from 0.25% up to 6.8% depending on which part of the ingots was used[3]. For the estimation of the samples, we have performed using CCD camera and fiber optics system. He-Ne laser was used for the excitation light source.

Magnetic field was applied with superconducting magnet up to 8T at 4.2K.

## Results and Discussions

For all Yb concentration samples, very sharp 4f shell luminescence lines were observed at around  $E=1.2\text{eV}$ . Figure 1 shows typical temperature dependence of the sample at around 4f shell PL[3]. At low temperature, PL intensity is very high compared with other high quality semiconductor samples such as GaAs and CdTe. With increasing temperature, PL intensity is maintained almost constant up to 70K and it shows rapid decrease above this temperature. At higher temperatures than 150K, 4f shell PL becomes almost invisible. Different from those samples grown by MOCVD, band edge PL at around 1.4eV are very weak at liquid He temperature; about  $10^{-4}$  of 4f-shell luminescence[2]. In Fig. 2, we show temperature dependence of band edge photoluminescence

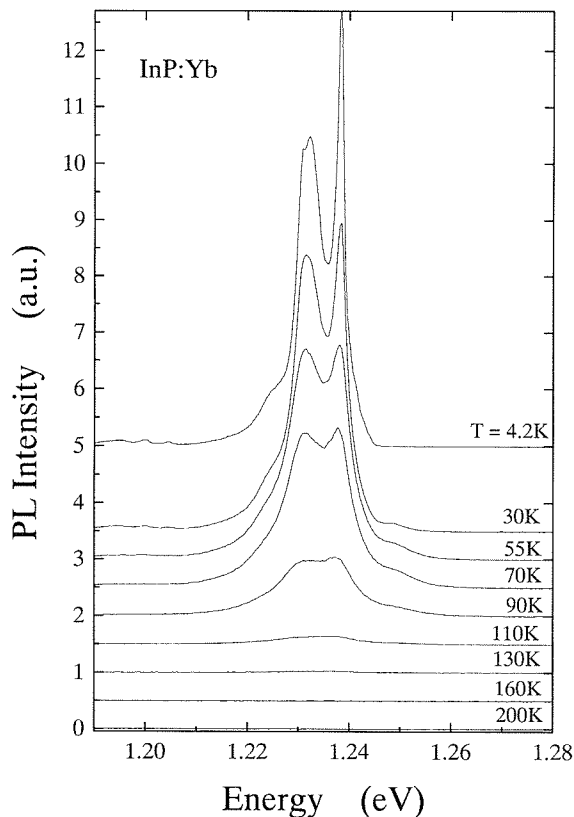


Fig. 1 Temperature dependence of 4f-shell photoluminescence.

pendence of band edge PL. At low temperature, very small PL peaks were observed at 1.35eV and 1.49eV. The origin of these PL peaks are not clear at present, however from the temperature dependence of the InP band gap, higher energy peak can be assigned to the band gap PL and lower peak to the acceptor level. These small PL peaks become invisible above 30K. When the temperature is increased to above 90K, PL peak appears again around 1.4eV. Intensity of 4f shell PL peaks and band edge peaks are plotted as a function of temperature in Fig. 3. It is very interesting that the appearance of the band edge PL and disappearance of 4f shell PL are in coincidence with each other, suggesting energy transfer occurs between these

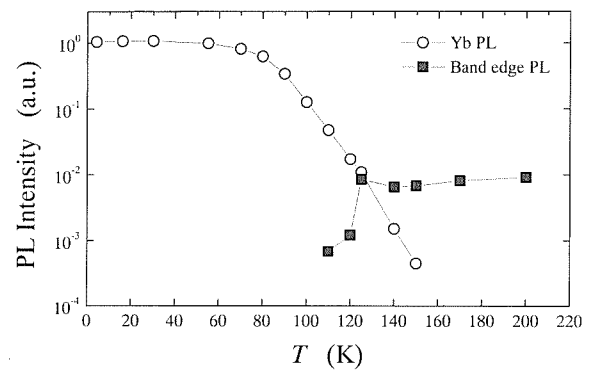


Fig. 2 Temperature dependence of band edge photoluminescence measured at the same time of Fig.1.

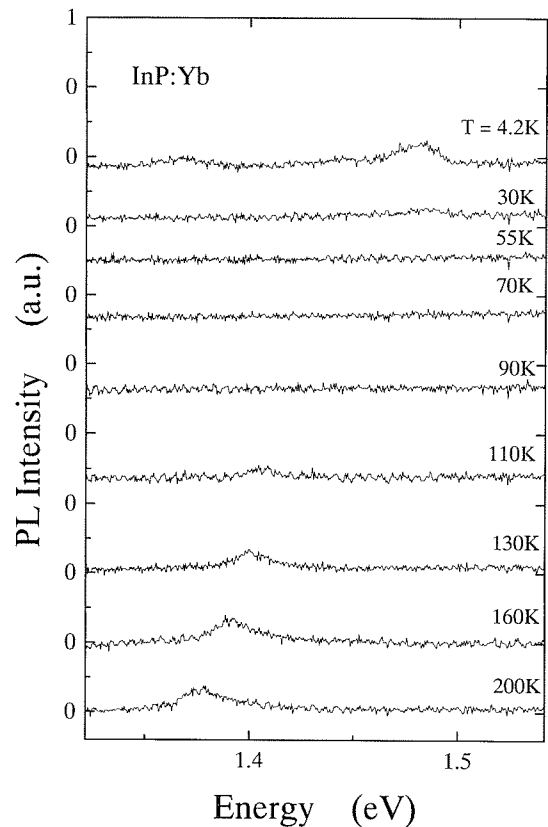


Fig. 3 PL intensity of Yb 4f shell and InP band gap as a function of temperature.

two PL centers.

For InP:Yb samples, Taguchi et al. have proposed PL mechanism as multiphonon-assisted energy transfer[5]. Qualitative discussion of their calculation is adaptable to the present case. However, in our sample band edge photoluminescence is invisibly weak which suggest that almost all excited electron-hole pairs should be recombined in non-radiative process. It is not likely that the coupling between electron and usual phonon system is so strong. Some additional mechanism such as resonant emission of localized phonon is needed for the quantitative explanation.

### Summary

In summary, we have grown the bulk crystal or InP:Yb using modified Bridgman method. Our sample shows very sharp and high efficiency PL peak of Yb 4f shell and almost invisible band edge PL up to about 100K, suggesting the high quality single phase crystal. Temperature dependence of these two PL intensities support energy transfer mechanism qualitatively.

**Keywords:** Yb doped InP, optical measurements

### References

- [1] See, e.g. G. H. Dieke, Spectra and Energy Levels of Rare Earth Ions in Crystals (Interscience, New York, 1968).
- [2] H. Suzuki, T. Takamasu, Y. Imanaka and G. Kido, in Proceedings of 4th international seminar of APF-4.
- [3] H. Suzuki, T. Takamasu, Y. Imanaka and G. Kido, Physica B 294-295 (2001) 475.
- [4] K. Takahei, A. Taguchi, H. Nakagome, K. Uwai and P. S. Whitney, J. Appl. Phys. 66, 4941 (1989).
- [5] A. Taguchi, K. Takahei and Y. Horikoshi, J. Appl. Phys. 76, 7288 (1994).

"Photoluminescence of Yb doped InP under High Magnetic Fields" H. Suzuki, T. Takamasu, Y. Imanaka and G. Kido, 6th International Symposium on Research In High Magnetic Fields.

"High efficient intra-4f-shell photoluminescence in bulk growth Yb doped InP" T. Takamasu, H. Suzuki, Y. Imanaka, and G. Kido, 25th International Conference of Physics of Semi conductors.

"Finite current effect on the photoluminescence at  $\nu=1$  quantum Hall regime In GaAs/AlGaAs heterostructures" T. Takamasu, Y. Imanaka and G. Kido, 25th International Conference of Physics of Semiconductors.

"High Field Optical Studies on Intra-4f shell

Photoluminescence in Bulk Growth Yb doped InP" T. Takamasu, H. Suzuki, Y. Imanaka, and G. Kido, International Conference in High Magnetic Fields in Semiconductor Physics.

"Finite Current Effect on the Photoluminescence in Quantum Hall Regime of GaAs/AlGaAs Quantum Wells" T. Takamasu, Y. Imanaka and G. Kido, International Conference in High Magnetic Fields in Semiconductor Physics.

"Photoluminescence study of CuInS<sub>2</sub>:Yb<sup>3+</sup> under High Magnetic Fields" N. Tsujii, Y. Imanaka, T. Takamasu, H. Kitazawa and G. Kido, International Conference in High Magnetic Fields in Semiconductor Physics.

## 9 Transport and Optical Properties of a Salmon-Sperm-DNA Film in High Magnetic Fields

KIDO Giyuu, KITAZAWA Hideaki, UJI Shinya and IMANAKA Yasutaka, Physical Properties Division

[April 1999 through March 2002]

Every year 6000 tons of salmon sperm must be disposed of in Hokkaido. Consequently, studies on ways to productively use the salmon sperm or to dispose of it with minimal impact on the environment have attracted much attention. Recently, a technique has been developed to fabricate a DNA-lipid complex from salmon sperm, and a DNA film and a DNA fiber from this complex.

We are evaluating the transport and optical properties of the DNA-lipid film in high magnetic fields in order to fabricate films in which the DNA chain is oriented either perpendicular or parallel to the film plane. The DNA chain is aligned along the direction of stretch of the film, so we

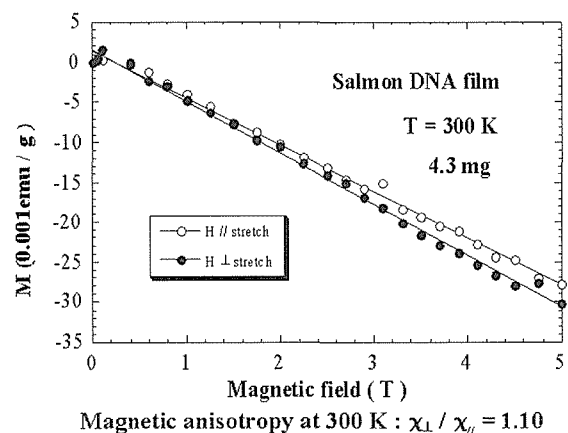


Figure 1. Magnetic susceptibility for a stretched film of salmon-sperm DNA-lipid complex at room temperature. The small anisotropy in the magnetic susceptibility suggests that the DNA chain has aligned itself with the high magnetic field.

suspected that there would be an anisotropy in the magnetization of the film. And indeed, we have measured an anisotropy of 10 % in the magnetic susceptibility, as shown in Fig. 1. This suggests that it might be possible to manufacture a DNA film with vertically oriented DNA chains by applying a high magnetic field during the manufacturing, a possibility of keen interest to researchers in this field.

**Keywords:** Salmon, DNA, alignment, anisotropy

#### 10 Theoretical study on atomic diffusion and electronic state in metal oxides

*T. Sasaki, Computational Materials Science Division*

[April 1999 to March 2002]

The properties of metal materials are changed by exposing its surface to air. The shiny surface of steel will corrode if it is not taken care of correctly; the rust will be made. On the other hand, aluminum surface can be protected by covering its surface by alumina. All these phenomena occur by the oxide formation. The study on the oxide formation on the metal surfaces has a long history. It contains not only the phenomenological analysis of the formation processes but also the model for the atomic diffusion and the chemical reaction. Nevertheless, the microscopic theory on the oxide formation, especially, based on the electronic theory has not been available. Previous studies have revealed that the oxide formation is governed by the atomic diffusion between oxides and the interior bulk metal. At this stage, the diffusion of atoms occurs with the help of vacancy or self-interstitial and their electronic states have significant influence to the diffusion. The present study aims to elucidate the diffusion processes of atoms in the oxides including defects theoretically, based on the state-of-the-art computation techniques; the first-principles electronic structure calculation methods in terms of the density-functional formalism. Thanks to the development of high-performance computers and the progress in the computational technique, the modern electronic theory can be successfully applied to the materials to explain and predict various physical properties. However, there are still some unresolved problems. The metal oxides are the cases. This study includes the investigation to explore how far the present electronic theory can be applied in the metal oxides. The computations are performed on the Numerical Material Simulator System (NEC-SX5/32) installed at

NRIM.

#### 11 Computer simulation on the vortex states and phase transitions of high- $T_c$ superconductors under an external magnetic field

*X. Hu, Y. Nonomura and A. Tanaka, Computational Materials Science Division*

[April 1999 to March 2004]

In the superconducting state, an external magnetic field applied parallel to the  $\text{CuO}_2$  plane of a high- $T_c$  superconductor induces the so-called Josephson vortices. The center of a Josephson vortex enters into a block layer, the layer between two superconducting  $\text{CuO}_2$  layers, in order to save the condensation energy of superconductivity. The thermodynamic phase transition and the lattice structure of interlayer Josephson vortices have been attracting considerable interests since the discovery of high- $T_c$  superconductivity. Using large scale computer simulations, we have observed a critical value in the product of the anisotropy parameter and the magnetic field in interlayer Josephson-vortex systems. Below (above) this critical value the thermodynamic phase transition between the normal and superconducting states upon temperature sweeping is first (second) order. It is clarified that the origin of this tricritical point in the B-T phase diagram is the highly anisotropic layered structure of high- $T_c$  superconductors.

**Keywords:** high- $T_c$  superconductivity, antiferromagnetism, vortex state, flux-line lattice melting

#### Recent Publications

"Possible tricritical point in phase diagrams of interlayer Josephson-vortex systems in high- $T_c$  superconductors", X. Hu and M. Tachiki, *Phys. Rev. Lett.* Vol.85 (2000), p.2577.

"Reply to the Comment by P. Olsson and P. Holme", X. Hu and M. Tachiki, *Phys. Rev. Lett.* Vol.85 (2000), p.2652.

"Spin-gap phenomenon by an  $\text{SO}(5)$  model", X. Hu, *Physica B*, Vol. 284-288 (2000), p.461.

"Antiferromagnetism and superconductivity transitions with  $\text{SO}(5)$  symmetry", X. Hu, *J. Low Temp. Phys.* Vol.117(1999), p.289.

"Inter-layer phase difference of HTSC in  $B \parallel c$ : Monte Carlo simulations", Y. Nonomura and X. Hu, *Physica B*, Vol. 284-288 (2000), p.435.

"Flux-line entanglement as the mechanism of FLL-melting transition in anisotropic HTSC", Y. Nonomura and X. Hu, *J. Low Temp. Phys.* Vol.

117 (1999), p.1447.

"Critical anisotropy in Josephson-vortex systems induced by magnetic fields along the ab plane of high- $T_c$  superconductors", X. Hu and M. Tachiki, *Physica C*, Vol. 341-348 (2000), p.961.

"Magnetic-field-induced first-order N to AF transition: a prediction by the SO(5) theory", X. Hu, *Physica C*, Vol. 341-348 (2000), p.239.

"Simulated phase diagram of high- $T_c$  vortex systems with point pins", Y. Nonomura and X. Hu, *Physica C*, Vol. 341-348 (2000), p.1307.

"Interlayer phase difference and flux-line entanglement at first-order melting transition of high- $T_c$  vortex systems", Y. Nonomura and X. Hu, *Physica C*, Vol. 341-348 (2000), p.1305.

## 12 Design Factors of Heat Resistant Ferritic Steels

*H. Onodera, T. Abe and M. Ohnuma, Computational Materials Science Division*

*K. Kimura, Materials Creation Research Station*

*H.Kushima, Strength and Life Evaluation Research Station*

[April 1999 to March 2001]

Since the capacity of earth is finite, the most efficient use of energy and other resources is necessary for sustainable development of the world as well as the minimization of environmental load. The concept of Minimum Alloying has been proposed by Kimura et al. to meet these requirements. The possibility of minimum alloying has been suggested from the analysis of NRIM creep data for heat resistant ferritic steels where the inherent creep strength depends mainly on the minute contents of Mo and C. We have examined the effect of minute solute elements on the long term creep strength of carbon steels from viewpoint of M-C atomic pairs between a substitutional solute atom, M and an interstitial solute atom, C. We have found a good correlation between the long term creep strength and the concentrations of Mo-C and Mn-C atomic pairs in the ferrite matrix estimated by thermodynamic calculations. This result suggests that the solid solution strengthening due to M-C atomic pairs plays an important role in the long-term creep tests of ferritic steels. Thus it is necessary to optimize the chemical compositions of alloys with the effect of M-C atomic pairs in order to improve long-term creep properties of ferritic steels.

In this study, the effect of solute atoms on the creep properties in Fe-M-C (M=Mo, Mn, Cr, Ti

and W) ternary systems has been studied from viewpoint of M-C atomic pairs. And the effect of each M-C pair has been evaluated in terms of binding energy of M-C pair and diffusivity of M atom. Fe-0.1at%M-0.02at%C (M=Mo, Mn, Cr, Ti and W) alloys and an Fe-0.02at%C binary alloy were prepared as ingots of 1 kg by vacuum induction melting. Ingots were hot-pressed at 1373K to a reduction of 40%, and cold-rolled to a reduction of 90%. Creep specimens with a gauge length of 30mm and a diameter of 6mm were machined from rods after annealed at 1523K for 5h. An average grain size of specimens was about 0.5mm. The creep tests were performed at 973K under Ar gas atmosphere. The results of the sudden stress increment tests suggest the existence of instantaneous plastic strain in all alloys. Thus, it is concluded that the rate controlling process of creep deformations in the present study is the recovery process due to the climb of dislocations. The recovery rate was measured by the stress decrement test proposed by Mitra and MacLean. The recovery rate of the Fe-M-C alloy normalized by that of the Fe-C alloy ( $\gamma_{MC}/\gamma_{Fe}$ ) is shown in Table 1. From these results, it is found that Mo has the largest strengthening effect and the effect decreases in the order of W, Ti, Cr and Mn. The recovery rate of the Fe-M-C alloys was calculated from the binding energy between M and C atoms and the diffusion coefficient of M atom based on the model proposed by Sandstrom. The calculated ratio ( $\gamma_{MC}^*/\gamma_{Fe}^*$ ) agrees well with the measured one ( $\gamma_{MC}/\gamma_{Fe}$ ) as shown in Table 1, suggesting that M-C pair reduces the climb rate of dislocations due to the interaction with dislocations.

**Keywords:** heat resistant ferritic steels, inherent creep strength, the minimum creep rate, M-C atomic pairs, dislocation climbing velocity

Alloys	The ratio of recovery rate	
	Measured	Calculated
	$\gamma_{MC}/\gamma_{Fe}$	$\gamma_{MC}^*/\gamma_{Fe}^*$
Fe-Cr-C	0.77	0.71
Fe-Mn-C	0.85	0.77
Fe-Mo-C	0.34	0.40
Fe-Ti-C	0.65	0.36
Fe-W-C	0.49	0.91

Table 1 The recovery rate of the Fe-M-C alloy normalized by that of the Fe-C alloy ( $\gamma_{MC}/\gamma_{Fe}$ ) and the ratio estimated from the model proposed by Sandstrom ( $\gamma_{MC}^*/\gamma_{Fe}^*$ ).

"Effect of M-C (M=Mo, Mn and Cr) Atomic Pairs on Creep Properties of Fe-M-C Ternary Alloys" T. Abe, H. Onodera, K. Kimura and H. Kushima, *J. Japan Inst. Metals*, 63, 717(1999).

### 13 First-Principles Theory of Dislocations in Solid

*T. Ohno, Computational Materials Science Division*

[April 1998 to March 2001]

Dislocations in solid play important roles in determining electronic, optical, and structural properties of real materials. The purpose of this work is to investigate theoretically dislocations in solid by using first-principles electronic structure calculations, and to clarify their effects on various properties of solid.

The atomic and electronic structures of misfit dislocations of InAs/GaAs(110) and GaAs/InAs(110) heterostructures have been investigated using first-principles calculations. It is found that the core confined at the InAs/GaAs(110) heterointerface has five-fold coordinated In atoms. The surface just above the dislocation line is depressed and the calculated vertical displacement is about 0.52 Å when the InAs epilayer thickness is 4 monolayer (ML), which is in good agreement with the STM observations. In the GaAs/InAs(110) heteroepitaxy, core structures drastically change with the increase of GaAs epilayer thickness.

A phenomenological theory of growth behavior in semiconductor heteroepitaxy has been developed that includes the effects of the formation of Stranski-Krastanov (SK) islands and misfit-dislocations (MDs). This theory can reproduce the various types of growth behavior observed in heteroepitaxial growth. Moreover, a procedure for determining the phenomenological parameters that includes atomistic calculations has been formulated. The critical thickness of InAs/GaAs(110) obtained by this procedure is in good agreement with the experimentally obtained value.

**Keywords:** dislocation, first-principles calculations

### Related Papers

Phenomenological Theory of Semiconductor Epitaxial Growth with Misfit-Dislocations, K. Okajima, K. Takeda, N. Oyama, E. Ohta, K. Shiraishi, and T. Ohno, *Jpn. J. Appl. Phys.* 39 (2000) L917-L920.

*H. Irie, Mechanical Properties Division*

*S. Matsuoka, K. Yamaguchi, A. Ohta, T. Abe, K. Miyahara, N. Nagashima, H. Hirukawa, K. Kobayashi, M. Shimodaira, E. Takeuchi, T. Ohmura, M. Hayakawa, Y. Furuya, M. Kimura, N. Suzuki and H. Maeda, Strength and Life Evaluation Research Station Frontier Research Center for Structural Materials*

[April 1997 to March 2002]

The project aims at the establishment of long term standard reference data on the fundamental fatigue properties of Japanese engineering materials most commonly used for machines and structures under fatigue conditions.

Since 1975, NRIM has established standard data base of conventional fatigue properties of various metals and their welded joints and published 83 data sheets and 16 technical documents. In the documents, fatigue fact data of various metals, their relationships with basic mechanical properties such as elasticity, the fracture mechanism and so on were summarized and described under fundamental investigations on fatigue phenomena.

Recently the life of machines and constructions has been strongly required to be elongated from the ecological and economical points of view. According to the classical theory of fatigue, many of steels have their fatigue limit and there is no problem for any longer time if they will be used below the fatigue limit. However it has been pointed out that the fatigue limit decreases again for longer use, for instance at, more than  $10^{10}$  cycles. Then we will start again the production of long term standard reference data even with some technical difficulties.

In this new project, (1)fatigue data of high strength steels for machine at more than  $10^{10}$  cycles, (2)fatigue data of heat resisting steels from low to high cycle fatigue regions under controlled strain, (3)fatigue data of titanium alloys for up to long term use and (4)fatigue data of welded joints for big constructions considering residual welding stress will be produced and published as data sheets. In addition, in each category of data production basic researches on fracture mechanism of metal due to fatigue from the micro and macro points of view and development of new evaluation methods will be carried out.

The data sheet project of NRIM has a programming system for deciding materials and testing methods in order data to be widely used. A committee, members of which are selected from engineer and/or researcher of typical steel making and

fabricating companies, is organized and discusses the testing program with NRIM.

In 1999, the following fatigue tests and researches have been conducted.

#### 1) Long-term fatigue test at room temperature

The first candidate of steel JIS SUP 7 for spring material has been being tested by rotary bending type testing facilities of up to 100Hz aiming  $10^{10}$  cycles fatigue data will be finished in 2000. In addition to this normal test, fatigue tests with an ultra-sonic fatigue facility with 20kHz have been tried and compared with the normal tested results in order to shorten the long-term testing. In longer testing time up to  $10^8$  cycles, the fatigue occurred inside of specimen not at the surface. However, no remarkable decrease in fatigue strength has been observed.

The nano-indentation technique with AFM, developed by NRIM will be used to make clear the relationship between the fracture orientation and inclusion inside of metal. For the 2<sup>nd</sup> and 3<sup>rd</sup> specimens, a carbon steel JIS S40C and a chromium and molybdenum steel JIS SCM440 were selected and sampled. After decision of heat treatment conditions, these metal will be tested.

#### 2) Long-term high temperature fatigue test

Recently developed and nearly practically used heat resistant steels NF616(9Cr-2W) and HCM12A (12Cr-2W) for power plant were selected to be tested under a strain control up to  $10^5$  cycles (partly  $10^7$  cycles). Testing temperatures were conducted at the room temperature and high temperature among 400 to 700°C. In 1999, all tests of HCM12A steel were finished and a fatigue data sheet has been edited for publication. According to the result, the S-N curve folded to the higher stress level at more than  $10^4$  cycles and fractures were occurred inside of specimen at more than  $10^5$  cycles. The next, specimen of NF616 tests started to be tested. And after NF616, 2.25Cr-1Mo steel and 25Cr-20Ni steel were selected to be tested.

#### 3) Fatigue test of Ti alloys

3 heats of Ti-6Al-4V alloy with a heat treatment at 930°C, one hour (air cooling) and annealed at 705°C, 2 hours (air cooling), have been fatigue tested from low cycle to high cycle fatigue region. The S-N curves were classified into two types, especially in low to middle region of fracture cycle. However, the fatigue limit of all heats was nearly the same value. All of fatigue tests of this alloy were finished and a fatigue data sheet has been edited for publication. For the next target, another Ti-6Al-4V alloy of a different strength level with a heat treatment at 955°C, one hour (air cooling) and annealed at 550°C, 4 hours (air

cooling) were selected and fatigue tests started.

#### 4) Fatigue test of welded joints

In order to obtain basic fatigue properties of practical are welded construction, fatigue test of large scale specimen were carried out and at the same time the influence of residual stress on fatigue properties has been investigated, by measuring residual stress. Large scale specimen and small rib cross welded joint of JIS SM570Q steel were produced. In large scale specimen, the slit type welding was carried out in order to get the maximum residual stress. Comparing of fatigue test results using both welded joint indicated that the small size rib welded joint can simulate practical large scale joint if residual stress is correctly evaluated. However, the rib cross welded joint with a slit could not obtain high weld residual stress comparable to yield stress of base metal because of shortage of restriction by previous welded beads. Then the other welding procedures were tested in order to obtain high residual stress. The same fatigue test will be carried out with specimens of JIS SM400B steel after SM570Q steel.

**Keywords:** fatigue properties, standard reference data, steel, aluminum alloy, titanium alloy

### 15 NRIM Creep Data Sheet Project-V

*H. Irie, Mechanical Properties Division  
F. Abe, H. Tanaka, K. Kubo, M. Murata, M. Tabuchi, E. Baba, M. Shimizu, K. Yokokawa, T. Ohba, H. Kushima, H. Miyazaki and K. Sawada, Strength and Life Evaluation Research Station Frontier Research Center for Structural Materials*

*K. Kimura and S. Muneki, Materials Creation Research Station Frontier Research Center for Structural Materials*

*M. Yamazaki, H. Hongo and T. Watanabe, Mechanical Properties Division*

[April 1996 to March 2001]

The major objectives of the NRIM Creep Data Sheet Project are to produce long-term creep and creep rupture data up to more than  $10^5$  hrs for heat resistant steels and alloys, which are produced in Japan, and to publish the data as a series of NRIM Data Sheets. This project has been continued since 1966 and the series of NRIM Data Sheets have been distributed not only in Japan but also in abroad. In fiscal year 1999, we published 3 sheets listed in the Table.

The data sheet No.33A is the second version of Fe based 21Cr-20Ni-20Co-3Mo-(Nb+Ta)-N superal-

loy steel widely used as material of turbine blade and contains long-term creep rupture data up to 14,000 hrs, tensile strength data at high temperature, typical microstructures of received and fractured steels, results of statistical analysis of creep rupture data, for example the rupture strength of 30,000 hrs and so on.

The data sheet No. 27B is the final version of NCF800H-P corrosion resisting and heat resisting superalloy. It contains creep rupture data up to 150,000 hrs creep strain data up to 100,000 hrs, tensile strength data at high temperatures, typical microstructures of as received and creep ruptured specimen, properties of as-received specimen, results of statistical analysis of creep rupture strength up to 100,000 hrs and others.

The data sheet No. 40A is the second version of STB 510 carbon steel tube for boiler and heat exchanger. It contains long-term creep rupture strength data up to 60,000 hrs, tensile strength at high temperature, microstructure of as received and creep ruptured specimens, results of statistical analysis of creep rupture strength up to 30,000 hrs and so on.

With the testing and publication program, we have done researches on long term creep and rupture behavior of heat-resistant steels and alloys. Long-term creep deformation behavior of ferritic Mod. 9Cr-1Mo and 2.25Cr-1Mo steels has been investigated and also microstructural evolution in creep stressed austenitic stainless steel(18Cr-8Ni) have been quantitatively investigated.

1) Long-term creep deformation behavior.

The relationship between long term creep strength up to 40,000 hrs and microstructural evolution of Mod. 9Cr-1Mo ferritic heat resisting steel was investigated. The creep rupture strength remarkably fell down at more than 100,000 hrs. It caused from that a local recovery of structure primarily progressed at prior austenitic grain boundary and the accelerating creep occurred at early time when the creep strain rate in low strain region has not reached at sufficient small value.

Comparison of long term creep properties between two 2.25Cr-1Mo ferritic heat resisting steels, one was sampled from a 190,000 hrs used steel in a plant and other was of not used steel. The initial creep strain rate of used one at high stress region was lower at smaller stress and the nearly same strain rate as the not used one was revealed under the critical stress. This critical stress corresponded to the yield stress at the same temperature.

2) Microstructural evolution in austenitic stainless steels

Following the data sheet publishing schedule, the investigation on structural evolution and its

analysis in long term crept SUS 316 austenitic stainless steels has started.

On the bases of already published Atlas of Microstructure Data Sheet M-1(March 31, 1998), an investigation while hardness change in crept steel can be used for the diagnostics of the deterioration degree of steel was carried out. The hardness of crept stainless steel depended on many positive and negative factors, such as the increase of dislocation density by creep deformation, the decrease in it by recovery, rearrangement of dislocation distribution, precipitation state of carbide particles, grain growth and so on. These phenomena depended strongly on the crept time, the stress level, and deformation. Then a simple or universal relationship between hardness change and material properties could not be recognized. However, while the hardness change under low level of stress showed the same behavior in steel under aging treatment, it was indicated that the material deterioration in practical plant can be evaluated using the hardness measurement in aging treatment.

**Keywords:** long-term creep, creep rupture, stress relaxation, microstructural evolution

Table Summary of NRI Data Sheets in fiscal year 1999

## 16 Fatigue Behavior and Microstructure of Metals

*F. Morito, Mechanical Properties Division*  
[April 1999 to March 2002]

When pure metals are subjected to cyclic plastic strains, they may harden or soften depending on their initial structures. Thus, metals in the annealed state usually become harder while those that are cold worked generally soften. Such a fatigue hardening or softening in deformation resistance can be detected by corresponding changes in indentation hardness, flow stress, damping response and the cyclic stress-strain response of the material.

Fatigue damage process develops preferentially at the sites of cyclic strain localization. As a direct consequence of strain localization, therefore, crack nucleation occurs and crack growth proceeds in the material.

In order to understand changes in the deformation resistance and the strain localization during fatigue, we must study the dislocation structure as well as the surface slip pattern associated with cyclic deformation process. It is also necessary to clarify any obvious correlation between the interior dislocation structure and the surface slip band structure.

We examined the fatigue behavior in pure nickel and 304 stainless steel with FCC structure. Specimen was bar type of 80 mm total length with 4 mm  $\psi$  and 8 mm gauge length. Fatigue tests at room temperature were carried out at a frequency of 4 Hz in the load control mode and a stress ratio of  $R=0.1$  or  $-1$ .

In fatigue of the work hardened materials under  $R=-1$ , the fatigue softening existed typically in pure nickel, but it did not occur in 304 stainless steel. Under  $R=0.1$ , no fatigue softening existed in both materials. In fatigue of annealed materials under both stress ratios, the fatigue hardening existed in both materials.

In the fatigue softened pure nickel, the microstructure was mainly subgrain formation. In the fatigue hardened pure nickel under  $R=-1$ , the loop patch formation was observed in low stress amplitude, while the subgrain formation was observed in high stress amplitude. In the fatigue hardened 304 stainless steel under  $R=-1$ , oriented dislocations and stacking faults were recognized in low stress amplitude, while cell-like structure with high dislocation density existed in high stress amplitude. The reason why no fatigue softening occurred under  $R=-1$  in work hardened 304 stainless steel is considered that cross-slip deformation was difficult due to lower stacking fault energy.

Based on the above results, particular attention is paid on the fatigue behavior and microstructure in iron and molybdenum with BCC structure. We examine details of the surface slip band structure, dislocation arrangement, crack nucleation and their relations during fatigue deformation. We compare the characteristics of fatigue damage process in BCC crystals with those in FCC crystals. It is possible to reveal the mechanisms of fatigue softening and hardening behavior.

**Keywords:** fatigue softening, fatigue hardening, stress ratio, microstructure

## 17 Dynamic Microstructural Change and Mechanical Properties in Ceramics at High Temperatures

*K. Hiraga, K. Nakano, B.-N. Kim and K. Morita Mechanical Properties Division*

[April 1998 to March 2001]

Most of polycrystalline ceramic materials show plasticity at high temperatures under the aid of grain boundary sliding accommodated by matter transport through or across grain boundaries. The failure of such accommodation at localized boundary regions leads to the occurrence of intergranular

cavities, which grow into facet sized ones and coalesce to form intergranular microcracks. This study aims to get basic information on microstructural factors relating to such deformation and fracture processes. Special attention is placed on the effects of dynamic microstructural changes on constitutive behavior and cavitation damage during deformation at relatively low tensile stressed ( $\sigma/E=10^{-4}$ ), at temperatures higher than 1600 K. The followings are within the scope of the present study.

(1) theoretical modeling and simulation for deformation and microstructural evolution: dynamic grain growth and grain boundary sliding during diffusional creep has been analyzed on the basis of grain boundary diffusion mechanisms. Superplastic deformation and microstructural evolution such as grain growth and grain elongation during deformation have been also analyzed by incorporating the mechanisms of Lifshits grain boundary sliding and static and dynamic grain growth. The analysis reveals a close relationship between grain boundary sliding and grain boundary migration, i.e., grain growth.

(2) deformation mechanisms in undoped and silica-doped zirconia polycrystals: the details of deformation behavior and relating microstructural aspects are under investigation as a function of stress, temperature and grain size using HRTEM and creep machines, by which concurrent tensile strains at gauge portion can be monitored directly with a resolution of 5  $\mu\text{m}$  using an optical extensometer. The study has revealed new aspects of high temperature deformation in tetragonal zirconia polycrystals such as intervention of a diffusional creep mechanism at low stresses and contribution of intragranular dislocations to an accommodation process at high stresses.

(3) cavitation and failure mechanisms in fine-grained oxides: stereological analysis of cavity size distributions have revealed the detailed features of cavity nucleation and growth behavior during high temperature tensile deformation in superplastic and superplastic-like oxide ceramics. The study have also revealed a close relationship between the occurrence of microcracks causing failure and the formation and growth of cavities growing into sizes larger the current grain size. The stress-, temperature- and grain-size-dependence of cavity nucleation and growth are under investigation in connection with stress concentration and relaxation at multiple grain junctions and constraints for cavity growth from surrounding grains.

**Keywords:** grain growth, grain boundary sliding, diffusional creep, superplasticity, stress concentration, dislocation activity, cavitation, microcrack,

modeling

## 18 Fracture Mechanism of Welded Structure of Stainless Steel at Cryogenic Temperature

*T. Ogata and T. Yuri, Mechanical Properties Division*

[April 1999 to March 2002]

In the applications of cryogenic technology, there are projects of constructing large scale facilities of superconducting magnets at liquid helium temperature (4K) and clean energy to transport and store liquid hydrogen (20K). It is very important to evaluate the mechanical properties of the materials including weld metals in practical environment to keep the reliability of large scale structures used at cryogenic temperatures and in high magnetic field. It is required to comprehend the mechanical properties such as continuous data of fracture toughness from room temperature to liquid helium temperature, and also to clarify the effects of hydrogen-gas environment at low temperatures on deformation and fracture behavior of structural materials for the design of structure and selection of materials. Especially, hydrogen embrittlement at low temperatures in the large scale structures of stainless steels is an important subject. In this study, we are going to carry out high-cycle and low cycle fatigue tests on stainless steel welds with delta ferrite but less weld defects and clarify the effects of brittle structure on fatigue properties, carry out the J-evaluation tensile tests by round bar with circumferential notch on the specimens sampled from the welds and hydrogen-charged to evaluate fracture toughness of the welds in detail and effects of hydrogen on the welded structure, and carry out tensile and fracture toughness tests from room temperature to liquid helium temperature in high magnetic field and investigate the effects of high magnetic field and weld structure on the mechanical properties of unstable austenitic stainless steels at each temperature.

In 1999, we investigated low-cycle fatigue properties of aluminum alloy base metal (A5083) and weld (A5183) at cryogenic temperatures, and we found that the degradation of low-cycle fatigue properties of A5183 at low temperature was due to intergranular failure caused by the  $\beta$ -phase at the grain boundary, and it is possible to minimize the degradation of fatigue properties in aluminum alloy welds at cryogenic temperatures if the occurrence of blowholes and intergranular failure can be controlled by optimizing the welding process. We also studied the effects of  $\delta$ -ferrite and long time

hydrogen-charging on fracture toughness of SUS 304L weld joints using the small tensile specimen, and found that fracture toughness is lower in weld metals than in base metals and decreases as the amount of  $\delta$ -ferrite increases, the toughness decreased in 5% and 10%  $\delta$ -ferrite welds by 9ppm hydrogen-charging, however, toughness decreased only in 10% welds by 4ppm hydrogen-charging, which means that less amount of  $\delta$ -ferrite weld has less influence of hydrogen embrittlement.

**Keywords:** structural material, stainless steel, cryogenic temperature, magnetic field, tensile properties, fatigue properties, hydrogen embrittlement

## 19 Search for Group IV Elements Compounds Including Alkaline-earth-metal Elements

*M. Imai and T. Hirano, Mechanical Properties Division*

[April 1999 to March 2001]

Si is still one of the important materials in the present LSI technology. With progress of the technology, the problems arise that cannot be solved with the materials used conventionally. Therefore, search for new Si-related materials with new function and properties becomes more important. Silicides are one of the potential constituents of microelectric and optoelectronic device. Among the silicides, silicides including alkaline-earth-metal elements have unique structures like a layer-by-layer packed structure, clathrate structure, and so on. For the reasons above, we studied alkaline-earth metal disilicides ( $M_A\text{Si}_2$ ,  $M_A=\text{Ca, Sr, Ba}$ ) for recent several years. We synthesized metastable phases of alkaline-earth metal disilicides  $\text{BaSi}_2$  under high-pressure and high-temperature condition, and studied structure and electronic properties of these phases.  $\text{BaSi}_2$  was chosen as samples because of their unique atomic configurations and large compressibility of Ba atoms.  $\text{BaSi}_2$  was found to be a semiconductor with an orthorhombic structure at ambient conditions. We synthesized  $\text{BaSi}_2$  with a cubic structure and a trigonal structure, and found that trigonal  $\text{BaSi}_2$  is a hole metal while cubic  $\text{BaSi}_2$  is an n-type semiconductor. It is rarely known that high-pressure metallic phase is quenched at ambient condition. Furthermore, it was found that trigonal  $\text{BaSi}_2$  is a superconductor with onset temperature of 6.8K. We also observed pressure-induced structural phase transition with in situ X-ray diffraction measurements, and discussed about the similarity among the transformation sequence under pressure in three  $M_A\text{Si}_2$ .

In this project, we are studying Si clathrate compounds, and  $\text{CaAl}_2\text{Si}_2$ , which has a layer-by-layer packed structure, and related materials.

The Si clathrate compounds were discovered in alkali-metal-Si system for the first time, and their physical properties were investigated many years ago. Crystal structure of the Si clathrate compounds consists of Si polyhedral cages, and alkali-metal atoms are incorporated inside the cages. After recent discovery of superconductivity of alkali-metal-doped fullerenes, the Si clathrate compounds has attracted attention again. This is because the shape of polyhedral cage is close to that of fullerene, and the expected Debye frequency for the tetrahedrally coordinated Si network seems to be favorable for the superconductivity of the BCS mechanism. Now two Si clathrate compounds,  $(\text{Na}, \text{Ba})_8\text{Si}_{46}$  and  $(\text{K}, \text{Ba})_8\text{Si}_{46}$ , are known as superconductors. In this study, we are trying to synthesize the Si clathrate compounds in the other system, and investigate their physical properties.

**Key words:** silicides, alkaline-earth metals, electrical resistivity

### Related Papers

Electrical resistivity of metastable phases of  $\text{BaSi}_2$  synthesized under high pressure and high temperature, M. Imai and T. Hirano, *J. Alloys and Compounds* 224 (1995): 111-116.

Superconductivity of trigonal  $\text{BaSi}_2$ , M. Imai, K. Hirata and T. Hirano, *Physica C* 245 (1995): 12-14.

Electrical resistivity of three polymorphs of  $\text{BaSi}_2$  and p-T phase diagram, M. Imai and T. Hirano, *Mat. Res. Soc. Symp. Proc.* 402 (1996): 567-572.

In situ measurements of the orthorhombic-to-trigonal transition in  $\text{BaSi}_2$  under high-pressure and high-temperature conditions, M. Imai, T. Hirano, T. Kikegawa, and O. Shimomura, *Phys. Rev.* B55 (1997): 132.

Phase transitions of  $\text{BaSi}_2$  at high pressures and high temperatures, M. Imai, T. Hirano, T. Kikegawa, and O. Shimomura, *Phys. Rev.* B58 (1998): 11922.

Single-crystal growth and electrical properties of  $\text{B}_n\text{Si}$  ( $n=18$ ), M. Imai, T. Kimura, K. Sato, and T. Hirano, *J Alloys and Compounds* 306 (2000): 197-202.

### 20 Characterization and Evaluation of Cryogenic Structural Materials

*T. Ogata and T. Yuri, Mechanical Properties*

### Division

[April 1997 to March 2002]

For design and development of large scale cryogenic applications, such as a nuclear fusion reactor, a superconducting power generator, a superconducting magnetic levitated train, and so on, it is very important to construct intellectual infrastructure through international pre-standardization for promoting practical use of advanced cryogenic structural materials, high-strength stainless steels, high-Mn steels, and large thickness weld joints. This research has been carried out with a close contact with the VAMAS Technical Working Area(TWA) 17, cryogenic structural materials, which has been organized in the Versailles Project on Advanced Materials and Standards to promote the prestandardization program on material properties tests of glass fiber reinforced polymer (GFRP) composite materials and alloys at liquid helium temperature. The base is to develop an understanding of mechanical-property determinations at liquid-helium temperature (4.2 K) and establish a unified method. A series of international interlaboratory comparisons of both tensile and fracture toughness tests for high-strength stainless steels, a titanium alloy, and an aluminum alloy, and compression and shear tests for composite material G-10CR were performed so far. Fifteen research institutes from eight nations have participated in the projects of TWA 17, such as the University of Tokyo, Tohoku University, National Institute of Fusion and Science, and Osaka University in Japan, FZK in Germany, RAL in United Kingdom, NHMFL, CTDI, and UCLA in USA, SEP in France, EMPA in Switzerland, Tech Univ. in Vienna in Austria, and so on.

In this research we are going to establish and report pre-standard testing methods of a) tensile test in high magnetic field, b) an advanced fracture toughness evaluation method by round bar with circumferential notch, and c) interlaminar shear test of G-10CR, glass fiber reinforced plastic, at cryogenic temperature.

In 1999, we have performed investigation, analysis, and international round robin tests on testing conditions and procedures of each research subjects. As a chairman and the office of TWA 17, we held the Technical Working Party meeting twice in USA and Japan attended by participants to this programs from each country, discussed and agreed the results so far and details of testing items and procedures of these round robin tests. According to the agreement of the 14th TWP meeting held on July 12, 1999, a draft of the international standards "Metallic Materials -

Tensile Testing in Liquid Helium" was discussed in TWA 17 and submitted to ISO TC164/SC1 the end of 1999 as a New Work Item for the SC1. The draft was distributed to the delegates to the SC1 and this proposal will be accepted with at least five countries approval. This draft is based on ASTM E 1450 and added a recent view of VAMAS activities and JIS Z 2277(Tensile Testing Method for Metallic Materials in Liquid Helium); a diameter of a standard specimen is 7 mm but alternatives are allowed, main strain measurement methods use extensometers but strain gages are also allowed and so on.

**Keyword:** structural material, cryogenic temperature, standardization, tensile test, fracture toughness test, shear test

**Publication:**

Results of VAMAS Activities on Pre-standardization of Mechanical Properties Evaluation at 4K, Advances in Cryogenic Engineering (Materials), Vol.46(2000)p.427-434

## 21 Microstructural Control for High Performance Refractory Metals

*T. Fujii and K. Kamihira, Materials Processing Division*

[April 2000 to March 2003]

For the wider utilization of b.c.c refractory metals such as molybdenum and tungsten, development of high performance refractory metals is necessary. However, those refractory metals undergoes a severe loss of ductility after recrystallization, welding or heavy neutron irradiation. It is generally accepted that such a problem is due to intergranular embrittlement. This is the greatest weak point of these metals.

Fortunately, NRIM (National Research Institute for Metals) has succeeded in establishing a new technology to develop commercial scale molybdenum and tungsten single crystals and their multi-layer crystals with a desired crystallographic orientation from hot-rolled sheet doped with a certain amount of oxides by means of secondary recrystallization. However, a few research and development for preparation of the polycrystalline refractory metals with high strength and toughness by a microstructural control, i.e. microstructure, grain boundary and texture control, have been carried out.

Thus, the main purpose of this study is to de-

velop a new microstructural control means for preparation of high performance polycrystalline-refractory metals such as molybdenum, tungsten and their alloys through solid state processes.

**Keywords:** microstructural control, refractory metal, solid state process

## 22 Crystal growth and dissolution mechanisms in peritectic system

*K. Maiwa and T. Fujii, Materials Processing Division*

[April 1998 to March 2000]

We intend to clarify the mechanisms of crystal growth and dissolution in a peritectic system in this subject. For this purpose, we chose  $\text{Sr}(\text{NO}_3)_2 - \text{H}_2\text{O}$  peritectic system as an example, in which the crystal growth and dissolution processes can be observed in situ in a transparent liquid at room temperature. Above and below the peritectic temperature,  $T_p = 29.3^\circ\text{C}$ ,  $\text{Sr}(\text{NO}_3)_2$  phase and  $\text{Sr}(\text{NO}_3)_2 \cdot 4\text{H}_2\text{O}$  phase are equilibrated with the liquid in this system, respectively. A peritectic reaction is expected at peritectic point in equilibrium. It was observed, however, that in the liquid of the composition of the peritectic point at the temperatures below  $T_p$ , both solid phases could grow. In these conditions, the growth rate of the low-temperature phase was much larger than that of the high-temperature phase and the difference in the growth rate between two phases increased with the decrease of the temperature. It is followed that the latter was engulfed in the former simply due to the difference in growth rate, which resulted in a 'peritectic texture'.

**Keywords:** peritectic reaction, incongruent melting, crystal growth

## Recent Publications

Atomic force microscopy observations of hollow cores on the  $\{111\}$  and  $\{100\}$  faces of barium nitrate, M. Plomp, K. Maiwa, W.J.P. van Enkevort, J. Crystal Growth 198/199 (1999) 246.

## 23 Application of Ionization Separation Technique to Gaseous Process

*Y. Ogawa and O. Kujirai, Materials Processing Division*

[April 1998 to March 2001]

Ionization separation methods are effective to remove impurities from a gaseous matrix by electrostatic field. The objective of this study is to investigate basically photoionization and surface ionization as the separation technique. It was found using photoionization that there were many unknown high-lying energy levels in lutetium which is the last member of the rare-earth elements and has the filled 4f electron shell. Light and middle rare-earth atoms have an unfilled 4f electron shell and complex spectral configuration. The research of unknown high-lying energy levels of these atoms is important to understand energy transition and electron configuration of rare-earth atoms and to apply photoionization to them.

The research is composed of the following two subjects.

1. Study of high-lying energy levels of light and middle rare-earth atoms by resonance photoionization.
2. Study of the basic features and characteristics of the surface ionization as the separation method.

**Keywords:** laser, resonance photoionization, surface ionization, high-lying energy level, rare-earth elements

#### Related Papers

Laser Material Purification of Neodymium, Y. Ogawa et al., J. Jpn. Inst. Met. 55(1991):545-552.

Study of Even-Parity Autoionization States of Lutetium Atom by Laser Resonance Photoionization Spectroscopy, Y. Ogawa and O. Kujirai, J.Phys.Soc.Japan,68(1999) 428-433

Odd-Parity Autoionization States of Praseodymium Atom by Optogalvanic Spectroscopy, O. Kujirai and Y. Ogawa, J.Phys.Soc.Jpn.,69(2000):67-71

#### 24 Fabrication and characterization of nano-structured materials

*Y. Sakka, K. Ozawa, T. Uchikoshi, T. S. Suzuki, H. Okuyama and O. O. Vasylyk\**, *Materials Processing Division, \*STA fellow*  
[April 1999 to March 2002]

Nano-structured materials can be classified into two general categories. One category consists of materials of only nanosized materials. The other consists of materials where nanosized particles are distributed within the intra- and/or inter-grains of micronsized grains. These nano-structured materials have been receiving increasing attention due to

their unique chemical and physical properties which cannot be obtained from the conventional materials. However, the processing of the nano-structured has not been established. In this study two types of processing are conducted to fabricate nano-structured materials. One is synthesized by consolidating fine powders through a colloidal processing followed by sintering. The other is nano-porous materials with layered perovskite structures through the soft chemical processing i.e. a sol-gel or a hydrothermal processing.

Nano-size Y-doped zirconia powder with controlled secondary particle size was synthesized by hydrolytic coprecipitation. Hydrous-zirconia gel produced by urea precipitation results in a nano-powder with a primary particle size of 5-8 nm and secondary aggregate size of 45-65 nm.

The colloidal processing is a useful tool for consolidating nano-sized particles with desired pore size distribution. An important factor is to control the interparticle interaction in liquid. Alumina and/or zirconia compacts with a narrow pore size distribution, which was determined by mercury porosimetry, was produced by slip cast, pressure filtration or electrophoretic deposition technique. Sintering characteristics of the green compacts and mechanism of preparing nano-structured materials are examined.

Powder and film of antimonite acid have been prepared by a direct reaction of  $\text{Sb}(\text{O}-n-\text{C}_3\text{H}_7)_3$  or Sb metal with  $\text{H}_2\text{O}_2$  aqueous solution. Bismuth or yttrium doped antimonite acids were prepared by reacting an  $\text{H}_2\text{O}_2$  aqueous solution with  $\text{Sb}(\text{O}-i-\text{C}_3\text{H}_7)_3$  and  $\text{Bi}(\text{O}-i-\text{C}_3\text{H}_7)_3$  or  $\text{Y}(\text{O}-i-\text{C}_3\text{H}_7)_3$ . The conductivity of 0.1 mol%  $\text{Bi}_2\text{O}_3$  (or  $\text{Y}_2\text{O}_3$ ) doped antimonite acids was found to be high ( $1.0^8 10^{-3} \text{Scm}^{-1}$ ). Effect of the water vapor pressure and nano-pore structure on the proton conductivity is studied.

**Keywords:** nanoparticle, colloid, antimonite acid, sintering, nanocomposite

#### Recent publications

Preparation and electrical conductivity of three types of antimonite acid films, K. Ozawa, Y. Sakka and M. Amano, J. Mater. Res. **13** (1998):830-33.

Preparation of fine-grained zirconia and alumina ceramic systems through colloidal processing, Y. Sakka, T. Uchikoshi, K. Ozawa, T. S. Suzuki and K. Hiraga, Advances in Science and Technology, **14B** (1999):593-604.

Nonisothermal synthesis of yttria-stabilized zirconia nanopowder through oxalate processing: I, characteristics of Y-Zr oxalate synthesis and its decomposition, O. Vasylyk and Y. Sakka, J. Am.

Ceram. Soc., **83** (2000):2196-202.

Synthesis of composite metal particles modified UFP using the RF-plasma CVD, H. Okuyama, K. Honma and A. Ohno, J. Jpn. Powder Powder Met., **47** (2000): 993-98.

## 25 Diffusion Bonding between Transition Metals (Cr, Fe, and Ni) and Metals of Group IV~VI

*T. Kasugai and K. Ei, Advanced Materials Processing Div.*

[April 1999 to March 2002]

It is difficult to apply fusion welding processes, such as an arc welding or an electron beam welding, to dissimilar metals joining because a large amount of brittle metallic compounds form in the weld metals. On the other hand, the size of metallic compounds and diffusion layer in dissimilar metal joints can be easily controlled by a solid state diffusion bonding.

The basic metallurgical knowledge on the dissimilar metal bonding zone has been scarce until now, and it is difficult to estimate the size/kind of metallic compounds at the bonding zone based on phase diagrams. The diffusion process in the bonding zone of dissimilar metals, moreover, is not simple, but a few negative diffusion or up-hill diffusion phenomena have been observed in bonding zone between Ni-Cr alloy or stainless steel and metals of group IV.

In this study, joinability of the diffusion bonding between transition metals (Cr, Fe, and Ni) and metals of group V, the formation of metallic compounds in the bonding zone between transition metals (Cr, Fe, and Ni) and metals of group V, diffusion processes, and bonding crack are investigated in the connection with the periodic table.

**Keywords:** Diffusion bonding, Cr, Fe, Ni, Metals of Group V

## 26 Cladding or Coating Processes by Utilizing Semi-Solid Processing

*T. Dendo, T. Shirota and T. Kimura, Advanced Materials Processing Division*

[April 1999 to March 2002]

In the recent years, much interest has been arisen in composite or combined materials because requirements of engineering materials become more and more severe and versatile. Accordingly, various processing techniques have been attempted

for manufacturing composite materials or for combining dissimilar materials. We also have been proposed new methods for combining dissimilar materials, in which cladding and forming are simultaneously performed by utilizing semi-solid processing. On the basis of our proposals, this study consists of two sub-themes as described in the following.

One is on cladding process combined plastic working of solid metal with squeeze forming of semi-molten metal. A metal block heated up in semi-molten state is inserted into a dissimilar hollow metal in solid state, and then the hollow metal is bulge-formed in a shaped die by pressurizing the semi-molten metal. Through this processing, a shaped part clad in a skin of dissimilar metal is manufactured. The experiments are being conducted so as to grasp feasibility and problems in this process. The semi-molten metals employed are Al-Si alloys. Three kinds of metallic pipe, stainless steel, copper and aluminum, are used as the hollow metals.

Another is on coating process with particle-dispersed composite by means of pressure infiltration under semi-molten state. When a pressure is applied to semi-molten metal covered partially with powder layer, liquid component oozes out and infiltrates into the powder layer. Consequently, a block or part coated partially in a composite layer is fabricated through this process. Some experiments are being carried out to explore the fundamental characteristics of this mode in combination of semi-solid Al-Si alloys and alumina powder.

**Keywords:** semi-solid processing, cladding, coating, composite, plastic working, infiltration

## 27 Effect of Interface Damage on Fatigue Crack Growth for Fiber-Reinforced Titanium Alloy Matrix Composite

*C. Masuda, Y. Tanaka and Y-F. Liu, Advanced Materials Processing Division*

[April 1999 to March 2002]

Continuous SiC fiber reinforced titanium alloy matrix composites are attractive for structural applications such as in gas turbines, because of their high specific modulus and strength, and good stability at high temperature. Improvement of fatigue resistance of the composite at high temperature is an important research subject which should be realized before application. The fatigue life of the composite in vacuum at high temperature is significant longer than that at room temperature. The fa-

tigue crack growth mechanism of the composite is fiber bridging which operated behind the tip of the matrix crack. It is suggested that the interface frictional sliding length is longer at high temperature than that at room temperature, and the interface shear sliding stress is due to the reduction of load transfer potential by the interface wear.

The effect of the interfacial damage on fatigue crack growth behavior of the composite was studied using in-situ observation technique in vacuum at room ( $T=293\text{K}$ ) and high temperature ( $T=823\text{K}$ ), and the following results were obtained.

(1) The fatigue crack growth rate of the composite decreases with increasing test temperature. and decreases with increasing applied stress intensity range. The acceleration of the crack growth is strong dependent on the fiber fracture by interface wear. The degradation of bridging fibers in the crack wake is severe at room temperature, and this behavior is dependent on the test temperature.

(2) The increase in the test temperature results in the decrease of the fatigue crack growth rate. The crack opening displacement along the crack wake at  $T=823\text{K}$  is smaller in comparison to that at  $T=293\text{K}$ , and this tendency is dependent on the applied stress range. The associated increase in the crack tip shielding is explained on the basis of crack closure due to matrix relaxation by fatigue creep behavior.

**Keywords:** fiber-reinforced Ti alloy matrix composite, fatigue crack growth rate, crack closure, interface wear

### Recent Publications

- 1) Y. Tanaka, Y. Kagawa and C. Masuda, "Observation of fatigue damage process in SiC fiber-reinforced Ti-15-3 composite at high temperature", *Metall. Trans. A*, 30A (1999) p221-229.
- 2) Y.-F. Liu, Y. Tanaka and C. Masuda, "In-Situ Detection of Fiber Break and Analysis of its Effect on Stress Transfer during Tensile Tests of a Metal Matrix Composite", *Composites Part A: Manufacturing and Applied Sciences*, Vol. 30, pp. 1243-1249, (1999).
- 3) Y.-F. Liu, Y. Tanaka and C. Masuda, "Effect of Interfacial Debonding and Sliding on Matrix Crack Initiation during Isothermal Fatigue of SCS-6/Ti-15-3 Composites", *Metall. Trans. A*, Vol. 31A, pp. 2637-2645 (2000).

### 28 Fabrication and characterization of nano-structured materials

Y. Sakka\*, T. Uchikoshi\*, K. Ozawa\*, T.S. Suzuki\*, H. Ohtsuka\*\* and K. Hiraga\*\*\* \*

\* *Materials Processing Division,*

\*\* *High Magnetic Field Research Station,*

\*\*\* *Mechanical Property Division*

[April 1998 to March 2001]

Concerted Amplification is defined as "Induced non-linear phenomena in the proceeding reaction fields by external stimulation". Research on advanced materials processing on the basis of concerted amplification started in 1998 by special coordination funds of STA. In this study to fabricate advanced ceramics by colloidal processing, external fields such as magnetic field, ultrasonication, electric field, etc. are applied during the consolidation stage.

The controlled development of texture in ceramics is a topic of recent interest in processing because it allows improved tailoring of various properties. Textured alumina was synthesized by using colloidal processing and a high magnetic field. Fine alumina powder dispersed in suspension was oriented under a high magnetic field (10T) owing to crystal magnetic anisotropy. When the green compact prepared by slip casting in a high magnetic field was annealed at high temperatures, grain growth occurred with grain alignment. During annealing at high temperatures plate-like grains grew, thus the degree of alignment increased. The c-plane of alumina was perpendicular to an applied magnetic field.

Electrophoretic deposition (EPD) usually requires the use of non-aqueous colloidal suspensions, to avoid the problems of void formation by the electrolysis of  $\text{H}_2\text{O}$ . We found that no voids were formed in the deposit prepared by aqueous suspension using a palladium. The preparation and characteristics of suspensions are important for factors such as deposition rate, zeta potential, and particle size distribution. The zeta potential and, hence, suspension stability, of TZ3Y-ethanol system were increased by washing. As a result, EPD rate increased dramatically from the as-received condition. There were no significant beneficial effects of washing on the aqueous system, indicating a much greater sensitivity to ionic contaminants in an ethanol suspension especially for the TZ3Y. Green densities prepared by EPD using aqueous suspensions were higher than those by EPD using ethanol suspensions and similar to those by slip casting using aqueous suspensions.

Cubic antimonite acid suspensions were synthe-

sized by a direct reaction of  $\text{Sb}(\text{O}-n-\text{C}_3\text{H}_7)_3$  or Sb metal with  $\text{H}_2\text{O}_2$  aqueous solution. Antimonic films were successfully prepared on the stainless steel and Si(100) substrates by the EPD using the synthesized suspensions. The proton conductivity of antimonic were evaluated by an ac impedance method at room temperature under controlled levels of relative humidity.

**Keywords:** colloidal processing, electrophoretic deposition, high magnetic field, antimonic acid, textured alumina

#### Recent publications

Fabrication of bubble-free compacts from aqueous suspensions by electrophoretic deposition, T. Uchikoshi, K. Ozawa, B. D. Hatton and Y. Sakka, *Trans. Mater. Res. Soc. Jpn.*, **25** (2000):107-10.

Preparation of polycrystalline antimonite acids films by electrophoretic deposition, K. Ozawa, Y. Sakka and M. Amano, *J. Sol-Gel Sci. Technol.* **19** (2000):595-98.

Synthesis of aligned alumina by slip casting in a high magnetic field and heat treatment, T. S. Suzuki, H. Ohtsuka, Y. Sakka, K. Hiraga and K. Kitazawa, *J. Jpn. Powder Powder Met.*, **47** (2000): 1010-14.

Slip casting and electrophoretic deposition of suspensions of alumina and zirconia fine particles, Y. Sakka, B. D. Hatton and T. Uchikoshi, *J. Jpn. Powder Powder Met.*, **47** (2000):1015-20.

#### 29 Evaluation of Mechanical Properties for Metal matrix Composites

*C. Masuda, Y. Tanaka and Y.-F. Liu, Processing Materials Division*

[April 1996 to March 2001]

Metal Matrix Composites (MMC) have numerous potential applications in situations requiring light weight and high stiffness materials with high temperature capability. As metal matrix composites have anisotropic structures, those mechanical properties are significantly depended upon the fiber direction in the composites compared with the conventional steels, aluminum alloys and so on. In order to obtain the reliable mechanical properties for metal matrix composites and to propose a test standard to ISO, an international cooperative research for the round robin test (RRT) of mechanical properties for MMC has been continued in operation carried out since 1992. About eight organizations from United State of America, United

Kingdom, Germany, France, and Japan are involved in this technical working area of VAMAS Project.

Up to now a tensile test has been carried out for a SiC whisker reinforced aluminum alloy matrix composite (SiCw/Al) supplied from NASA and machined into testpieces by NRIM. Recommended test procedures include appropriate test-piece dimensions, testing rates, methods of gripping and strain measurement techniques. Methods for measuring Young's modulus, proportional limit, proof stress, tensile strength and elongation to failure at room and 200°C were also defined. Data obtained from RRT were analyzed and the tensile test method for MMC at room temperature will be proposed to ISO. The scatter and uncertainties in the modulus measurements at 200°C were lower than those measured from an earlier RRT at room temperature on the same material. The main reason for the variation in strength was the temperature profile and thermal history of the testpiece.

There are no standards for the fatigue testing of MMC, although a large number of different test methods and conditions have been reported. This makes accurate comparison of data and test methodology difficult. Titanium alloy matrix composite and SiCw/Al composite were tested for fatigue condition at room temperature and/or high temperature. The fatigue lives of the composites were dependent on the surfacing process of the test-piece. RRT will be started after the test conditions are decided.

**Keywords:** metal matrix composites, standardization of test method, tensile test, fatigue test, aluminum alloy matrix composite, titanium alloy matrix composite

#### 30 The Development of High Strength High Conductive Cu Base In-Situ Composite

*H.G. Suzuki, C. Masuda, E. Takakura, S. Sakai and S. Sun, Materials Processing Division*

[Sept 1998 to March 2000]

Cu base in-situ composites, Cu-15%Cr-X alloys, have been studied to increase the strength keeping the electrical conductivity high level. The X elements are Sn, Fe, Si. The combination of Fe-C and Fe-P was examined, but results were not successful because of the failure of melting practice. Main results are as follows.

1) The addition of 0.1 to 0.5wt% of Sn causes the retardation of recovery and recrystallization of

dislocation structures introduced by a heavy cold rolling and resulted in a banding structure. This effect leads to the increment of strength by about 100MPa compared with that of Cu-15%Cr. It is noted that Cr phase work-hardens in the early stage of cold rolling, but after  $\eta > 2$  work softening occurs. The aging treatment after cold rolling accelerates the precipitation hardening due to the Cr precipitation in Cu matrix and the recovery of electrical conductivity are remarkable. The addition of Sn appears to accelerate the precipitation of Cr in Cu matrix and does not precipitate itself.

2) The addition of 0.2 to 0.5% of Fe is not so effective to increase the strength, because 80% of Fe partitions to Cr phase and work-softens the Cr phase and also Fe lowers electrical conductivity. Additional studies on the elements such as Si and Ni are studying now.

**Keywords:** Cu alloy, high strength, electrical conductivity, cold rolling, composite

#### Recent Publications

- 1) H.G. Suzuki and D. Eylon: *J. Materials Sci. & Eng.*, A243 (1998), 126-133 "Hot ductility of titanium alloys"
- 2) Y. Jin, K. Adachi, T. Takeuchi and H.G. Suzuki: *J. Materials Science*, 33(1998), 1333-1341 "Aging characteristics of Cu-Cr in-situ composite"
- 3) Y. Jin, K. Adachi, T. Takeuchi and H.G. Suzuki: *Metall. Mater. Trans. A*, 29A(1998), 2195-2203 "Correlation between the cold working and aging treatments. in a Cu-15wt%Cr in situ composite"
- 4) H.G. Suzuki, T. Takeuchi, T. Mihara, K. Adachi, Y. Jin and S.T. Subokawa: in *Processing and Fabrication of Advanced Materials VII*, TMS(1998), 359-367 "Development of high strength high conductive copper base in-situ composites"
- 5) D.L. Zhang, K. Mihara, E. Takakura and H.G. Suzuki: *Mater. Sci. Eng.*, A266(1999), 99-108 "Effect of the amount of cold working on the ductility of a Cu-15%Cr-0.2%Ti in-situ composites"
- 6) K. Mihara, K. Adachi, S. Tsubokawa and H.G. Suzuki: *Proc. 4th Int. Conf. Recrystallization related phenomena*, ed by T. Sakai and H.G. Suzuki, (1999), 327-332 "Thermomechanical processing of high strength high conductive Cu base in-situ composites"

#### 31 Development of Brazing Technique for the Fabrication of Rocket Engine

*Ken Sasabe, Jeremy Paul Weston\*, Takayoshi Kasugai, Materials Processing Division*

*\* Frontier Research Center for Structural Materials, Joining and Interface Research Station [Oct. 1999~March 2001]*

A lot of parts of engines for the launching rocket of satellites are fabricated using brazing technique. Many quantities of brazed joints are exposed to the cryogenic hydrogen and to the high temperature combustion gas during running of rocket engine. By means of the marked temperature difference, large thermal strain is developed in joints very often. Such a radical condition for brazed joint can never be experienced in other cases without in the case of rocket engine, and the very high performance and the very high reliability are required for brazed joint of rocket engine.

The most important property of brazed joint of rocket engine is low cycle fatigue at high temperature induced by cyclic temperature change caused by the repetitions of running and stop of combustion. Therefore, the properties of low cycle fatigue of brazed joint at high temperature must be understood enough.

The design and fabrication of rocket engines are carried out under the evaluations owing to the combustion tests of the real models and the results based on the past flights, and the evaluations of joint properties under the operating conditions of rocket components has not been carried out enough.

On the other hand, mechanical properties of brazed joint, especially the properties under cyclic load, are dependent on stress and/or strain distributions of filler metal layer of joint. Therefore, it is not reasonable to evaluate mechanical properties of brazed joint using usual evaluation methods for homogeneous materials. The evaluation methods should reflect the behaviors of filler metal in joint under real operating conditions.

Furthermore, the analysis of mechanisms of low cycle fatigue of brazed joint is an unexplored academic field, and the approach to it is not known. From these viewpoints, we are carrying out the analyses of the elements to clarify the mechanisms of low cycle fatigue of brazed joint and the fundamental research to establish the evaluation methods of joint characteristics.

### 32 Preparation of Ionic Conductors by Pressurization

*H. Nakamura, Team of Director of Special Research*

[April 1998 to March 2002]

There have been many researches related to solid-state electrolytes consisting of oxide ceramics, some of which have been in practical use as an oxygen sensor. For the real-time measurements of the chemical species specific to a solid-state electrolytes, it is necessary to synthesize solid-state ionic conductors that show selectivity to individual species. Since many compounds that show selectivity to air pollutants decompose readily at elevated temperature, there has been little attempt of synthesizing complex compounds that can be used as an electrochemical sensor to air pollutants.

In this study, pressurized sintering was applied to prevent the decomposition of otherwise degradable compounds such as nitrates for the synthesis of solid state electrolytes. The technique made it possible us to create types of solid electrolytes derived from complex compounds that show ionic conductivity sufficient for the use as a sensor at relatively low temperature. The purpose of this study is to produce solid electrolytes for determining corrosive gases quantitatively.

**Keywords:** ionic conductor, solid-state electrolyte, charge carrier, electrical conductivity

### 33 High Temperature Materials 21 Project

*H. Harada, High Temperature Materials 21 Project*

[June 1999 to March 2004]

In June 1999, NRIM launched an R&D project, "High Temperature Materials 21 (HTM 21) Project", the Phase 1 (1999.6-2004.3), within a scheme of "Leading Programme for Independent Administrative Corporations". The budget is 314M. ¥ (about 3M.\$) / year.

In this Project we develop high temperature materials for advanced power engineering systems, including ultra-high efficiency (65%) gas turbines for power generations, advanced jet engines, high performance space rockets and so on.

Guided by knowledge obtained through materials design and experimental microstructural/deformation analysis researches, we develop Ni-base superalloys, ceramics(Si<sub>3</sub>N<sub>4</sub>), and refractory superalloy, which are the main three materials to start with in

this Project.

We have clear targets for developments; the temperature capability under 137MPa for 1000h creep rupture is to be 1100°C for Ni-base superalloys, 1500C for ceramics, and 1800°C for refractory superalloys. With Ni-base single crystal superalloys, we have reached up to 1075°C and the alloys, TMS-75 and TMS-82+, are now being tested in an industrial gas turbine generating power to Tokyo. With ceramics, Yb addition to crystallise grain boundaries has been found effective to improve the temperature capability. For refractory superalloys, Ir- and Rh-base refractory superalloys were invented by us and investigated extensively in terms of microstructure and mechanical properties up to 1800°C.

A wide range of materials design methods, including statistical thermodynamics, thermodynamics, and empirical approaches, are being investigated and applied to actual development of the materials. In-situ high temperature analysis methods are being developed. As an example, high temperature (1250°C) TEM observation of Ni-base superalloys has been successfully made and for the next step in-situ creep observation is scheduled. To enhance practical use of the new materials we develop a virtual gas turbine in computers to evaluate the materials performance and the gas turbine efficiency we can reach before actual gas turbine test.

We collaborate internationally with many research organisations and companies based on fifty-fifty contributions and co-ownership of the results. (see High Temperature Materials 21 Project in <http://www.nims.go.jp>)

**Keywords:** Ni-base superalloy, Ir/Rh-base Refractory Superalloys, Si<sub>3</sub>N<sub>4</sub>, Materials Design, Microstructure Analysis, Virtual Gas Turbine

### 34 Control of the In-plane Texture of High-Tc Superconducting Thin Films for Microwave Applications

*M. Fukutomi, K. Komori, K. Kawagishi and K. Togano, 1st Research Group*

[April 1998 to March 2001]

A near term application of high temperature superconducting (HTS) thin films is microwave devices such as resonators and filters, where large area, high quality films deposited onto technologically important substrates are required. The HTS thin films dealt with in this research falls into two categories: 1) YBCO thin films on lattice-mismatched substrates such as MgO, sapphire and silicon; and 2) YBCO thin films on substrates having

no template for epitaxial growth such as polycrystalline metal or ceramic substrates. In order to successfully obtain these films, in-plane misorientations, i.e., the high-angle tilt boundaries need to be kept to a minimum because they severely increase the microwave surface resistance  $R_s$  of the film. Therefore, the development of suitable buffer layers for epitaxial growth of HTS films is one of the main goals of our work. In the past years, efforts have been made to develop YBCO films with a fairly low  $R_s$  on polycrystalline copper substrates with a Cr/in-plane textured YSZ double buffer layer. An interesting potential application for this material is in the construction of rf resonant cavities for particle accelerators. As for the films of the first category, we have recently developed smooth and epitaxial YBCO films on large area (100)MgO(30x30mm<sup>2</sup>) substrates. The use of CeO<sub>2</sub>/YSZ(Y<sub>2</sub>O<sub>3</sub>-stabilized ZrO<sub>2</sub>) double buffer layers was found to greatly improve superconducting properties with high reproducibility. Preliminary results on  $R_s$  measurements indicate that YBCO films grown on CeO<sub>2</sub>/YSZ buffered MgO have apparently good microwave properties compared with those on bare MgO.

Part of this research has been performed in a collaboration with High Energy Accelerator Research Organization.

**Keywords:** YBCO thin film, buffer layer, in-plane texture, microwave surface resistance

#### Related Papers

1. J. Liu, K. Asano, E. Ezura, S. Inagaki, S. Isagawa, H. Nakanishi, M. Fukutomi, K. Komori, M. Saito, "Precise measurement of the microwave surface impedance of a YBa<sub>2</sub>Cu<sub>3</sub>O<sub>7-δ</sub> film on copper substrate" J.Appl.Phys.87 (2000)3912-3919
2. K. Kawagishi, K. Komori, M. Fukutomi, K. Togano, "Preparation of in-plane textured large-area YBCO films on (100)MgO with CeO<sub>2</sub>/YSZ buffer layers" (submitted to J. Supercond.)

#### 35 High-Resolution Real-Time Investigation on Defect Formation under Surface and Interface-reactions

*M. Kitajima, K. Ishioka, A. Nakamura(Itakura) and M. Hase, 2nd research Group  
T. Hirano, M. Demura and K. Kishida, Mechanical Property Division  
[April 1999 to March 2004]*

A control of reaction at the atomic level on the solid surface and/or film/substrate interface is essential for developing materials with higher quality and microscopic devices. This study is to elucidate kinetics and dynamics on reactions of ions, neutral atoms and plasmas with solid materials. There are two main targets in this study:

1) Using a pump/probe technique with ultrashort pulse laser, we are observing lattice vibrations in solids on a time scale of 10-100 fs. This gives us direct information to understand lattice dynamics for phonon-defect interactions and carrier excitations in damaged materials. The dephasing of the coherent phonons in bismuth due to the lattice defects has been successfully observed. Dynamics of non-equilibrium carriers and the phonon-plasmon interactions in defective semiconductor are also being discussed, based on the time-resolved reflectivity measurements.

2) We are also going to measure the mechanical properties of Ni<sub>3</sub>Al bicrystal specimens under an environment of hydrogen atoms, in order to examine the effect at interface defects induced by hydrogen atoms from viewpoint of kinetics. A method of highly-ductile Ni<sub>3</sub>Al thin foils at room temperature has been developed. For testing hydrogen embrittlement, the bicrystals having different  $\Sigma$ -values have been also fabricated, and the kinetic properties on the hydrogen embrittlement will be studied.

**Keywords:** defect, ultrashort pulse laser, coherent phonons, hydrogen

#### Related papers

"Dephasing of coherent phonons by lattice defects in bismuth films", M. Hase, K. Ishioka, M. Kitajima, K. Ushida and S. Hishita, Appl. Phys. Lett. 76, 1258(2000).

"Effect of lattice defects on LO phonon-plasmon coupled modes in n-GaAs", M. Hase, K. Ishioka, M. Kitajima and K. Ushida, ULTRAFAST PHENOMENA XII, 387 (2001).

"Fabrication of Ni<sub>3</sub>Al thin foils by cold rolling, submitted.

#### 36 Understanding and Improvement of Radiation-Induced Degradation in the Advanced Nuclear Materials

*J. Nagakawa, Y. Murase, N. Yamamoto, Y. Fukuzawa and K. Yagi, 2nd Research Group  
K. Fukutomi, 1st Research Group  
[April 1998 to March 2002]*

Changes in microstructure and degradation in mechanical properties induced by the irradiation with energetic particles are critically important for the structural materials of nuclear application. They significantly influence the endurance of structural components of nuclear reactors. In this research project, deformation and fracture of materials under irradiation are being studied experimentally and theoretically for the nuclear materials to be used in the advanced nuclear energy sources like the fusion reactors and the next-generation light water reactors. Emphasis is placed on the understanding of deformation and fracture properties of the advanced materials under irradiation, and also on the development of new methods to suppress the radiation-induced degradation.

Damage by energetic particles causes atomic displacements and introduces migrating point defects and stable defect agglomerates in the material. Migration of point defects, especially the interstitial atom that has a very strong strain field, is influenced by the external stress field and induces unique material degradation phenomena. One of the most important degradation for the nuclear reactor materials is the radiation-induced deformation. Very active plastic deformation is produced by the synergistic effect of migrating point defects and external stress even at rather low temperatures and stress levels<sup>1)</sup>.

It is, on the other hand, well known that a metal fatigue is one of the crucial mechanical properties those determine the life of structural components. We have revealed that the fatigue fracture is affected by the simultaneous irradiation in 316 stainless steel<sup>2)</sup>. Fatigue life under the irradiation with 17 MeV protons at 60 °C was larger than that of the unirradiated condition, and even that of the post-irradiation after the same amount of irradiation as the *in-situ* fatigue, in a load-controlled tensile-tensile fatigue testing of side-notched specimens. Investigation has been carried out to clarify whether the elongation of the fatigue life is caused by the irradiation hardening or by the dynamic effect of irradiation. Yield stress was measured as a function of irradiation up to that at the fracture of the *in-situ* irradiation fatigue, i.e. the pre-irradiation dosage of the post-irradiation testing. The increment of yield stress was roughly proportional to a square root of the number of atomic displacements, and the yield stress had been possibly increased by 25% prior to the post-irradiation testing from that for unirradiated specimens. During the *in-situ* irradiation, yield stress started from the original value and gradually reached to this pre-irradiation value at last on the point of fracture. The number of fatigue cycles to

initiate crack was also evaluated from the SEM analysis of the striation pattern on the fracture surface, which corresponds to the advance of fatigue crack at each cycle. It was found that both crack initiation and crack propagation were suppressed under *in-situ* irradiation. These two sets of experiments clearly indicate that the elongation of fatigue life under *in-situ* irradiation is not directly caused by the irradiation hardening, i.e. the interaction of stable defect clusters and moving dislocations. Rather, it appears to result mainly from the dynamic interaction of migrating point defects and dislocations, in other words, the dynamic effect of *in-situ* irradiation.

**Keywords:** radiation damage, point defects, deformation, fatigue

### Recent Publications

1. Theoretical and Experimental Study on the Significant Creep Deformation of SUS 316 Induced by Irradiation at 60 °C, J. Nagakawa, Y. Murase, N. Yamamoto and Y. Fukuzawa, Key Engineering Materials, 171-174 (2000), 313-320.
2. Creep-Fatigue Response of 20%CW 316 SS under Irradiation at 60C, Y. Murase, J. Nagakawa, N. Yamamoto and Y. Fukuzawa, Effect of Radiation on Materials, ASTM STP 1366, ASTM, (2000), pp.713-724.

### 37 Influence of Nuclear Transmutations on Low Activation Structural Materials for Fusion Reactor Application

N. Yamamoto, J. Nagakawa, Y. Murase and Y. Fukuzawa, 2nd Research Group  
[April 1996 to March 2001]

Radio-activation of materials has been recognized as one of the most crucial issues in the field of nuclear fusion technology from the viewpoint of waste management, environmental safety and public acceptance for the utilization of fusion power. The problem is much intensified for first wall/blanket structural materials used in a prototype reactor and the beyond, owing to large radiation doses of fusion neutrons. Because such heavy irradiation causes material deterioration in many cases, the development of radiation-resistant structural materials with low activation characteristics has been hence strongly demanded on the establishment of fusion reactors. In order to contribute such activities, we have investigated the

influence of nuclear transmutational elements on material integrity using accelerator irradiation technique with a primary concern on gaseous elements (helium and hydrogen) which are known to often induce severe grain boundary embrittlement.

The means of  $\alpha$ -particle irradiation with a cyclotron was employed for the purpose of simulating neutronic helium production in a fusion reactor. Using this method, creep test specimens of a representative low activation martensitic steel, F82H (Fe-8Cr-2W-0.2V-0.04Ta-0.1C), were irradiated with  $\alpha$ -beam at 823 K with a helium concentration of about 1000 appm. These temperature and helium content roughly correspond to the conditions specified in a typical DEMO reactor design. Creep tests were subsequently performed at the same temperature so as to obtain creep data up to 3.6 Ms. To clarify the effects of helium, unirradiated reference samples which underwent the same histories as those of helium implanted ones were similarly examined.

No meaningful degradation was detected in terms of the creep lifetime, and the stress dependence of creep rupture time was nearly the same between implanted samples and helium free controls. The elongation at rupture also seems to have been identical. The data of each set lay within a commonly acceptable error band regardless of the presence or the absence of helium. In addition, the fracture appearance remained perfectly transcrystalline and ductile even after such a large helium introduction, and there observed no indication of grain boundary separation caused by helium. These facts, which are well in agreement with the previous results on 100 and 300 appmHe implantations, imply that materials of this kind would have a promising potential to endure helium-induced mechanical deterioration for long time service in fusion environments.

**Keywords:** helium embrittlement, hydrogen embrittlement, ferritic steel, vanadium alloy

### Recent Publications

An Evaluation on Helium Embrittlement Resistance of Low Activation Ferritic/Martensitic Steel F82H, N. Yamamoto, J. Nagakawa and K. Shiba, *J. Nucl. Sci. Technol.* 36 (1999) 713-715.

Creep Rupture Properties of Helium Implanted Low Activation Martensitic Steel for Nuclear Fusion Application, N. Yamamoto, J. Nagakawa and K. Shiba, *Key Engrg. Mater.* 171-174 (2000) 115-120.

Effects of Helium Implantation on Creep Rupture Properties of Low Activation Ferritic Steel

F82H IEA Heat, N. Yamamoto, J. Nagakawa and K. Shiba, *J. Nucl. Mater.* 283-287 (2000) 400-403.

Creep Behavior of 8Cr2WVTa Martensitic Steel Designed for Fusion DEMO Reactor -An Assessment on Helium Embrittlement Resistance-, N. Yamamoto, Y. Murase, J. Nagakawa and K. Shiba (submitted to *Int. J. of JSME*)

### 38 Isotope Separation and Its Application to Materials

*T. Noda\*1, H. Suzuki\*2, H. Araki\*2, K. Yagi\*2, M. Fujita\*3 T. Hirano\*3 and F. Abe\*4*

*\*1: High Resolution Beam Station*

*\*2: Nuclear Materials Group*

*\*3: Mechanical Properties Department*

*\*4: Strength and Life Evaluation Research Materials Evaluation Station*

[April 1997 to March 2002]

### 1. Introduction

Materials composed of isotopically selected elements realize the essential solution of subjects such as induced activity, He embrittlement, and compositional change caused by reactions with energetic particles. Moreover, the isotopically controlled materials have been pointed out to improve various physical properties of crystallines.

The objectives of the program are (1) to develop CO<sub>2</sub> laser with oxygen isotope, which expands the infrared wavenumber region of the laser emission and to search infrared laser with a wide range of wavenumber, (2) to synthesis isotopically controlled materials such as silicon and boron compounds, and (3) to utilize isotopes by transmutation, including simulation studies.

### 2. Main Results

2.1 Development of isotopically controlled laser and searching infrared laser with a wide range of wavenumber

Usual pulse CO<sub>2</sub> laser is limited in emission of wavenumber as 931-956cm<sup>-1</sup>, 966-983cm<sup>-1</sup>, 1033-1057cm<sup>-1</sup> and 1069-1085cm<sup>-1</sup>. If <sup>12</sup>C or <sup>16</sup>O is replaced by the other isotope such as <sup>13</sup>C or <sup>18</sup>O, then new emission lines appear due to the different stretching and bending modes of isotopic CO<sub>2</sub> from those of usual CO<sub>2</sub> gas.

In order to achieve the isotope laser, a closed-cycle CO<sub>2</sub> laser system is examined. It is necessary to use isotope CO<sub>2</sub> effectively because of its high cost. When the laser is emitted by discharge, isotope CO<sub>2</sub> is consumed with the reaction as



Then the catalyzer composed of CuO is installed in the circulation system to recombine CO and O<sub>2</sub>

to return CO<sub>2</sub>. The system was operated with a mixture gas of CO, CO<sub>2</sub>, N<sub>2</sub> and He where the ratio of <sup>16</sup>O and <sup>18</sup>O is 1:1 in volume. Odd lines of P17 and P19 which were not available for natural gas, were first observed.

Free Electron Laser (FEL) is also examined to be used as the other laser covering a wide wavenumber region. The one which is available in the infrared wavenumber region and has a considerable high power is the FELIX of the FOM in the Netherland. The FELIX emits the infrared laser at 5-30 μm(333-2000cm<sup>-1</sup>) and at 5MW. The use of this laser also is being examined under the cooperation with the FOM institute and Los Alamos National Laboratory. The enrichment of silicon isotopes in the SiF<sub>4</sub> formed and residual Si<sub>2</sub>F<sub>6</sub> was observed in 10, 12 and 25 μm absorption bands.

## 2.2 Synthesis of isotope silicon films and growth of isotope single crystals

It is necessary to take out silicon metal from isotopically concentrated SiF<sub>4</sub> or Si<sub>2</sub>F<sub>6</sub> gas to examine various physical properties of isotopically controlled silicon and its compounds. Silicon flake was deposited by a plasma CVD method. Natural SiF<sub>4</sub> gas was used to find the optimum condition of Si film formation prior to isotopically enriched gases. Microwave of 2.45GHz with a power of 8.4x10<sup>-4</sup>Wm<sup>-2</sup> was applied to the gas at 13.3Pa-266Pa at a flow rate of 30-500SCCM. Ar and H<sub>2</sub> are added as a plasma assisting and scavenging gases, respectively. The substrate temperature was kept at 523-873K. The films formed were examined with SEM, XRD and weighed for measuring formation rates. It is found that polycrystalline Si films were formed in the present experimental temperature range. That is, silicon can be produced through the decomposition reactions of fluoro-silane gases by the plasma CVD. The optimum temperature to obtain silicon films with a high efficiency was 623-723K. The maximum conversion efficiency from fluoro-silane to silicon metal was 28%.

Natural boron is composed of <sup>10</sup>B of 19.9% and <sup>11</sup>B of 80.1%. Since relative mass difference between <sup>10</sup>B and <sup>11</sup>B is very large, mass effect on physical properties of boron is expected. In the present study, single crystalline isotope boron was tried to be prepared using zone melting technique. The starting materials were 99.5%<sup>10</sup>B and 99%<sup>11</sup>B powders. After isostatically pressed to a cylindrical shape under hydrostatic pressure of 2000kgW/cm<sup>2</sup>, the isotopic boron powders were sintered in a vacuum at 1873K. The sintered rod was then zone melted on the seed crystal under flowing Ar gas.

Finally isotope boron single crystals with a size of 10mm φx40mm could be formed. The observa-

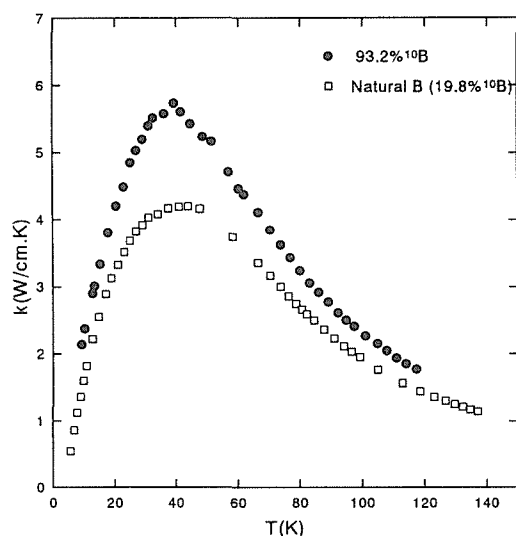


Fig.1 Thermal conductivity of  $\beta$ -Boron single crystals with a natural isotope abundance and 93%<sup>10</sup>B.

tion of the cross section of the crystals indicated a smooth surface and the growth direction was identified to be <100> by X-ray Laue back reflection analysis.

The boron single crystals prepared are 93.2%<sup>10</sup>B, 99%<sup>11</sup>B and natural boron (19.9%<sup>10</sup>B and 80.1%<sup>11</sup>B). Physical properties such as lattice constant, thermal diffusivity, and heat capacity for boron single crystals are being measured.

Fig.1 shows the temperature dependence of thermal conductivity of natural boron and <sup>10</sup>B. The boron with single isotope clearly improved the thermal conductivity.

## 2.3 Utilization of isotopes by transmutation

The simulation code, IRAC, calculating transmutation was improved by combining with a neutron transport calculation code and introducing multi-step reactions to predict more precisely the transmutation of materials including isotopically controlled materials. FENDL2.1 was introduced as a newest nuclear data file covering both stable and unstable nuclides for various nuclear reactions. Using the improved calculation code, synthesis of new materials through the transmutation and annihilation of radioactive nuclides with a long half-life are being examined.

SiC has excellent nuclear properties and has been considered as a structural material of fusion reactors. Since SiC itself is intrinsically brittle, SiC composites with a high purity and favorable mechanical properties are being developed using chemical vapor infiltration process.

**Keywords:** isotopically controlled materials, isotope separation, free electron laser, silicon, boron, chemical vapor infiltration, silicon carbide, transmu-

tation

### Related papers

- 1) N. Nogi, T. Hirano, K. Honda, S. Tanaka and T. Noda: Preparation of the isotopically controlled  $\beta$ -B105 single crystals by the FZ technique, *J. Surface Analysis*, 3, (1998) 280-283.
- 2) H. Suzuki, Y. Takeuchi, S. Ito, I. Shiota, T. Noda: On-line formation of isotopically controlled Si films from fluoro-silane, *J. Surface Analysis*, 3, (1998) 372-376.
- 3) T. Noda, H. Suzuki and H. Araki: Silicon Isotope Enrichment for Low Activation, *Fusion Eng. & Design*, 41, (1998) 173-179.
- 4) J.L. Lyman, B. Newnam, T. Noda and H. Suzuki: Enrichment of Silicon Isotopes with Infrared Free-Electron Laser Irradiation, *J. Physical Chemistry A*, 103, (1998) 4227-4232.
- 5) N. Nogi, S. Tanaka, T. Noda and T. Hirata: Infrared-active A<sub>2u</sub> and E<sub>u</sub> modes in isotopically enriched  $\beta$  rhombohedral boron, *Solid State Communication*, 111, (1998) 447-451.
- 6) T. Noda, H. Suzuki and N. Nogi: Prospect of Isotope Controlled Materials, *Bulletin of ISIJ*, 3, (1998) 23.
- 7) N. Nogi, T. Numazawa, S. Tanaka and T. Noda: Thermal conductivity of isotopically enriched  $\beta$  rhombohedral boron, *Mater. Trans. JIM*, 40, (1999) 950-952.

### 39 Development of Light Weight High Strength Ti<sub>2</sub>AlNb Titanium Intermetallic Alloy

*M. Hagiwara, Third Research Group*

[April 1999 to March 2003]

The ordered orthorhombic Ti<sub>2</sub>AlNb (O phase)-based titanium intermetallic alloys are considered as potential materials for aircraft engine applications due to their higher room temperature strength, ductility and fracture toughness than conventional Ti<sub>3</sub>Al( $\alpha_2$ ) and TiAl( $\gamma$ ) alloys. Among various O phase-based alloys, two phase O+B2 (ordered bcc phase) alloy such as Ti-22Al-27Nb is said to have the best balance of tensile, creep and fracture toughness. One main drawback of these O phase-based alloys is that the service temperature is limited to 750 °C due to a degradation of tensile strength, creep resistance, thermal stability and environmental resistance. Moreover, they exhibit lower elastic modulus and higher density compared to those for  $\alpha_2$  and  $\gamma$  alloys.

The objective of the present research project is to develop advanced light weight high strength O

phase-based alloys having superior combinations of mechanical properties in the temperature range up to 1,000 °C.

So far, a systematic study was conducted to improve room and high temperature mechanical properties of O phase-based alloys by microstructural and compositional modifications, and the homogeneous dispersion of fine ceramic particulate such as TiB.

The spherical  $\alpha_2$  particles which were formed during the hot rolling in the ( $\alpha_2$  +B2) two phase region just below the B2 transus temperature were found to be very stable when the hot-rolled material was reheated in the B2 single phase region, and therefore relatively small prior B2 grains ranging from 50  $\mu$ m to 80  $\mu$ m in diameter were obtained by the pinning effect of these undissolved  $\alpha_2$  particles. This fine-grained microstructure showed an excellent combination of room temperature tensile strength and ductility. For example, room temperature tensile elongation of 7 % and tensile strength of 1,371MPa were obtained for a Ti-22Al-27Nb alloy.

The transition metal elements such as Mo, W and V were substituted for a portion of Nb in a Ti-22Al-27Nb alloy. The substitution was made so that the  $\beta$  phase stability in the modified alloy is equal to that in Ti-22Al-27Nb. It was found that the substitution of 2 %W for 7 %Nb (Namely Ti-22Al-20Nb-2W) was quite effective in increasing the tensile strength at temperatures above 923 K and reducing the steady state creep rate and primary creep strain.

In order to further improve the high temperature mechanical properties of orthorhombic alloys, TiB-reinforced particulates composites were produced using the gas atomization P/M method. The dispersion of TiB was very fine (less than 2  $\mu$ m in diameter) and uniform. The high temperature tensile strength, creep and Young's modulus of the composites were found to be superior than those of the corresponding unreinforced matrix alloy.

**Keywords:** titanium intermetallics, particulate composites, powder metallurgy, microstructure, mechanical properties

### Related Papers

1. Microstructures and Mechanical Properties of Blended Elemental Powder Metallurgy Ti<sub>2</sub>AlNb Intermetallics, S. Emura, J.H. Liu, M. Hagiwara, Y. Kawabe and A. Okada, *Titanium '95* edited by P.A.Blenkinsop, W.J.Evans and H.M.Flower, The Institute of Materials, (1996): 404-410

2. Modulated Microstructure in Ti-22Al-11Nb-4Mo Alloy, F. Tang, S. Emura and M. hagiwara, *Scripta Materialia*, 40(1999):471-476
3. Reinforcing effect of in situ grown TiB whiskers on Ti-22Al-11Nb-4Mo alloy, F. Tang, S. Emura and M. hagiwara, *Scripta Materialia*, 43(2000):573-578
4. Tensile properties of tungsten-modified orthorhombic Ti-22Al-20Nb-2W alloy, F. Tang, S. Emura and M. hagiwara, *Scripta Materialia*, 44(2001):671-676
5. Creep behavior of tungsten-modified orthorhombic Ti-22Al-20Nb-2W alloy, F. Tang, S. Emura and M. hagiwara, *Scripta Materialia* 43(2000):1065-1070

#### 40 Improvement of Thermal and Mechanical Properties of L<sub>12</sub>-type titanium trialuminide

*K. Hashimoto, K. Kasahara, E. Abe, T. Kimura, M. Nakamura, Y. Yamamoto, 3rd Research Group*  
[1997~2000]

##### Introduction

L<sub>12</sub>-type titanium trialuminides, (AlM)<sub>3</sub>Ti modified from DO<sub>22</sub>-type Al<sub>3</sub>Ti by alloying of transition metals, M are interesting materials for engineering applications because they are very light and oxidation resistant, and show good strength up to fairly high temperatures. However application is limited by their brittleness. Much work relating to microalloying and microstructural modification has been carried out on the ductility improvement of the trialuminides. Unfortunately, these studies have not yet accomplished the satisfactory tensile elongation more than 1%, while they recognized that the ductility depended on the amount and kind of the alloying elements, M and/or additive quaternary elements.

Recently, it has been confirmed in our laboratory that ductility of intermetallic compounds exhibits a positive linear relationship with the residual strain, which is obtained by peak profile analysis from the X-ray diffraction of powder specimen after milling of the intermetallic alloy. Since the X-ray diffraction analysis and the preparation of the powder specimen of the intermetallic alloy are so easy that ductility evaluations of many intermetallic alloys are carried out with lower cost, smaller labor, and shorter time compared with mechanical testing, i.e., bending or tensile testing.

Thus, by applying the relation between the residual strain and the ductility to the titanium trialuminides of (AlM)<sub>3</sub>Ti alloys with Cr or Mn as a

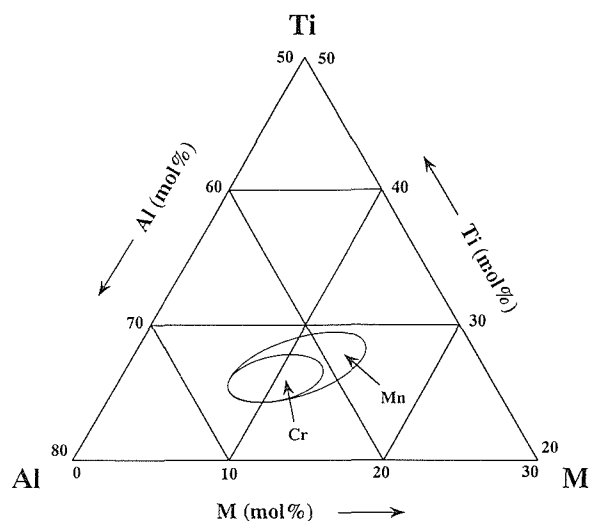


Fig.1 Single-phase regions of the L<sub>12</sub>-type titanium trialuminide in ternary Al-Ti-Mn and Al-Ti-Cr systems at 1450K. Small ellipse; (AlCr)<sub>3</sub>Ti single-phase region, Large ellipse; (AlMn)<sub>3</sub>Ti single-phase region

ternary element, M, the screening of alloy compositions which may exhibit good ductility has been performed and then the tensile elongation has been estimated by three-point bending test for the alloys with the selected compositions.

##### Composition screening

Firstly, to change widely the compositions of the (AlMn)<sub>3</sub>Ti or (AlCr)<sub>3</sub>Ti single-phase alloy, the L<sub>12</sub>-type titanium trialuminide single-phase region at 1450K has been determined by EPMA and X-ray diffraction analysis for many alloys heat-treated at 1450K for 24h. Thus, the L<sub>12</sub>-type titanium trialuminide single-phase regions at 1450K are confirmed to be large and small ellipses in Figure 1 for the Al-Ti-Mn and Al-Ti-Cr ternary systems, respectively<sup>[1][2]</sup>. For the Al-Ti-Mn-V and Al-Ti-Cr-V quaternary systems, the L<sub>12</sub>-type titanium trialuminide single-phase regions at 1450K has been also determined by changing the amount of V up to 12 mol% with holding the constant content ratio of Al:Ti:Mn or Al:Ti:Cr in the ternary alloys. The results obtained are shown in Figures 2(a) and (b)<sup>[1][2]</sup>. The maximum solubilities of V in Al-Ti-Mn-V and Al-Ti-Cr-V systems were determined to be 9mol% and 5mol%, respectively.

Secondly, the effects of Cr or Mn as a ternary element, M on the residual strain of (AlM)<sub>3</sub>Ti single-phase alloys which were selected based on Figure 1 have been examined using powdered specimens. The results obtained are summarized in Figure 3<sup>[3][4]</sup>. In both of the Al-Ti-Cr and Al-Ti-Mn ternary systems, relatively large residual strains are observed at alloy compositions of about 25mol% Ti contents with relatively higher Cr or Mn contents in the L<sub>12</sub>-single phase regions in each ter-

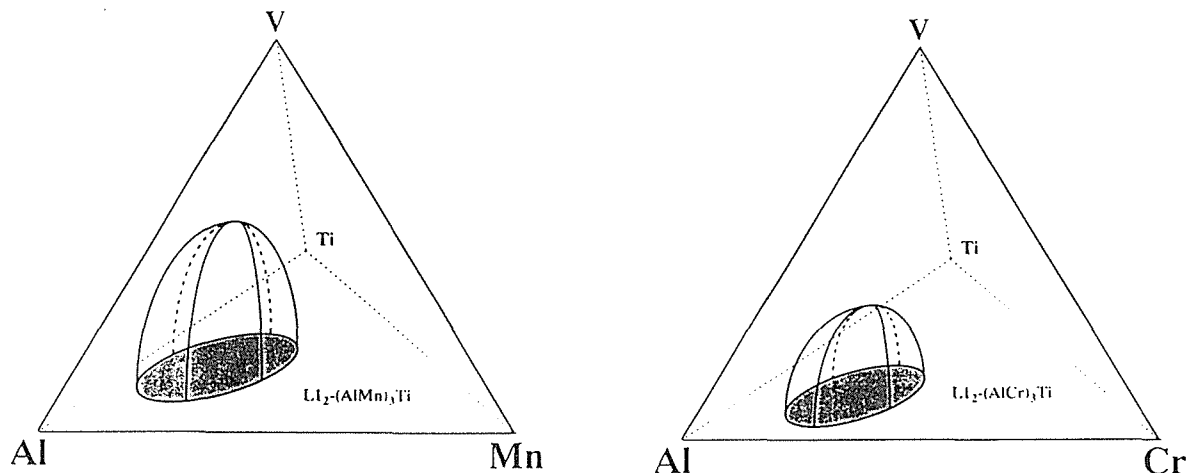


Fig.2 Single-phase regions of the  $L_{12}$ -type titanium trialuminide in quaternary Al-Ti-Mn-V and Al-Ti-Cr-V systems at 1450K. The maximum solubility of vanadium in the regions in quaternary Al-Ti-Mn-V and Al-Ti-Cr-V systems is 9 and 5 mol%, respectively.

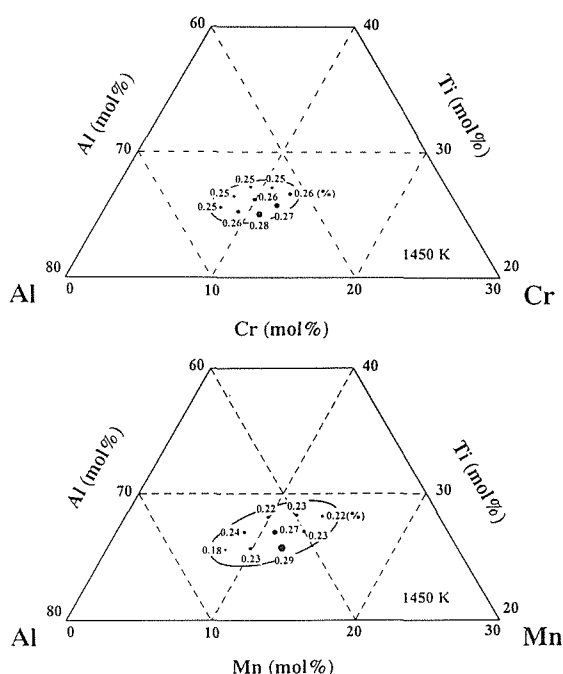


Fig.3 Composition dependence of the residual strains for ternary Al-Ti-Mn and Al-Ti-Cr Alloys. The larger residual strains are observed at composition with lower Ti content and with relatively higher ternary element content. The maximum value was obtained for the alloy with manganese.

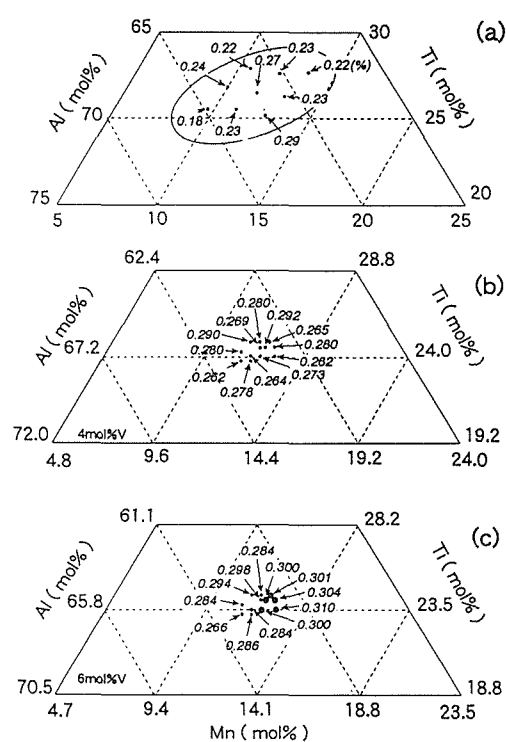


Fig.4 Residual strains of the  $L_{12}$ -single phase alloys in the quaternary Al-Ti-Mn-V system. (a) ternary alloys, (b) alloys with 4 mol% vanadium, and (c) alloys with 6 mol% vanadium.

nary system. The maximum residual strain was obtained from Mn ternary system. By the similar way, the effect of V as a quaternary element on the residual strain of  $(AlMn)_3Ti$  alloys with several compositions, which exhibited relatively large residual strain in Fig.3(a), has been examined. The representative results obtained are shown in Figure 4<sup>[4]</sup>. The addition of 6mol% vanadium shows relatively larger residual strain among those alloys with the addition of vanadium of 4 -7 mol%.

#### Effect of microstructure on the room temperature ductility and thermal properties

Bending tests and microstructure analysis have been performed for the alloys, which have rela-

tively large residual strain. Actually, the maximum bend strain at room temperature was obtained for the alloy having the largest residual strain and its elongation of 0.8% exceeded well the strain reported in the previous papers regarding to the  $L_{12}$ -type titanium trialuminide alloys. On the other hand, it is confirmed from this experiment that the residual strain is a necessary condition, but it is not a sufficient condition for the good ductility of the  $L_{12}$ -type titanium trialuminide alloys. Based on this result, further precise composition screening has been carried out in the vicinity of the maximum ductility alloy composition including reconfirmation of the vanadium content. One of the

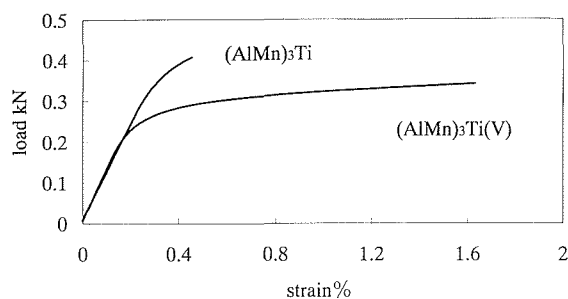


Fig.5 Load-strain curves at room temperature for alloys with and without vanadium addition.

results is shown in Figure 5. The load-strain curve exhibits about 1.5% elongation and softening due to vanadium addition.

For the alloy having 1.5% elongation, oxidation resistance and thermal shock resistance have been examined by mass gain measurement at 1273K for up to 100h in air and by Ar-arc remelting in a water-cooled Cu crucible, respectively. The good oxidation resistance comparable with Al<sub>3</sub>Ti and the good thermal shock resistance which did not exhibit any crack during remelting have been confirmed.

#### Conclusion

This paper describes a development process of an L1<sub>2</sub>-type titanium trialuminide alloy with good ductility and thermal properties. The results obtained are as follows.

The L1<sub>2</sub>-single phase regions in the ternary Al-Ti-Mn and Al-Ti-Cr systems and in the quaternary Al-Ti-Mn-V and Al-Ti-Cr-V at 1450K were confirmed by experimental methods. Screening of appropriate alloy composition for good ductility was performed by using the positive relation between ductility and residual strain obtained from X-ray diffraction measurement. After screening of the alloy composition, the room temperature ductility of the alloys was determined by bending test. The maximum bend strain of 1.5% was obtained for the quaternary Al-Ti-Mn-V alloy containing about 2 mol%V. The alloy also exhibited good oxidation resistance and thermal shock resistance.

**Keywords:** Intermetallic compound, L1<sub>2</sub>-type titanium trialuminide, Room temperature ductility, Aluminum-titanium-manganese ternary system, Aluminum-titanium-manganese-vanadium quaternary system, Oxidation resistance, Thermal shock resistance

#### Reference

1. Y. Yamamoto, H. Hashimoto, T. Kimura, H. Moriya, M. Nobuki and N. Kohno: J.Japan

Inst.Metals, 62,1998,pp.844-852.

2. H. Moriya, Y. Yamamoto, H. Hashimoto, T. Kimura and N. Kohno: J.Japan Inst.Metals, fall meeting proceeding, 1997,p.386
3. Y. Yamamoto, H. Hashimoto, T. Kimura, M. Nakamura and N. Kohno: J.Japan Inst.Metals, 64, 2000, pp.327-330.
4. K. Hashimoto, Y. Yamamoto, T. Kimura, M. Nobuki: Materials Trans., JIM, 40, 1999, pp.400-403.

41 Functions of hydrogen in environmental degradation of structural materials (Environmental embrittlement behavior and hydride formation of intermetallic compounds)

*Morihiko Nakamura, 3rd Research Group*  
[1998 ~ 2000]

TiAl based intermetallic alloys have attractive high temperature characteristics like high strength, high elastic moduli and relatively good oxidation resistance, and they are expected to be used for high temperature applications such as airplane and rocket engine components as well as automobile engine systems. In particular, the development of hydrogen propulsion systems is expected for aerospace vehicles in the near future. This means that the alloys will be exposed to severe environments, which can be hydrogen ranging from liquid hydrogen to high-temperature gaseous hydrogen, and then it is required to examine the degradation of the alloys exposed to a high temperature hydrogen gas and to study the suppression of the degradation. Meanwhile, TiAl based alloys are known to exhibit environmental embrittlement in laboratory air at room temperature, which is one of the reasons why they exhibit poor room temperature ductility in air, although their ductility is affected by microstructure and alloy composition. The environmental embrittlement in air is considered to be the embrittlement which is caused by hydrogen generated through reaction of moisture in air with the alloy surface. Thus it is required to study the mechanical properties of TiAl based alloys in a gaseous hydrogen atmosphere in a wide temperature region. When the alloys are exposed to a high temperature hydrogen gas, a large amount of hydrogen permeates into the alloys and may cause hydride formation, hydrogen-induced microstructure change, etc. These changes may result in embrittlement of the alloys.

The purpose of this work is to clarify the microstructure change like formation of hydrides and embrittlement behavior for TiAl base alloys which

are exposed to hydrogen environments, and to discuss the relationship between them.

1. Tensile properties of TiAl based alloys exposed to a high temperature hydrogen gas

Ti-49at%Al was prepared by vacuum arc melting, hot-isostatic-pressed at 1473 K under an argon atmosphere of 120 MPa, and homogenized at 1473 K for 24 h, followed by isothermal forging at 1473 K to a thickness reduction of about 80%. Tensile specimens with a gauge section of  $15 \times 4 \times 1.5$  mm were cut from the forged ingot, and annealed at 1423 K for 4 h or at 1573 K for 2 h in an argon gas, followed by cooling in the argon gas. Then, all the specimens were electro-polished. These heat treatments resulted in the equiaxed grained  $\gamma$  single phase structure and the dual phase structure (the equiaxed  $\gamma$  grains with the laths consisting of fine  $\gamma/\alpha_2$  lamellae), respectively.

Before tensile testing, some of the specimens were exposed to a flowing hydrogen gas of 0.1 MPa at 1073 K for 3 h, followed by furnace-cooling in the flowing hydrogen gas. Tensile tests were carried out at a strain rate of  $2 \times 10^{-4}$  s<sup>-1</sup> in vacuum (better than  $2 \times 10^{-5}$  torr). The test temperature was room temperature, 473 K and 573 K. The hydrogen content in the exposed specimens was evaluated from weight change before and after thermal desorption analysis.

The embrittlement caused by exposure to a high temperature hydrogen gas was affected by the microstructure of the Ti-49at%Al, and the dual phase specimens exhibited less embrittlement than the single phase ones. That is, the dual phase specimens contained a larger amount of hydrogen (about 340 wppm) than the single phase ones (about 250 wppm), when they were exposed to hydrogen in the same condition. However, the former exhibited relatively good elongation of 1.5% to 2% in vacuum at temperatures from room temperature to 573 K, while the latter exhibited no elongation, and fractured below the 0.2% offset stress. The fracture surfaces of the dual phase specimens were scarcely different from those of the single phase ones, and exhibited transgranular cleavage fracture with a small amount of intergranular facets. The increase in 0.2% offset stress and work hardening rate were observed for the dual phase specimens. No hydrides were observed by optical microscopy, transmission electron microscopy and x-ray diffractometry for the hydrogen-exposed specimens of both the dual phase structure and the single phase. Thus, the change of the tensile properties with exposure to the high temperature hydrogen was considered to result from not hydrides but solute hydrogen.

2. Microstructure change with Ti-49at%Al exposed to a high temperature hydrogen gas

The microstructure of Ti-49at%Al with the dual phase structure was investigated using high-resolution transmission electron microscopy (HREM). The dual phase specimens cut from the forged Ti-49at%Al ingot were exposed to a high temperature hydrogen gas in the same condition as mentioned above. In the single  $\gamma$  phase specimens, no change of the microstructure with the hydrogen exposure was observed by TEM. So, only the dual phase specimens were observed in detail using HREM. The results obtained are as follows.

- 1) No hydride was observed in the matrix  $\gamma$  phase of the dual phase specimen.
- 2) No hydride was also observed in the  $\alpha_2$  phase of the laths composed of the fine  $\gamma/\alpha_2$  lamellae.
- 3) Amorphous regions were observed along the fine  $\gamma/\alpha_2$  lamellar interfaces, and the chemical composition of the amorphous region is approximately equal to that of the  $\alpha_2$  phase and is much different from that of the  $\gamma$  phase. Thus, the amorphous regions were considered to form in the  $\alpha_2$  phase along the interfaces.
- 4) The amorphous regions formed in the Ti-Al-H system, when the hydrogen content was high, because the regions were existent along the  $\gamma/\alpha_2$  interfaces, which might be the paths of hydrogen flow in the dual phase specimen. The amorphous regions changed to the nanocrystalline  $\alpha_2$  phase regions when the specimen was heated in the TEM.

#### Related papers

- 1) M. Nakamura and T. Kumagai, "Environmental Embrittlement Caused by Hydrogen for Intermetallic Compounds: Preliminary Model of Ductility", *Met. Mater. Trans. A*, 30A, (1999) 3089-3107.
- 2) K.W. Gao and M. Nakamura, "Microstructures and hydrogen embrittlement of Ti-49Al alloy", *Intermetallics*, 8, (2000) 595-597.
- 3) E. Abe, K.W. Gao and M. Nakamura, "Local amorphization in hydrogen-charged two-phase TiAl alloy", *Scripta Mater.*, 42 (2000), 1113-1118.
- 4) K.W. Gao and M. Nakamura, "Effect of hydrogen on tensile properties of Ti-49Alat%Al alloy", *Scripta Mater.*, 43 (2000) 135-140.

*K. Inoue, Y. Yoshida, Y. Iijima and A. Kikuchi, 4th Research Group*

[April 1997 to March 2002]

Because the stored energy density of SMES (Superconducting Magnetic Energy Storage) is increased rapidly with increasing the magnetic field, the increase of the operation field make the fabrication of micro-SMES (compact SMES) possible. The operation field is determined mainly by the  $J_c$ -B properties of superconducting wire used for SMES. There are two kinds of commercialized superconducting wires; Nb-Ti wires for low fields and Nb<sub>3</sub>Sn wires for high fields. Although Nb<sub>3</sub>Al, Nb<sub>3</sub>Ge, Nb<sub>3</sub>Ga, Ni-2212, and Bi-2223 have not yet been commercialized, they are the most promising candidate superconducting materials for increasing the operation field of SMES because of their large potentialities due to higher  $H_{c2}$ (4.2 K)'s than that of Nb<sub>3</sub>Sn. Recently we found that the Nb<sub>3</sub>Al multifilamentary wire, fabricated through the rapid-heat, quench, and transformation (RHQT) process, showed not only 2-5 times larger  $J_c$  in high fields than that of the commercialized Nb<sub>3</sub>Sn multifilamentary wire but also excellent strain tolerances. The large  $J_c$  in high fields and the excellent strain tolerance are the most required properties for the superconductor used for the micro-SMES. In this study we are investigating the coil fabrication technique, stabilization, and improvements of superconducting properties for the Nb<sub>3</sub>Al multifilamentary wire and other high-field superconductors. Superconducting current lead and superconducting magnetic shield are also being studied as the basic technologies for the micro-SMES.

We studied the Ge addition to the Nb<sub>3</sub>Al multifilamentary wire, which improved remarkably not only  $T_c$  from 17.9 K to 19.4 K, but also  $H_{c2}$ (4.2 K) from 26.2 T to 40 T, but drastically reduced  $J_c$ (4.2 K) in fiscal 1998. In fiscal 1999, we succeeded in drastic improvement of  $J_c$  with Al-Ge core reduction to 0.3  $\mu\text{m}$ .  $J_c$ (25 T, 4.2 K) of 150 A/mm<sup>2</sup> was obtained for the Nb<sub>3</sub>(Al, Ge) multifilamentary wire. According to the transmission microscope observations the filament included Nb<sub>3</sub>(Al, Ge) phase, Nb<sub>2</sub>Al phase, Nb<sub>5</sub>Ge<sub>3</sub> phase, and remaining Nb phase. With decreasing the Al-Ge core size, the volume fraction of superconducting Nb<sub>3</sub>(Al, Ge) phase increased, which caused the drastic improvement of  $J_c$ . However, the Nb<sub>3</sub>(Al, Ge) volume fraction were still much smaller than 50 % for the wire with 0.5  $\mu\text{m}$  core. Therefore the intrinsic  $J_c$  of Nb<sub>3</sub>(Al, Ge) filament are 2-3

times larger than the obtained  $J_c$ . The additional effects of Ge to the Nb<sub>3</sub>Al wire should be studied in more detail.

For stabilizing the superconductivity of Nb<sub>3</sub>Al wire, we studied pure-Cu coating on the wire. At first we tried Cu-electroplating on the Nb<sub>3</sub>Al wire rapidly-heated/quenched. However, the firm Nb oxide layer on the Nb surface, which has large electrical resistance and thermal one, prevent the stabilization of the Nb<sub>3</sub>Al wire. Therefore we studied Cu-ion plating on the Nb<sub>3</sub>Al wire in the next step. We found that the Cu-ion plating with thicker than 1  $\mu\text{m}$  in thickness removed the Nb oxide layer efficaciously, and prevented the reformation of oxide layer on the Nb surface. We found that Cu-electroplating after Cu-ion plating on the Nb<sub>3</sub>Al wires stabilized their superconductivity remarkably.

In collaboration with Nippon Keiki Works, Ltd. and Mitsui Mining & Smelting, Co. Ltd., we fabricated a large-scaled superconducting Bi-2223 magnetic shield through plasma spraying. In a large zero-field chamber surrounded by the magnetic shield, we have succeeded in measuring the magnetic pulsed fields caused by human brain activities in fiscal 1998. In fiscal 1999, we studied the Bi-2223 formation mechanism during the heat treatment on the as-sprayed layer. As sprayed layer was composed of amorphous phase, which is transformed rapidly to Bi-2212 phase, 3-5 Cu phase, and 2-1 Pb phase. Bi-2223 phase were formed gradually by the reaction among Bi-2212, 3-5 Cu, and 2-1 Pb at about 838 °C.

The current lead, transporting current from an ac-dc converter at room temperature to a superconducting magnet at cryogenic temperature in the SMES, must be high conductive for current, and low conductive for heat. In many oxide superconductors, Y-123 film is the most promising material for the current lead in SMES, because of its high  $J_c$ (77 K) in high fields. However, only Y-123 films with good alignment in crystal orientations show high  $J_c$ . We studied on the fabrication process of Ni substrates with 2-axis alignments for using them the substrates of Y-123 films in fiscal 1998. In fiscal 1999, we tried to fabricate Y-123 films with good 2-axis alignments by electron-beam evaporation. As a buffer layer, we used an Y<sub>2</sub>O<sub>3</sub> layer between the Ni-substrate and the Y-123. We selected simple mono-layer as the buffer layer in order to reduce the fabrication cost.

**Keywords:** Nb<sub>3</sub>Al, Bi-2223, Rapid-Heat, Quench, Transformation,  $J_c$ , Superconducting Shield, Current Lead

Magnetic Shielding Properties of Bi-2223 Superconducting Hollow Cylinder Made through Plasma Spraying Process, Y. Yoshida, K. Inoue, Y. Kamekawa, K. Nakayama, K. Hoshino, A. Koike and E. Sudou, *Cryogenic Engineering* (in Japanese), Vol. 33 (1998): 60-67.

Nb<sub>3</sub>(Al, Ge) Multifilamentary Conductor Fabricated by Continuous Rapid-Heating/Quenching Process, Y. Iijima, K. Inoue, M. Kosuge and T. Takeuchi, *Proc. of MT-15* (1998): 1040-1043.

New Nb<sub>3</sub>Al Multifilamentary Conductor and Its Application to High Field Superconducting Magnet, K. Inoue, Y. Iijima, T. Takeuchi, T. Kobayashi, K. Fukuda, K. Nakagawa, G. Iwaki and H. Moriai, *Physica B*, Vol.246&247 (1988): 364-367.

Structure and Irreversibility Field of Tl-1223 phase Synthesized through the Substitution of TlF for Tl<sub>2</sub>O<sub>3</sub>, A. Kikuchi, K. Inoue, K. Tachikawa, *Physica C*, Vol. 337, (1999): 180-186.

Effects of Additional Elements to Nb<sub>3</sub>Al Multifilamentary Wire Fabricated by Rapid-Heating/Quenching Process, Y. Iijima, A. Kikuchi, K. Inoue and T. Takeuchi, *IEEE Trans. on Appl. Supercond.* Vol. 9, (1999): 2696-2701.

Preparation and Characterization of Y<sub>2</sub>O<sub>3</sub> Buffer Layer and YBCO Films on Textured Ni Tape, A. Ichinose, G. Daniels, N. Heing, D.C. Larbalestier, A. Kikuchi, K. Tachikawa and S. Akita, *IEEE Trans. on Appl. Supercond.* Vol. 9, (1999): 2280-2283.

New Nb<sub>3</sub>Al-Based A15 Multifilamentary Wires with High *J<sub>c</sub>* in High Fields, Y. Iijima, A. Kikuchi and K. Inoue, to be published in *Cryogenics*, (2000).

Development of Nb<sub>3</sub>Al Conductors Having Great Potentialities in High Energy Physics, K. Inoue, to be published in *Proc. of ELOISATRON Workshop*, (2000).

Improved Critical Current Density of Rapidly-heated/Quenched and Transformed Nb<sub>3</sub>(Al, Mg) and Nb<sub>3</sub>(Al, Ge) Multifilamentary Wires, A. Kikuchi, Y. Iijima, K. Inoue, T. Asano and M. Yuyama, to be published in *Proc. of 4<sup>th</sup> EUCAS*, (2000).

43 Investigation of New Nonlinear Optical Crystals for Wavelength Modulation, Single Crystal Growth and Principle Technology Development for Optical Devices

*H. Kimura, A. Miyazaki, T. Fukuda<sup>1</sup>, T. Sasaki<sup>2</sup>, T. Katsumata<sup>3</sup> and M. Sato<sup>4</sup>: 4th Research Group*

Crystal on BaO-B<sub>2</sub>O<sub>3</sub>-Al<sub>2</sub>O<sub>3</sub> system is one of the SHG (Second Harmonic Generation) crystals. We have already reported that a substitution of Al or Ga for B on the β-BaB<sub>2</sub>O<sub>4</sub> was effective to improve properties of the β-BaB<sub>2</sub>O<sub>4</sub> crystal, such as an increase of viscosity and surface tension, a stabilization of low temperature phase and an increase of hardness, and an intensity increase of the SHG. There are many crystal phases on the BaO-B<sub>2</sub>O<sub>3</sub>-Al<sub>2</sub>O<sub>3</sub> system according to the JCPDS card. One of the phases (BaAl<sub>2</sub>B<sub>2</sub>O<sub>7</sub>) was reported as a high SHG active phase by Chen et al.

In this work, forming crystal phases were investigated by means of a solid state reaction method and a liquid state reaction method for crystals listed in the JCPDS card on the BaO-B<sub>2</sub>O<sub>3</sub>-Al<sub>2</sub>O<sub>3</sub>, BaO-B<sub>2</sub>O<sub>3</sub>-Ga<sub>2</sub>O, Li<sub>2</sub>O-B<sub>2</sub>O<sub>3</sub>-Al<sub>2</sub>O<sub>3</sub>, Li<sub>2</sub>O-B<sub>2</sub>O<sub>3</sub>-Ga<sub>2</sub>O<sub>3</sub> systems. Single crystals were tried to grow by our original pulling down method. Furthermore, formed crystals were characterized on a viewpoint of the SHG. Since there is no date on the BaO-B<sub>2</sub>O<sub>3</sub>-Ga<sub>2</sub>O<sub>3</sub> system in the JCPDS card, we assume the crystal phase on the BaO-B<sub>2</sub>O<sub>3</sub>-Ga<sub>2</sub>O<sub>3</sub> system is similar to that on the BaO-B<sub>2</sub>O<sub>3</sub>-Al<sub>2</sub>O<sub>3</sub> system.

Crystals, from BaCO<sub>3</sub>, Li<sub>2</sub>CO<sub>3</sub>, B<sub>2</sub>O<sub>3</sub>, Al<sub>2</sub>O<sub>3</sub> and Ga<sub>2</sub>O<sub>3</sub> (99.99%) source materials, were formed by the solid state reaction at 700-800°C or by the liquid state reaction at 950-1000°C for 5 hours using a Pt crucible in an air atmosphere. Formed phase was investigated by powder X-ray diffraction. Melting mode was investigated by TG-DTA as a congruent melting or not. The SHG properties were investigated by a radiation of the YAG laser to the powder samples prepared by the formed crystals.

For the Ba-type systems, the phases by the solid state reaction were almost in agreement with those in the JCPDS card. The phases by the liquid state reaction were almost glass not crystal. Melting mode was almost incongruent melting. On the other hand for the Li-type systems, crystals were formed by the liquid state reaction and by the solid state reaction. The melting mode was almost congruent melting.

For the SHG properties, the SHG was observed on the BaO-B<sub>2</sub>O<sub>3</sub>-Al<sub>2</sub>O<sub>3</sub>, BaO-B<sub>2</sub>O<sub>3</sub>-Ga<sub>2</sub>O<sub>3</sub> and Li<sub>2</sub>O-B<sub>2</sub>O<sub>3</sub>-Ga<sub>2</sub>O<sub>3</sub> systems and not on the Li<sub>2</sub>O-B<sub>2</sub>O<sub>3</sub>-Al<sub>2</sub>O<sub>3</sub> system.

Crystals were grown by the pulling down method, but transparent crystals were difficult to grow yet.

We think on a viewpoint of the melting mode and the SHG properties that the crystals on the Li<sub>2</sub>O-B<sub>2</sub>O<sub>3</sub>-Ga<sub>2</sub>O<sub>3</sub> system are promising for the

SHG applications.

This research was performed in collaboration with the Institute for Materials Research, Tohoku University, and the Institute of DEO for a crystal growth and a characterization on nonlinear optical oxides.

**Keywords:** frequency modulation, crystal asymmetry, substitution, refractive index, dielectric constant

### Recent publications

1. "Growth and characteristics of long duration phosphor crystals", T. Katsumata, R. Sakai, Y. Ohshiba, Y. Isoda, S. Komuro, T. Morikawa and H. Kimura: *J. Crystal Growth* 198/199 (1999)869-871.
2. "Growth of small diameter  $Ba(B_{1-x}Al_x)_2O_4$  single crystals", A. Miyazaki, H. Kimura, X. Jia, K. Shimamura and T. Fukuda: *Cryst. Res. Technol.* 34(1999)817-820.
3. "Stability of  $Ba(B_{0.9}Al_{0.1})_2O_4$  molten zone by floating zone technique on earth", X. Jia, A. Miyazaki and H. Kimura: *J. Crystal Growth* 209(2000)850-854.
4. "Crystal growth of  $Ba(B_{1-x}Al_x)_2O_4$  using a new Fz furnace with double ring halogen lamp heater", H. Kimura, X. Jia, K. Shoji, R. Sakai and T. Katsumata: *J. Crystal Growth* 212 (2000)364-367.
5. "Crystal properties of  $Li_2(B_{1-x}Al_x)_4O_7$  grown by Czochralski method", H. Kimura, A. Miyazaki and X. Jia: *J. Mater. Sci. Lett.* 19(2000)745-747.

\*1 Visiting Researcher (Tohoku Univ.)

\*2 Visiting Researcher (Osaka Univ.)

\*3 Visiting Researcher (Toyo Univ.)

\*4 Visiting Researcher (Kitami Institute of Technol.)

### 44 Surface modification by plasma source ion implantation

*H. Shinno, M. Kaise, and S. Ikeno, 2nd Subgroup, 4th Research Group*

Plasma-source ion implantation is a coating method, which is useful for ion implantation to surfaces of three-dimensional complex shaped substrates, with much lower expenses than beam-line ion implantation. In this experiment, DLC (diamond like carbon) coatings were fabricated by plasma-source ion implantation in a plasma of acetylene, and dependence of deposition rate on im-

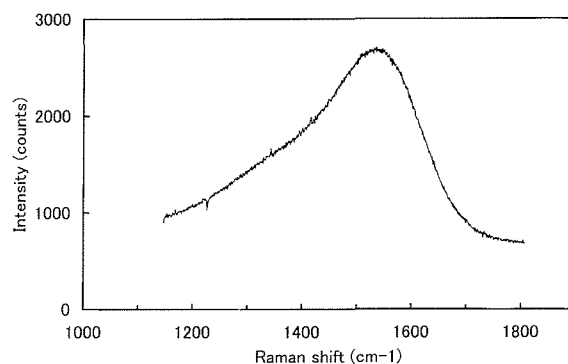


Fig.1 Raman spectrum of a carbon film deposited by plasma-source ion-implantation using glow-discharge plasma by pulse voltages.

plantation conditions was studied. The plasma was ignited using an r. f. generator with a frequency of 13.56 MHz. Two glass substrates ( $15 \times 15 \times 1$  mm) were mounted on an aluminum substrate holder ( $30 \times 40 \times 1$  mm). Positive ions in the plasma were accelerated and implanted to the substrates by pulse voltages applied to the substrate holder. Pulse voltages were  $-5 \sim -20$  kV, pulse widths were  $10 \sim 20 \mu s$  and pulse frequencies were  $100 \text{ Hz} \sim 1 \text{ kHz}$ . When the gas pressure was higher than about 2.6 Pa, glow-discharge plasma was ignited by the pulse voltages, and the plasma-source ion implantation could be performed without the r. f. discharge. Without the r. f. discharge, plasma was concentrated around the substrate, so that contamination of inner wall of the chamber by carbon coatings was eliminated. Fig. 1 shows a Raman spectrum of one of obtained films. Analysis of the Raman spectrum suggested that the film was DLC.

Optically transparent DLC coatings are desirable for hard coatings on glassware, so that mixed gases of acetylene and oxygen was used to make DLC coatings, because residual graphite in DLC films might be removed by oxygen. Effects of gas composition on deposition rate of DLC films were studied using two kinds of mixed gases A and B. A is a mixed gas of acetylene ((100-X)%) + argon ( $(X \times 0.95)$ %) + oxygen ( $(X \times 0.05)$ %), and B is that of acetylene ((100-Y)%) + oxygen (Y%). With increasing X or Y, deposition rate decreased and became zero when  $X \sim 90$  and  $Y \sim 10$ . From this result, it was concluded that oxygen decreased deposition rate of DLC films effectively, while argon didn't. In this experiment, all the films were colored and transparent DLC films were not obtained.

While hard coating such as DLC or c-BN (cubic boron nitride) are well known, CN (carbon nitride) is expected to be harder than diamond. One of the purposes of this experiment is to synthesize

CN films using ion implantation technique. CN films were synthesized by nitrogen ion implantation into carbon films deposited by magnetron sputtering. The carbon films had compressive or tensile internal stress when the sputtering gas was argon or nitrogen, respectively. Nitrogen ions were implanted into the carbon films at room temperature and at a low temperature near that of liquid helium. During the room-temperature ion-implantation, most nitrogen atoms escaped from the films and radiation damages of the films were severe. On the other hand, during the low-temperature ion-implantation, nitrogen stayed in the films and formed blisters. This suggested that the formation of CN compounds were possible in these films.

Sintered TiAl - 3 ~ 40 at% TiN, TiAl - 3 ~ 40 at% TiB<sub>2</sub>, TiAl - 3 ~ 40 at% SiC and TiAl - 3 ~ 40 at% TiC complex alloys were produced from TiAl and ceramics powder. Micro-Vickers hardness of inner part of the complex alloys was increased from 300 to 670 with ceramic concentration. In surface of the complex alloys, Al<sub>2</sub>TiO<sub>5</sub> + Ti<sub>2</sub>AlC, Al<sub>2</sub>TiO<sub>5</sub> + Ti<sub>3</sub>AlC and Al<sub>2</sub>TiO<sub>5</sub> + Ti<sub>2</sub>SiC were grown. Micro-Vickers hardness of the surface layers in TiAl - 20 ~ 40 at% TiB<sub>2</sub> and TiAl - 20 ~ 40 at% SiC was Hv1200 ~ Hv2000. Wear properties of the surface layers was superior to that of stellite. In complex alloys of less than 20 at% ceramics, low toughness of the surface layers brought low wear resistance.

#### 45 Research and Development of High-Performance Light Alloys for Hydrogen Storage

*C. Nishimura, S. Hwang, M. Komaki, T. Ozaki and H. Numata, 4th Research Group M. Amano, Materials Physics Division [April 1997 to March 2001]*

Hydrogen can be regarded as an ideal energy intermediary for the following reasons: (1) it is almost inexhaustible, (2) clean and tender to ecology, (3) easy to be stored and transported. There is no doubt that hydrogen will play an important role in the near future after the fossil-energy era. In scope of the large-scale use of hydrogen as an energy intermediary, it is inevitable to establish the technological fundamentals of materials related to hydrogen-energy applications. In this study, it is aimed to give guidelines for developing high-performance light alloys for hydrogen storage, based on magnesium, which can be applied in automobiles as gas-containers or batter-

ies.

Mechanical alloying was used to synthesize B2 and other structures for the following two reasons: (1) it produces alloys with nanometer-sized grains (typically <100nm) enhancing the chemical and physical properties, (2) it is a room temperature process based on solid state reaction with low production cost. Synthesized powders were tested for their hydrogen storage performance using PCT measurements.

Thus far, Mg-Ag, Mg-Ag-M (where M = Pd, Ti or V, atomic percent  $\leq 10$ ) and Mg-La have been extensively studied, among B2-type intermetallic compounds having 50:50 atomic percent of each element. In all cases, B2 structure was readily formed by mechanical alloying. In most cases, hydrogen was absorbed during the first activation process in PCT measurements. The highest hydrogen absorption was obtained in Mg-La B2 alloy, at approximately 1.2 wt.%.

Other alloys such as MnV (B2 structure), MnVZr (amorphous), TiAg (B11 structure) and LaMg<sub>3</sub> (DO<sub>3</sub> Structure) were also examined using the same procedure. Amorphous MnVZr alloy absorbed some amount of hydrogen ( $H/M < 0.5$ ) due to the inclusion of Zr. LaMg<sub>3</sub> alloy was found to absorb relatively large amount of hydrogen, similar to that of B2 structured alloy LaMg.

**Keywords:** hydrogen storage, magnesium, mechanical alloying, B2 structure

#### Recent Publications

Effects of Oxidation of Mg-Ni-H and Mg-Ni-Al-H Alloys on Hydrogen-Thermal-Desorption Characteristics, M. Komaki, M. Amano, H. Numata and C. Nishimura, *J. Japan Inst. Metals* 62 (1998): 111-116 (in Japanese)

Hydride formation on Ti<sub>3</sub>Al by Cathodic Hydrogen Charging in Sulfuric Acid Containing Sb<sub>2</sub>O<sub>3</sub>, *J. Japan Inst. Metals* 63, 561 (1999).

Hydrogen Permeation through Magnesium, C. Nishimura, M. Komaki and M. Amano, (*J. Alloys and Compounds* 293-295 (1999): 329-333.

Deformation mechanism of nanocrystalline magnesium in compression, S. Hwang, C. Nishimura and P.G. McCormick, (submitted to *Scripta Materialia*).

#### 46 Designing of function and structure for functionally graded system

*Y. Shinohara, 4th Research Group [April 1999 to March 2002]*

Use of waste heat is demanded to save the limited energy resource in the earth. Most of waste heat is not easy to use efficiently, because it is released not continuously but intermittently and from small equipments in our living environment. Low temperature of waste heat, less than 800K, also makes it difficult to use. One answer to how to use waste heat is a small power generating device that can work intermittently at the heat source less than 800K.

Lead telluride PbTe is typical thermoelectric material applied in the temperature range from 300K to 800K. It has been already used for power generating devices at special locations, *i.e.* space, deep sea, desert, pole, *etc.*, which have not been applied to use of waste heat. We need more than 30% higher thermoelectric energy conversion efficiency  $\eta$  of PbTe. The higher  $\eta$  is achieved by the higher figure-of-merit  $Z(= \alpha^2/(\rho \kappa))$ ,  $\alpha$ : Seebeck coefficient,  $\rho$ : electrical resistivity,  $\kappa$ : thermal conductivity). PbTe has variations of  $Z$  with temperature and the  $Z$  has a maximum at the corresponding temperature  $T_m$ , as shown in Fig.1. The  $T_m$  can be shifted by increasing its carrier concentration  $n$ . When the  $n$  changes gradually in PbTe, the  $Z$  can be kept high in a wide temperature range, as indicated by a dotted line in Fig.1. The graded carrier concentration can improve  $\eta$  of PbTe by 30% theoretically.

The graded carrier concentration has, however, not been realized, because the ordinary P/M process to form metal/ceramics compositional gradient cannot be applied to. We need a new process for

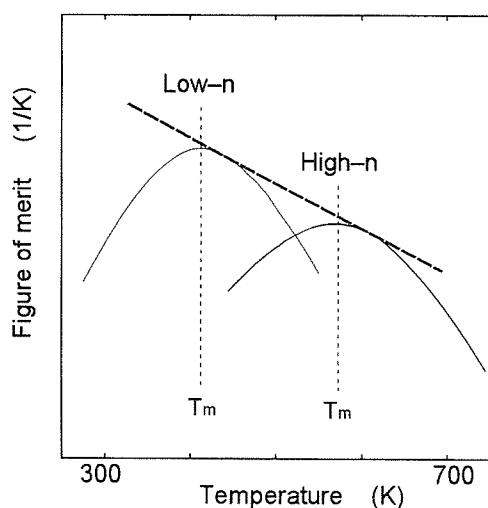


Fig.1 Variations of figure-of-merit with temperature for low- $n$  and high- $n$  PbTe

PbTe. Generally, the diffusion process forms continuous gradient of diffusant. When the dopant can

diffuse from one side of the non-doped PbTe ingot, the graded carrier concentration should be successfully formed. However, there are few reports on dopant diffusion in PbTe, especially n-type dopants. In this research, a high purity of the non-doped PbTe ingot has been prepared and the diffusion of n-type dopants into the PbTe has been investigated as a fundamental research of the controlled diffusion process. As a result, it was clarified that the diffusion of  $ZrCl_4$  n-type dopant into the PbTe was as slow as the self-diffusion of Pb in PbTe.

#### 47 Development of Essential Technique for Improving Coil Current Density in Superconducting Magnet

*K. Inoue, Y. Yoshida, Y. Iijima and A. Kikuchi, 4th Research Group*

[April 1998 to March 2001]

Recently we succeeded in development of new process, called as Rapid Heating/Quenching and Transformation (RHQT) process, in order to fabricate  $Nb_3Al$  multifilamentary wire. Through the RHQT-process, we can obtain  $Nb_3Al$  wire having 3-5 times larger  $J_c$  than those of commercialized wires. However, to improve coil current density in superconducting magnet by using the  $Nb_3Al$  wire, stabilization of the  $Nb_3Al$  wire is very important for low field applications. On the other hand,  $J_c$  of the RHQT-processed  $Nb_3Al$  reduced severely in fields above 20 T so that the improvement of  $J_c$  in higher fields than 20 T is required for high field applications.

The RHQT process includes a short heat treatment at 2000°C, which is much higher than the melting points of excellent electrical conductors, such as Cu, Ag, and Al. Simple electrical Cu-plating after the RHQ-treatment could not stabilize sufficiently the  $Nb_3Al$  wire, because the Nb oxide layer on the surface of Nb matrix prevents the thermal and electrical contact between Cu and Nb. In order to break the Nb oxide layer, we studied the Cu-ion plating on the RHQT-processed  $Nb_3Al$  in fiscal 1998. The combination of Cu-ion plating and Cu-electrical plating was found to be very effective to stabilize the  $Nb_3Al$  wire. However the process increases the wire stabilization cost. In order to reduce the wire stabilization cost, we studied the bonding between Cu and Nb under high pressures and high temperatures in fiscal 1999. We found that good metallurgical bonding between Cu and Nb were obtained under 10 kg/mm<sup>2</sup> and 500 °C, when we used oxygen-free Cu. On the other hand the good bonding could not obtained be-

tween Nb and tough-pitch Cu. By using the new point of view, we are developing a new economical stabilization method.

In order to clear up the cause of high  $J_c$  in the RHQT-processed Nb<sub>3</sub>Al, we performed electron transmission microscope observations. We found 3 kinds of lattice defects in the Nb<sub>3</sub>Al; grain boundaries, subgrain boundaries, and stacking faults. The stacking faults are formed parallel with space of 10-20 nm in each subgrain, and seem to be main effective pinning centers in this superconductor. Ordinarily, grain boundaries are well known act as the main pinning centers in superconducting A15 compounds, such as Nb<sub>3</sub>Sn and V<sub>3</sub>Ga. However, the grain sizes of Nb<sub>3</sub>Al are 0.5-2  $\mu$ m, and too large to explain the high  $J_c$  in Nb<sub>3</sub>Al. According to the EDX analysis, the Al concentration around the stacking faults is higher than that between the stacking faults. Therefore the composition of Nb<sub>3</sub>Al matrix shifts from the stoichiometric composition to Nb-rich composition with the formation of stacking faults, and reduces its  $T_c$  and  $H_{c2}$  a little. The stoichiometric Nb<sub>3</sub>Al is known to have the best values of  $T_c$  and  $H_{c2}$ .

According to the microstructure observations and the Nb-Al phase diagram, we obtained some ideas to fabricate Nb<sub>3</sub>Al wire with stoichiometric composition, resulting into Double Rapidly-Heating/Quenching (DRHQ) process. In this process, an Nb/Al microcomposite wire is applied to the RHQ treatment to obtain Nb-Al supersaturated bcc filaments. The resulting wire is applied to the second RHQ treatment to obtain stoichiometric Nb<sub>3</sub>Al filaments, and then annealed at 750-800°C to improve the long-range ordering in the Nb<sub>3</sub>Al crystal structures. The peak temperature during the second RHQ treatment is controlled to be about 1900°C, while that of the first one is about 2000°C. The Nb<sub>3</sub>Al wire, fabricated by the DRHQ process, shows  $T_c$  of 18.4 K and  $H_{c2}$ (4.2 K) of 30 T, which are similar to those of arc-melted stoichiometric Nb<sub>3</sub>Al. The most interesting result is its excellent  $J_c$ (4.2 K) in fields above 20 T, e.g., 200 A/mm<sup>2</sup> at 25 T, 270 A/mm<sup>2</sup> at 24 T, and 270 A/mm<sup>2</sup> at 23 T.

**Keywords:** Nb<sub>3</sub>Al, Y-123, Rapid-Heat, Quench, Transformation,  $J_c$

### Recent Publications

Nb<sub>3</sub>(Al, Ge) Multifilamentary Conductor Fabricated by Continuous Rapid-Heating/Quenching Process, Y. Iijima, K. Inoue, M. Kosuge and T. Takeuchi, Proc. of MT-15 (1998): 1040-1043.

New Nb<sub>3</sub>Al Multifilamentary Conductor and Its

Application to High Field Superconducting Magnet, K. Inoue, Y. Iijima, T. Takeuchi, T. Kobayashi, K. Fukuda, K. Nakagawa, G. Iwaki and H. Moriai, Physica B, Vol.246&247 (1998): 364-367.

Structure and Irreversibility Field of Tl-1223 phase Synthesized through the Substitution of TlF for Tl<sub>2</sub>O<sub>3</sub>, A. Kikuchi, K. Inoue and K. Tachikawa, Physica C, Vol. 337 (2000): 180-186.

Effects of Additional Elements to Nb<sub>3</sub>Al Multifilamentary Wire Fabricated by Rapid-Heating/Quenching Process, Y. Iijima, A. Kikuchi, K. Inoue and T. Takeuchi, IEEE Trans. on Appl. Supercond. Vol. 9 (1999): 2696-2701.

Preparation and Characterization of Y<sub>2</sub>O<sub>3</sub> Buffer Layer and YBCO Films on Textured Ni Tape, A. Ichinose, G. Daniels, N. Heing, D.C. Larbalestier, A. Kikuchi, K. Tachikawa and S. Akita, IEEE Trans. on Appl. Supercond. Vol. 9 (1999): 2280-2283.

New Nb<sub>3</sub>Al-Based A15 Multifilamentary Wires with High  $J_c$  in High Fields, Y. Iijima, A. Kikuchi and K. Inoue, to be published in Cryogenics (2000).

Improved Critical Current Density of Rapidly-Heating/Quenching Processed Nb<sub>3</sub>(Al, Mg) and Nb<sub>3</sub>(Al, Ge) Multifilamentary Wires, A. Kikuchi, Y. Iijima, K. Inoue, T. Asano and M. Yuyama, to be published in the Proc. of 4<sup>th</sup> EUCAS, (2000).

Development of Nb<sub>3</sub>Al Conductors Having Great Potentialities in High Energy Physics, K. Inoue, to be published in Proc. of ELOISATRON Workshop (2000).

Development of Nb<sub>3</sub>Al Conductor, K. Inoue, T. Takeuchi, Y. Iijima, A. Kikuchi, N. Nakagawa, G. Iwaki, H. Moriai and K. Watanabe, to be published in Advances in Materials Research, Vol.1 (2000).

Microstructures of Rapidly-Heated/Quenched and Transformed Nb<sub>3</sub>Al Multifilamentary Superconducting Wires, A. Kikuchi, Y. Iijima and K. Inoue, to be published in IEEE Trans. on Appl. Supercond. Vol. 11 (2001)

Nb<sub>3</sub>Al Conductor Fabricated by DRHQ (Double Rapidly-Heating/Quenching) Process, A. Kikuchi, Y. Iijima and K. Inoue, to be published in IEEE Trans. on Appl. Supercond. Vol. 11 (2001).

Cu-Added Nb<sub>3</sub>Al Multifilamentary Superconductors Having High  $J_c$  in High Fields, Y. Iijima, A. Kikuchi, K. Inoue and M. Yuyama, to be published in IEEE Trans. on Appl. Supercond. Vol. 11 (2001).

Nb<sub>3</sub>(Al, Ge) Multifilamentary Wires Made by the Rapidly-Heating/Quenching Process, A. Kikuchi, Y. Iijima, K. Inoue, M. Kosuge and K. Itoh, to be published in IEEE Trans. on Appl. Supercond. Vol. 11 (2001).

*N. Shinya, M. Kobayashi, T. Dan, M. Egashira, T. Konno, H. Fudouzi and M. Hase, 5th Research Group*

[April 1997 to March 2002]

Research on intelligent materials is one of the most important frontiers in the material science. The intelligent materials are the materials which have systematized and cooperative functions. They work as mechanical parts or electronic devices.

We proposed a particle assemblage to create intelligent materials. We must give materials multiple functions and make the functions work cooperatively. It will be realized through accurate three dimensional arrangement of various particles, each of which has a primitive function such as sensor, processor and actuator. In other words, we consider that micro-meter sized particles are the unit of materials and unit of function.

A key of the particle assemblage is a method to integrate various kinds of particles. Each kind of the particles must be placed at a prescribed position. More accurate positioning is required than achieved by the conventional methods. Thus, we have developed three methods, i.e., ordered mixture, manipulation by a microprobe, and particle arrangement using electron/ion beams. Detail of each method is described below.

### 1. Ordered mixture

The ordered mixture of semiconducting BaTiO<sub>3</sub> particles and In particles are formed by an forced electrification process. The particles are separately enclosed in a metallic vessel, and electrified at the opposite polarity by applying high voltage at the vessel. When both particles are sprayed in the same space at the same time, the ordered mixture is formed by the electrostatic force.

The packed bed of the ordered mixture of BaTiO<sub>3</sub> and In particles shows the same PTC property with the sintered bulk BaTiO<sub>3</sub>. The PTC property of a packed bed of semiconducting BaTiO<sub>3</sub> particles, however, is different from that for the bulk. The resistance is more than 100 times higher than that of the packed bed of the ordered mixture. It is attributed to high contact resistance between the semiconducting particles. While for the ordered mixture, In particles existing between the BaTiO<sub>3</sub> particles remove the high contact resistance.

PTC materials are expected to be good heater materials, because of their self-temperature controllability. We, therefore, made a prototype heater as follows. The ordered mixture was packed between two electrodes of thin copper plates, and they

were enveloped in a polyimide bag. The bag was sealed after evacuation. Then, the electrodes and the particulate layer were isotropically suppressed by the atmospheric pressure and fixed each other.

It is noticeable that the heater is formed without sintering process and is flexible despite BaTiO<sub>3</sub> is the ceramic materials.

### 2. Manipulation by a microprobe

The manipulation system is composed of a tungsten microprobe, a probe positioning system, stages for movement of substrates, and a CCD camera for the observation. Particles of less than 100  $\mu\text{m}$  on a metallic substrate can be adsorbed to the tip of the probe, carried to any positions on the substrate, and welded by controlling the applied voltage between the probe and the substrate.

The welding has done by the two-step discharge. High voltage of about 10 kV is applied to the probe in touch with the particle (contact discharge). The probe is lifted up for about 50  $\mu\text{m}$ , and 2kV is applied again to the probe (non-contact discharge).

The strength of welded particles was measured by pushing the particles with the tip of the sheet spring till the bond is broken. The breaking shear strength was calculated from the maximum strain of the sheet spring. When the gold particles were welded only by the contact discharge, the strength is too weak to measure by the device. The bond became tougher after the non-contact discharge. The estimated strength is fairly good comparing with that for the matrix material.

Microscopic observation also supported the above results. Ring-like upheaval existed at the fractured surface of the substrate. The welded particle touched the substrate at the ring, i.e., the interface was the inside the ring. When the particle was welded by the contact discharge, the particle is bonded at a little part of the interface. When the particle was welded by the two step discharge, the bonding area increased equal to the interface area.

Characters "N", "R", "I" and "M" are assembled from gold particles of 50  $\mu\text{m}$  as an example of the microstructure fabricated by our apparatus. Each character stands on a gold substrate by itself. The character "M" cannot be assembled, unless each particle is bonded together.

### 3. Particle arrangement using electron/ion beams

An electrified pattern is drawn on an insulating substrate by irradiation of an electron beam or an ion beam. A suspension is prepared from the particles to be arranged and an inert non-polar solvent. The substrate is dipped into the suspension for about 30 seconds. Since the particles are attracted to the electrified pattern by the electrostatic force

in the suspension, they are arranged as the electrified pattern.

Silica particles of 5  $\mu\text{m}$  can be arranged on a electrified line. The line composed of the particles is about 30  $\mu\text{m}$  wide. The arranged particles are fixed by a heat treatment or by a coating treatment. When the electrified spots are formed at a distance of 50  $\mu\text{m}$ , we can arrange one particle of 10  $\mu\text{m}$  diameter at each spot.

The measurement of zeta potential showed that the silica particles are charged negatively in the suspension. Thus, both the Coulomb's force and the gradient force will work on the particles in the suspension. The value of each force is numerically estimated by using the electric field analysis software. The results showed that the Coulomb's force is larger than the gradient force at which the particles are far from the electrified pattern. The gradient force, however, dominates near the electrified pattern.

**Keywords:** Intelligent materials, multiple functions, particle assemblage

#### 49 Development of Advanced Shape Memory Thin Films by Sputtering

*A. Ishida, T. Sawaguchi and M Sato, 5th Research Group*

[April 1997 to March 2002]

The effects of film composition and heat treatment conditions on the microstructure and shape memory behavior of Ti-rich Ti-Ni thin films have been investigated. Ti-rich Ti-Ni thin films of five compositions, Ti-45.2, 46.1, 47.0, 47.9 and 48.5 at.%Ni were prepared with a carousel type magnetron sputtering apparatus. The sputter-deposited thin films were annealed at 773, 823 and 873K for 1h. Transmission electron microscopy revealed that Ti-45.2at.%Ni thin films contain randomly oriented  $\text{Ti}_2\text{Ni}$  particles, while the other films contain  $\text{Ti}_2\text{Ni}$  precipitates with the same orientation as that of the TiNi matrix. In addition to these  $\text{Ti}_2\text{Ni}$  precipitates, GP zones were also observed in Ti-47.9 and 48.5at.%Ni thin films annealed at 773K for 1h. The shape memory behavior of these annealed Ti-Ni thin films was investigated with a thermomechanical tester. Every specimen showed a two-stage transformation in a low stress range, while it showed a single-stage transformation in a high stress range. The martensitic transformation temperature was found to decrease with increasing Ti content and decreasing annealing temperature. However, thin films containing GP zones showed sig-

nificantly low transformation temperatures despite of low Ti content (Fig. 1). On the other hand, the R-phase transformation temperature was not found to be sensitive to film composition, except for thin films with GP zones, which showed slightly low R-phase transformation temperatures. The critical stress for slip deformation was found to increase with increasing Ti content and decreasing annealing temperature. GP zones were helpful in increasing the critical stress of Ti-47.9 and 48.5at.%Ni thin films. The recoverable strain was found to increase with decreasing Ti content and annealing temperature. In particular, the thin films containing GP zones showed large recoverable strains. A plastic strain could not be detected when the two-stage transformation took place in a low stress range, but it appeared when the transformation behavior changed from a two-stage manner to a single-stage manner at a high stress. In general the transformation temperatures of Ti-rich Ti-Ni thin films are considered to be relatively higher than those of Ni-rich Ti-Ni thin films. Especially the R-phase transformation temperatures were found to be nearly 340K, regardless of composition and heating conditions. This characteristic seems to make Ti-rich Ti-Ni thin films applicable to practical devices.

**Keywords:** microactuator, shape memory effect, thin film, Ti-Ni, sputtering

#### Recent Publications

1. Microstructure and Mechanical Properties of Sputter-Deposited Ti-Ni Alloy Thin Films, A. Ishida and S. Miyazaki, Journal of Engineering Materials and Technology, ASME, 121 (1999): 2.
2. Mechanical properties of Ti-Ni shape memory

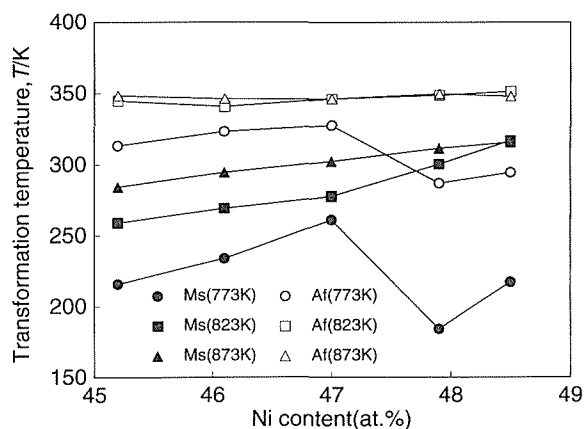


Fig.1 Martensitic transformation start temperature (Ms) and reverse martensitic transformation finish temperature (Af) of annealed Ti-rich Ti-Ni thin films as a function of Ni content

thin films formed by sputtering, A. Ishida, M. Sato and S. Miyazaki, *J. Mater. Sci. Eng. A*, 273(1999): 754.

3. Effects of Composition and Annealing on Shape Memory Behavior of Ti-rich Ti-Ni Thin Films Formed by Sputtering, *J. Japan Inst. Metals*, 64(2000): 62.
4. Stress-strain curves of sputter-deposited Ti-Ni thin films, A. Ishida, M. Sato, T. Kimura and S. Miyazaki, *Phil. Mag.A*, 80(2000): 967.

## 50 Study on the Processing and Assessment of Ecomaterials

*K. Halada, K. Minagawa, K. Ijima and H. Yoshizu, Ecomaterials Research Team*  
[April 1997 to March 2000]

ECOMATERIALS, which have high recyclability and give less environmental load to the eco-sphere without deteriorating their properties, are expected to be coming materials adapting to the sustainable development. It is an approach from materials science and engineering to the Industrial Ecology towards the coming Sustainable Society. The coming paradigm of the Post mass production is often called Dematerialization. This comes from the reconsideration of mass production, in which it was believed that the resources were infinite and the capacity of global environment was also infinite. Dematerialization means to decrease the mass of materials which the mankind uses, but does not mean needlessness of materials. Materials will circulate mainly among producers and service providers to realize effective circulation system to decrease the input/output of material from/to the environment. In this coming era, the material technology will become more important, because we have to circulate materials and products with higher quality adequately. Materials should have the properties of 1) lower environmental loading, 2) flexibility of production, 3) long life and the possibility of progressive maintenance.

This study consists of two parts. One part is the experimental feasibility study on the new processing technology for the coming dematerialization era. The processing with higher materials efficiency is the key concept of this study. The materials efficiency does not mean the direct amount of materials per product, but the total amount, in which fuel materials and raw materials are included, of materials in the lifecycle per intended service. The expected processing technology is not only the process with lower energy consumption nor lower emission but the process which can con-

trol the microstructure of material to assemble into proper part of the aimed material. From this viewpoint, powder-metallurgical technology is selected as one of the most available process. Following the Fe-Fe composite, utilization of Cu in the recycled steel is investigated.

It has been a great problem to separate Cu from the scrap of Fe-based alloys. Powder-metallurgical technology can solve this problem by using the Cu as a reinforcement element instead of removing Cu in Fe. Rapidly solidified powder and warm heavy-rolling consolidation was used to control the dispersion of Cu. As the result, a refined microstructure in which the disperse precipitate pinned the crystal grain was obtained in a Fe-Cu composite material, with the tensile strength of 1000MPa and about 8% elongation.

The other part of this study is to establish the assessment technology of ecomaterials. In the earlier work on ecomaterials, MLCA(materials life cycle analysis) was established as an assessment method, and the environmental load data of metals and alloys were calculated and collected into database. In this work, further development of MLCA is investigated to give the guideline of DfE (design for environment) and Eco-Design of products to the user of materials. As the utilization of MLCA in future should be used as an environmental element of life cycle engineering, the exchangeability of data with CAD and STEP is sought. And, the predictability of the environmental data change in the improvement of the process is also the required property of the database in order to deal with the development of flexible processes. At the first part of the study, the retrieval interface and the data structure of "the environmental load database of steel alloys" is modified.

These works had prepared the new research project named "Barrier-Free processing for Design for Environment" and were succeeded to the project research.

**Keywords:** ecomaterials, materials efficiency, recyclability, powder processing, materials environmental life-cycle analysis, computerized materials data

### Recent Publication

Barrier-Free Processing to improve Resource-efficiency through Life Cycle of material, Kohmei.Halada, *Proc. 4<sup>th</sup> Intl. Conf. on Ecomaterials 1999 Gifu (1999)*

## 51 Materials Efficiency Accounting based on MLCA

*K. Halada, K. Ijima, H. Yoshizu, K. Minagawa, Ecomaterials Research Team*  
[April 1999 to March 2002]

A National Research Project "Barrier-Free Processing of Material for Life-Cycle Design for Environment" has launched by Science & Technology Agency from 1999 for 5 years with 34 participants and collaborators. "Materials Efficiency Accounting based on MLCA" plays an important part of the Research Project.

Outline of the Barrier-Free Processing Project is the process innovation which can connect the "Materials Selection of Ecomaterials" and "Design for Environment (DfE)".

Here the relation among barrier-free processing, ecomaterials and Design for Environment is simplified as follows.

$$\begin{aligned} & \text{(Barrier-free processing)} \\ & = \text{(Materials Selection of ecomaterials)} \\ & \quad \times \text{(Innovation of materials-processing)} \\ & \quad \times \text{(DfE oriented)} \end{aligned}$$

The research project consists of three parts; 1) Innovative Processing for Materials' Circulation, 2) Materials Tailor-processing for Design for X, 3) Materials Efficiency Accounting.

"Innovative Processing for Materials' Circulation" is the investigation focused on the appropriate processing for the recycled materials which contains man-made impurities and have various shapes. "Materials Tailor Processing for Design for X" is the investigation on the noble processings which can control the shape and properties together and are suitable to Design for Environment. Regarding "Materials Efficiency Accounting", basic concept of materials efficiency is determined by;

$$\begin{aligned} & 1 / \text{(Materials efficiency)} \\ & = \text{(Total Materials Requirement)} \\ & \quad / \text{(factor for DfE for objected service)} \end{aligned}$$

Factors for DfE are started to investigated by making inventory of demands of DfE on materials. The method for estimation of Total Materials Requirement will be established based on the investigation of practical mining process and theory of extraction. "Materials Efficiency Accounting based on MLCA" takes the part of accounting TMR (Total Materials Requirement) base on the methodology of our developed MLCA.

TMR is just the amount of the materials which are moved from the earth by mankind. In the work of World Resource Institute, TMR was underestimated. Accounting was based on the amount of ore which is the output of mining but the input

from the earth in that work., and the related material flows such as induced one by energy were not considered. When we calculate TMR, ① all materials which are associated should be accounted, and ② socially induced material flow also should be concerned. In 1999, the fundamental data of TMR of Fe, Cu, Al, Zn, Pb, and coal are collected. The dispersion of the data and the universality of the data are investigated.

**Keywords:** ecomaterials, materials efficiency, recyclability, materials environmental life-cycle analysis, total materials requirement

## Recent Publications

Barrier-Free Processing to improve Resource-efficiency through Life Cycle of material, Kohmei. Halada, Proc. 4<sup>th</sup> Intl. Conf. on Ecomaterials 1999 Gifu (1999)

## 52 Fabrication of quasicrystals and investigations of their properties

*A.P. Tsai, Aperiodic Materials Research Team*  
[October 1, 1996 to November 30, 2001]

In this year, we have achieved three topics: 1) discovery of new stable quasicrystals in ternary Cd-Mg-RE and binary Cd-Yb and Cd-Ca alloys, 2) approach to a catalyst for quasicrystal and 3) developing new method for structural analysis for icosahedral quasicrystals.

1) Discovery of new quasicrystals in ternary Cd-Mg-RE and binary Cd-Yb and Cd-Ca alloys. A new stable icosahedral quasicrystal has been found in Cd-Mg-Dy system in annealed states. The new icosahedral phase was examined to possess a simple icosahedral lattice and have stoichiometry approximating Cd<sub>66</sub>Mg<sub>21</sub>Dy<sub>13</sub>. Peak widths of powder x-ray diffraction patterns claims that the icosahedral phase has same level of perfection as that of icosahedral Al-Pd-Mn. Following this work, we have confirmed stable icosahedral quasicrystal in a series of Cd<sub>65</sub>Mg<sub>20</sub>RE<sub>15</sub>(RE=Y, Eu, Gd, Tb, Dy, Ho, Er Tm, Yb and Lu) alloys.<sup>(1)</sup> This is the largest group of alloys among all the known quasicrystalline alloys found till now. Among these alloys icosahedral quasicrystal in Cd-Mg-Yb system is specially stable which formed in as-cast state as well as in annealed state. This led us revisiting the binary phase diagram of Cd-Yb. Interestingly, a phase remained unknown at Cd<sub>5.7</sub>Yb existing neighbor to a crystalline phase at Cd<sub>6</sub>Yb. The Cd<sub>6</sub>Yb is a body centered cubic phase with a

space group of  $Im\bar{3}$  and a lattice parameter of 1.5 nm. By analyzing the detailed structure, we found the Cd<sub>6</sub>Yb could be regarded as an approximant of icosahedral phase, in which a cluster structure locates at origin and body center. This convinced that the Cd<sub>5.7</sub>Yb is probably an icosahedral quasicrystal.<sup>(2)</sup> An alloy of Cd<sub>5.7</sub>Yb prepared by induction furnace was identified to be an icosahedral quasicrystal. According to the similarity in phase diagram the other binary stable quasicrystal was found in a CdCa alloy.<sup>(3)</sup>

#### 2) Approach to a catalyst for quasicrystals

Steam reforming of methanol ( $\text{CH}_3\text{OH} + \text{H}_2\text{O} \rightarrow 3\text{H}_2 + \text{CO}_2$ ) has been performed on a stable AlCuFe quasicrystal for the first time.<sup>(4)</sup> The AlCuFe quasicrystal after leaching in NaOH aqueous solution reveals excellent activity. Catalytic reaction is estimated by the production rate of H<sub>2</sub> of the above-mentioned reaction equation which reaches 235 l/kgmin at 573K for steam reforming of methanol. The activity is due to Cu nanoparticles at the surfaces of quasicrystalline grains which are generated by the leaching treatment. The quasicrystals have two advantages: one is their brittle nature, which allows them to be crushed efficiently; the other is the involvement of Fe, which suppresses the sintering effect of Cu particles. The catalytic activity of the Al-Cu-Fe quasicrystal reaches to the same level of industrial catalyst. The quasicrystals have potential to use as a catalyst.

#### 3) developing new method for structural analysis for icosahedral quasicrystals

A novel density modification method is applied for the first time to phase reconstruction of X-ray single crystal data of quasicrystals.<sup>(5)</sup> The structure of icosahedral Zn-Mg-Ho quasicrystal has been determined by means of this *ab initio* structure determination with a framework of 6D description. The location, size and the shape of the occupation domains are deduced. This suggested Ho sites in the 3D structure are consistent with the results of magnetic diffuse scattering and the present method is available to quasicrystal structure.

**Keywords:** quasicrystal, binary stable quasicrystal, cadmium-magnesium-rare earth metals system, cadmium-ytterbium

- 1) J.Q. Guo, E. Abe and A.P. Tsai, Jpn.J.Appl. Phys., 39(2000)L770.
- 2) A.P. Tsai, J.Q. Guo, E. Abe, H. Takakura and T.J. Sato, Nature, 408(2000)537
- 3) J.Q. Guo, E. Abe and A.P. Tsai, Phys. Rev.B62(2000)R14605.
- 4) A.P. Tsai and M. Yoshimura, J.Appl. Catal., in press.

- 5) H. Takakura, M. Shiono, T.J. Sato, A. Yamamoto and A.P. Tsai, Phys. Rev. Lett., 86(2001)236

### 53 Study on Combustion Synthesis of Useful Intermetallic Compounds

Y. Kaieda, N. Oguro, Y. Hosoya, Combustion Synthesis Research Team  
[April 1999 to March 2002]

The reactions in combustion synthesis to produce the intermetallic compounds are revealed fundamentally. The propagation of the reaction front and the synthesis process of the intermetallic compounds synthesized through the reaction are also studied. Investigation by the thermal analysis with rising temperature at constant and/or in alternating velocity is carried out to reveal the conditions for the initiation of the reaction, the propagation and the synthesis. The influence of pressure and convection on the phenomena in the reaction process of the system containing gaseous phase or liquid phase is studied using a high gaseous pressure apparatus.

The selection of the combinations of elements, which is focused in the present study, will be investigated. The system of the combination that might exhibit the effect of convection and pressure during the reaction and synthesis process is selected considering the system that performs the effect of liquid and gaseous phase. The system of elements, in which the safety during the experiment is assured, is selected.

The processes including high frequency induction vacuum melting and casting conventionally produce most intermetallic compounds. It is difficult to control accurately the chemical components of intermetallic compounds produced by the conventional process. The industrial process including a combustion synthesis method, which is a newly developed manufacturing process in the present institute, produces homogeneous intermetallic compound. The chemical components and the impurities in the specimens industrially produced by the process are revealed. These properties are vitally important when the combustion synthesis method is applied to an industrial mass production process for producing intermetallic compounds.

**Keywords:** combustion synthesis, intermetallic compound

**Related Paper**

1. Y. Kaieda, "Morphology Change in the Optical Microscopic Microstructure of Titanium by Nitriding Reaction and Combustion Synthesis Under Normal and Microgravity", *J. Mater. Synthesis Process.* 7(1999) 67-82.

#### 54 Promotion of Collaborative Studies Using User Facilities of Center for Advanced Physical Fields

*K. Yoshihara*

[From April 1999]

In the Center for Advanced Physical Fields, the world's leading facilities have been installed, such as a 40 T class hybrid magnet system, a 1000 keV ultra-high-voltage transmission electron microscope and an XHV integrated process. They are very powerful facilities and have potentialities to create new research fields by joint studies with researchers in the broad area.

As the first step to promote collaborative studies between the Center for Advanced Physical Fields and external researchers, high magnetic field facilities are now open to the domestic and international users. In 1999 we accepted 73 proposals from external users (58 from universities, 7 from public laboratories and 8 from private companies). They included a basic experiment of an MHD helical type thruster for a superconducting electromagnetic ship. This was an international effort in collaboration with the Institute of Electrical Engineering, China and Kobe University of Mercantile Marine, Japan. It was performed successfully.

Experimental apparatus commonly used for wide area researches have been prepared for promotion of the collaborative studies. A tensile test machine working in a condition of high magnetic fields and high temperatures was developed in 1999.

**Keywords:** collaborative study, user facility, high magnetic field, high-resolution beam, extremely high vacuum

#### 55 Development of New Superconductors for Nuclear Fusion Use

*T. Takeuchi, High Magnetic Field Station*

[April 1999 to March 2004]

The main purpose of this study is to develop the new superconductors to be used for the nuclear fusion reactor. The superconducting conductors for the nuclear fusion are required to have (1) large critical current density ( $J_c$ ) in high fields,

(2) high tolerance to mechanical stress and strain, (3) large current carrying capacity, (4) low sensitivity to radiation, (5) high stability to electromagnetic disturbances, (6) low ac losses. Recently, we have developed a new Nb<sub>3</sub>Al multifilamentary superconductor, which is based on a Jelly-Rolled (JR) Nb/Al composite and fabricated by rapid-heating and quenching a wire of such composites with subsequent transformation annealing to form Nb<sub>3</sub>Al phase. In contrast to the conventionally fabricated Nb<sub>3</sub>Al conductors, the transformation from super-saturated bcc-solid-solution Nb(Al)<sub>ss</sub> enables the highly stoichiometric A15-Nb<sub>3</sub>Al to form with fine grains, and the  $J_c$  characteristics are significantly improved over the whole range of magnetic fields, in particular, in the fields more than 20 T. The resulting substantially improved high-field performance is compatible with the excellent strain tolerance. Thus, the transformed Nb<sub>3</sub>Al conductor is promising as a realistic alternative to Nb<sub>3</sub>Sn for the fusion reactor use.

However, the rapid-quenching process does not allow Cu to be included as a basic composite constituent of the strand, because the conductor is heated up to 2000°C far above the melting point of Cu. The Cu sheath would be melted and reacted with the JR Nb/Al composites and form unwanted ternary compounds of Cu (Fig. 1(a)). Thus, an important and urgent issue with regard to

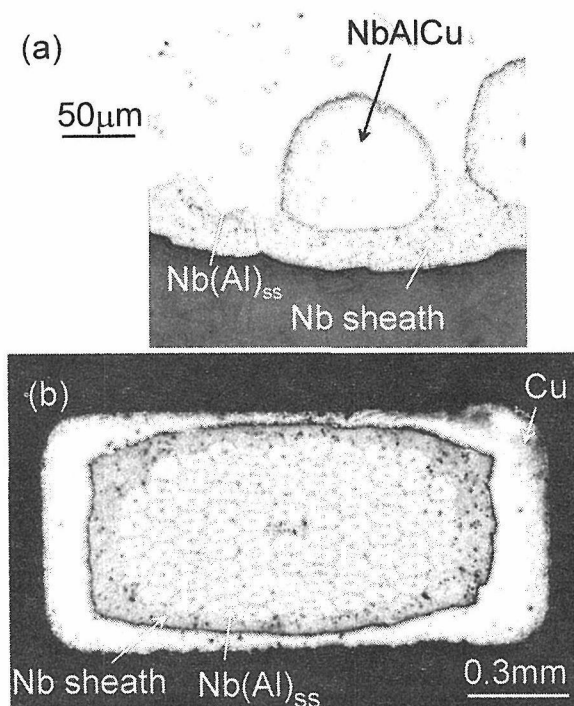


Fig. 1. (a) Cross-section of as-quenched wire with Cu stabilizer and without diffusion barrier to JR Nb/Al filaments. The Nb-Al-Cu ternary compound forms at the JR Nb/Al filaments side, and Nb dissolves in Cu at the Nb-sheath side. (b) Cross-section of Cu-cladding JR Nb/Nb(Al)<sub>ss</sub> conductor.

the practical use of Nb<sub>3</sub>Al is the incorporation of stabilizers into Nb<sub>3</sub>Al conductors. An electroplated thick-layer of Cu would be peeled off by the heat-cycle of soldering, etc, since the oxidation of the strand's surface makes it difficult to ensure both electrical and mechanical bonding between the Cu and the Nb. All the methods we have developed for the external incorporation of Cu to the strand's surface are based on the ductile nature of the as-quenched JR Nb/Nb(Al)<sub>ss</sub> composite at room temperature. The as-quenched JR Nb/Nb(Al)<sub>ss</sub> withstands a variety of subsequent deformation of bending, bundling, drawing, flat-rolling etc., without a serious degradation in  $J_c$  after transformation, as reported previously. In this year, we have developed a so-called "mechanical-cladding method" where an as-quenched composite is wrapped longitudinally with Cu and groove-rolled for ensuring mechanical bonding. Fig. 1 (b) shows the cross-sectional structure of a Cu-cladding Nb/Nb(Al)<sub>ss</sub> composite (1.5<sup>w</sup> x 0.72<sup>t</sup> mm<sup>2</sup>). The volume ratio of Cu to Nb/Nb(Al)<sub>ss</sub> strand is 0.45; this value can be increased by using a thicker Cu. The starting 1.26 mm $\Phi$ -Nb/Nb(Al)<sub>ss</sub>-wire is plastically deformed to an almost rectangular shape (1.2<sup>w</sup> x 0.62<sup>t</sup> mm<sup>2</sup>), with a total reduction of area,  $RA$ , of 42 % at Cu-cladding.

As reported previously,  $J_c$  was rather enhanced at the beginning of deformation of Nb/Nb(Al)<sub>ss</sub> strand;  $J_c$  of the Cu-cladding Nb/Nb(Al)<sub>ss</sub> composite is increased from 80 A/mm<sup>2</sup> to 220 A/mm<sup>2</sup> at 22 T by 42%  $RA$ . Such an enhancement in  $J_c$  well compensates the reduction in cross sectional area;  $I_c$  at 22 T is increased by 60% for 26%  $RA$ . Thus, mechanical cladding with an appropriate amount of deformation is quite an effective way to incorporate a large-volume-fraction Cu-stabilizer; this is true, for example, for monolithic Nb<sub>3</sub>Al conductors of a 1 GHz NMR magnet where a rectangular cross-section of conductor is allowed.

**Keywords:** transformed Jelly-rolled Nb<sub>3</sub>Al, current carrying capacity, Nb-matrix ratio, wire diameter

## 56 Development of 1 GHz NMR Spectrometer

*H. Wada, T. Kiyoshi, T. Takeuchi, K. Itoh, A. Sato, T. Numazawa, M. Yuyama, M. Kosuge, H. Nagai and F. Matsumoto, High Magnetic Field Research Station*

*T. Shimizu, A. Goto, T. Terashima and S. Uji, Physical Properties Division*

*H. Kumakura and H. Kitaguchi, 1st Research Group*

[April 1995 to March 2002]

High  $T_c$  oxide superconductors (HTS) are expected to be able to induce much higher magnetic fields than low  $T_c$  metallic superconductors (LTS) when used at 4.2 K. We have initiated a program in which we will develop a 1 GHz superconducting NMR spectrometer including a 23.5 T superconducting magnet; such magnet must be constructed using HTS coils in combination with LTS coils. In our design the LTS coils are operated in persisting mode at a field of 21.1 T in a 132 mm diameter bore. The HTS coil is expected to generate an additional field of 2.4 T in a 54 mm room temperature bore. The cryostat has been designed to replace the HTS coil when necessary. This enables parallel development of the LTS and HTS coils. Those coils are cooled with atmospheric superfluid helium at 1.8 K.

Development of high performance metallic superconductors is one of the key issues of this program. We have developed high critical current (Nb,Ti)<sub>3</sub>Sn conductors and Ta reinforced (Nb,Ti)<sub>3</sub>Sn conductors for this project. The former conductors are made from Cu-15wt.%Sn-0.3wt.%Ti bronze matrix and their critical current density is improved. The latter conductors have 0.2 % yield strength of over 300 MPa at 4.2 K. We have finished winding all the LTS coils.

The development of the oxide inner magnet is the most critical issue in this project. From the viewpoint of field generation, we succeeded in generating a field of 23.4 T by the combination of LTS and HTS magnets. A persistent mode of operation to achieve field stability of less than 0.01 ppm/h is considered the most difficult to achieve. To realize it, we have developed superconducting joint techniques between Bi-2212 and NbTi conductors and between Bi-2212 conductors themselves. A newly developed multi-layered coil generated a field of 2.8 T at 4.2 K without a back-up field. It used one continuous Bi-2212 round conductor with a length of 254 m and no joint in the winding. As a persistent current switch made of NbTi/CuNi was connected with joints between Bi-2212 and NbTi, its persistent mode of operation was carried out. A central field at the start point was 2.43 T. Observed field stability after 50 hours was 6720 ppm/h, but a central field of 1.4 T could be maintained at that time.

A test operation of the constructed cryostat was performed. A tank of wax whose volume was as same as that of the magnet was installed in the cryostat instead of the magnet. It took 18 days to cool down from room temperature to 2.2 K. The atmospheric superfluid helium bath was cooled down to 1.55 K.

**Keywords:** NMR spectrometer, high field magnet, oxide superconductor

## 57 Fundamental Studies on Very High Magnetic Field Generation

*T. Kiyoshi, T. Asano, S. Matsumoto, M. Kosuge, M. Yuyama, A. Sato, F. Matsumoto, H. Nagai, T. Numazawa, T. Takeuchi, K. Itoh and H. Wada, High Magnetic Field Research Station*

[April 1998 to March 2001]

Generation of very high magnetic fields is expected to open new frontiers of science and technology. To realize such high fields, continuous studies on magnet design, magnet fabrication, cooling system and materials should be performed.

New applications of magnetic fields often require special magnets based on new concept. Uniform magnetic force field magnets are now under development for a new application to structural biology. A magnet is usually designed and fabricated to achieve uniform magnetic field as well as uniform magnetic field gradient. In this new application, uniform magnetic force field is important because it has recently been found that the growth of protein crystals is affected by the presence of magnetic force.

Uniform magnetic force field magnets are superconducting magnets because they must be continuously run for several days to grow protein crystals. The first magnet generating uniform force fields up to  $224 \text{ T}^2/\text{m}$  is in operation for protein crystal experiments. In a cylindrical space of 10 mm in diameter and 10 mm in height, the magnetic force field fluctuation along the z-direction is better than 0.4 %, and the ratio of radial component to axial component is less than 1.9 %. It was made of NbTi conductors and cooled with a G-M refrigerator. From October 1999 to April 2000, it has operated continuously at  $202 \text{ T}^2/\text{m}$  (a central field of 8.24 T) without any trouble.

In order to cancel gravity by magnetic force, a magnetic force field of  $1400 \text{ T}^2/\text{m}$  is required in the case of water. The second uniform force field magnet using Nb<sub>3</sub>Sn and NbTi conductors is now under development. It is designed to generate magnetic force fields up to  $880 \text{ T}^2/\text{m}$  with a central field of 17.1 T. In a sample space of  $10 \text{ mm}^\phi \times 10 \text{ mm}$ , the force field fluctuation along the z-direction is better than 1 %, and the ratio of radial component to axial component is less than 2 %.

This study has been carried out in cooperation with the National Institute of Bioscience and

Human-Technology and the National Institute of Materials and Chemical Research and partially supported by CREST of JST.

**Keywords:** high magnetic field, superconducting magnet, water-cooled magnet, uniform magnetic force field

## 58 Development of Magnetic Separation System

*T. Ohara and H. Wada, Strong Magnetic Field Research Station*

[April 1999 to March 2001]

Recent progress in magnet technology has realized economically and operationally favorable cryocooler-cooled superconducting magnets. These types of magnets are now being used in much broader areas of science and technology than before, resulting in the establishment of a new scientific area called New Magneto-Science. One of the promising applications in this area is magnetic separation. The primary advantages of energy savings, compact size, and increased speed are only fully realized when magnetic separation systems are operated with superconducting magnets. The full-scale application of these systems will contribute greatly to the preservation of the global environment.

We constructed a Bi-2223 magnet system with a 200mm room temperature bore, and operated it for both a test run and for demonstration of the separation of slurries containing fine  $\alpha$ -hematite paramagnetic particles. The magnet generated 1.7T at the center and more than 1T in its 11-liter room temperature bore. It was excited up to its maximum magnetic field in one minute, and the magnet temperature gradually increased during the excitation from the initial temperature of 12K. After being cyclically excited up to the maximum magnetic field about twenty times within a period of nine minutes, the magnet temperature stabilized to between 35-38K. For a magnetic separation system, to obtain high running efficiency rapid energizing and de-energizing are very important because the separation should be done at maximum field strength, and the separated particles should be removed at zero field strength. Our test results showed that nearly 100% of the hematite particles were successfully separated from the slurry, and that the Bi-2223 magnet was thermally stable against repetitive excitation. This indicates that the Bi-2223 magnet is suitable for magnetic separation applications.

We also developed a numerical simulation

method of High Gradient Magnetic Separation (HGMS) processes. We use a computational fluid dynamics (CFD) computer program to simulate the effect of fluid flow, particle diffusion, and magnetic forces on the transport of particles. Using this method, we can simulate the time-dependent spatial and temporal concentration of particles in an HGMS system. In this numerical method, we first calculate the steady-state fluid velocity and magnetic fields. We then simulate the unsteady migration of particles through these velocity and magnetic fields, yielding the particle size-dependent concentration at every point in the system, and as a function of time. By calculating the fraction of particles that penetrate through the system, we can calculate the capture efficiency of the system, which is an important parameter for magnetic filter systems. This CFD-based simulation technique is effective for designing and evaluating HGMS systems.

We conducted this research in collaboration with the Electrotechnical Laboratory, Agency of Industrial Science and Technology, Ministry of International Trade and Industry, Iwate Industrial Promotion Center, and Iwate University.

**Keywords:** ultra-fine particles, high gradient magnetic separation, Bi-2223magnet, computer simulation, CFD

#### Related Papers

Development of Bi-2223 Magnetic Separation System, H. Kumakura, T. Ohara, H. Kitaguchi *et al*, presented at Applied Superconductivity Conference 2000

Simulation of High Gradient Magnetic Separation by Computer Fluid Dynamics, H. Okada, T. Tada, A. Chiba, T. Ohara and H. Wada, *ibid*

#### 59 Materials Development through Control of Phase Transformations by High Magnetic Field

*H. Ohtsuka, High Magnetic Field Research Station*

[April 1998 to March 2002]

Structural and functional control of materials through solid/solid phase transformations in a high magnetic field is investigated for the development of new materials or the improvement of materials characteristics. Effects of a high magnetic field on diffusional transformation behavior and transformed structure in Fe-based alloys have been investigated. The specimens used in this study are

Fe-0.4C (mass%) and Fe-1.5Mn-0.1C-0.05Nb for ferrite transformation, and Fe-13Mn-1.0C and Fe-0.8C for pearlite transformation. Ferrite and pearlite transformations are accelerated by a magnetic field. The acceleration of ferrite transformation is due to (1) increase of nucleation rate, (2) increase of growth rate at some temperature range and (3) decrease of austenite grain size by magnetic field, and the effect of (1) is the dominant factor. The Fe-C phase diagram was calculated under various magnetic fields using the susceptibility of ferrite and austenite at high temperatures, and by the Weiss's theory and it was found that (1)  $A_3$  temperature, (2) carbon content of ferrite and (3) eutectoid carbon content are all increased by a magnetic field. The direction of lamella of pearlite observed on the specimen surface was affected slightly by a magnetic field. Effects of a high magnetic field on transformed structure in austenite to ferrite transformation were studied and it was found that aligned structure along the direction of applied magnetic field is formed in austenite to ferrite transformation. This result shows that the application of high magnetic field is useful for the control of structure and variants of transformed phase.

**Keywords:** phase transformation, magnetic field, structure, ferrite, pearlite

#### Related Papers

1. J-K. Choi, H. Ohtsuka, Y. Xu and W-Y. Choo: "Effects of a Strong Magnetic Field on the Phase Stability of Plain Carbon Steels", *Scripta mater.* 43(2000), 221-226.
2. H. Ohtsuka, Y. Xu and H. Wada: "Alignment of Ferrite Grains during Austenite to Ferrite Transformation in a High Magnetic Field", *Materials Trans. JIM*, 41(2000), 907-910.

#### 60 Advanced cryogenic system for ultra low temperature

*A. Sato, T. Numazawa, H. Nagai, F. Matsumoto, S. Nimori and M. Maeda, High Magnetic Field Research Station*

[April 1999 to March 2004]

Superconducting magnet performance will be increased when operated at low temperature below 4 K. The stability of the magnet will be also increased by improvement of heat transfer characteristics especially in the superfluid helium.

In the conventional method, we need a vacuum

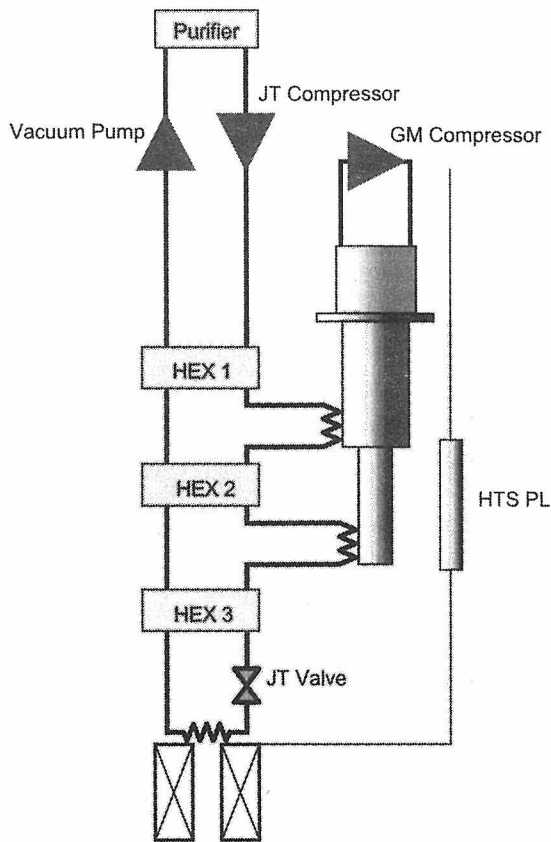


Figure 1 Cooling system overview.

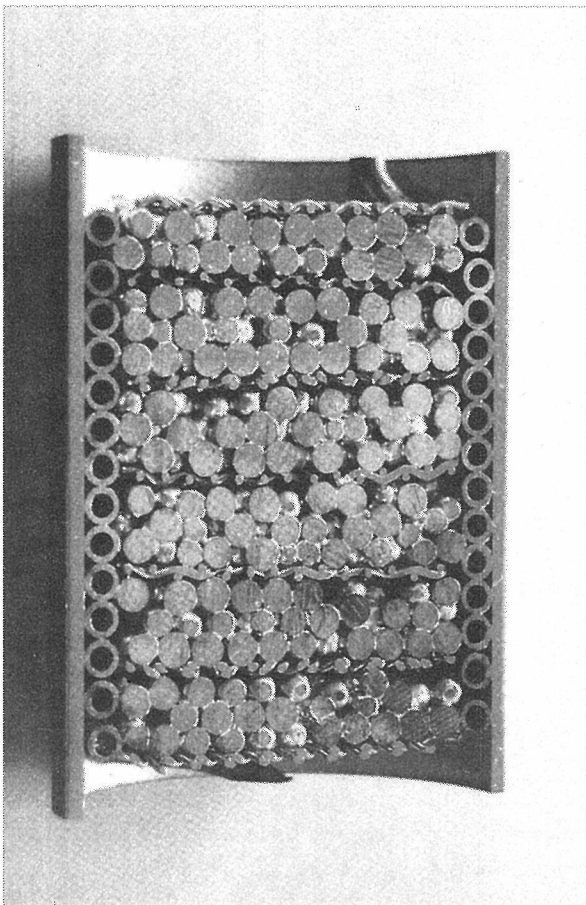


Figure 2 Cross section photograph of the heat exchanger.

pump to get a saturated superfluid helium and a cryostat with complex structure. As the result the cooling system will become larger and more complicated. So the use of the low temperature is limited by the surrounding space.

In this research, we aim to develop a handy, small cooling system with a practical cooling power at temperature below 2 K. We will develop an advanced 0.3 K cryogenic refrigerator by using our research results on the 2 K refrigerator and the regenerator. The 2 K refrigerator will be used in the conduction cooled high magnetic field magnet system, in which the safety against magnet quench will be highly improved.

This research consists of the following two research items.

### 1. Cooling system

The Joule-Thomson (JT) expansion cooling system combined with GM refrigerator has been developed to prove the validity of our system (Fig.1). JT circuit of an existing GM/JT refrigerator was modified by adding vacuum pump and purifier. The heat exchanger was used without modification. Cooling test was performed using a helium gas cylinder as a high pressure source. The minimum temperature of 2.03 K was achieved. To achieve lower temperature and higher cooling power, we need a heat exchanger of more highly efficiency and less pressure loss. We have developed the heat exchanger packed with copper spheres for low pressure side. The copper sphere surface will increase the heat transfer area. Figure 2 shows the cross section of the heat exchanger. The optimum conditions of size of the copper spheres and thickness of silver-plating and the temperature for the heat treatment were decided. These results can be applied to an experimental model of 2 K refrigerator.

### 2. regenerator with high heat capacity

A magnetic material is promising as a regenerator to achieve ultra low temperature. A new magnetic regenerator materials for refrigerator has been studied. Some rare-earth oxide magnetic materials have potential to provide a high heat capacity below 4 K. We found that perovskite  $GdAlO_3$  (GAP) had considerably large volumetric capacity below 4 K. The volumetric capacity of the GAP is four times larger than the one of  $HoCu_2$  at 3.5 K. A great improvement of the cooling power is expected compared with a refrigerator using a conventional regenerator. Fine particle of the polycrystal GAP between 100 and 500 microns in diameter were fabricated by a chemical process. We have established the fabrication condition of the high quality GAP polycrystalline sphere.

The refrigeration test was done with a 4 K pulse

tube refrigerator with a 3.3 kW compressor unit from a practical point of view. The cooling power was increased remarkably from 165 mW to 250 mW at 4.2 K by changing the HoCu<sub>2</sub> to the GAP in the low temperature portion of the second regenerator. The minimum temperature without heat load was reduced from 2.9 K to 2.5 K.

## 61 Test Methods for Superconductors

*H. Wada, K. Itoh, M. Yuyama, A. Sato, T. Takeuchi and M. Kosuge, High Magnetic Field Research Station*

*H. Kitaguchi, T. Kuroda and K. Kumakura, 1st Research Group*

[April 1997 to March 2002]

It is very important to establish and standardize the test methods for metallic and oxide superconductors in order to promote their development and utilization. In this study we work on pre-standardization of test methods, together with a large number of domestic and overseas research laboratories, in the framework of VAMAS. Results obtained will be the base of the international standards at the IEC/TC90; an international organization responsible for the standards of superconductors.

In this study we intend to establish and pre-standardize;

- 1) critical current measurement methods of Ag-sheathed oxide superconductors,
- 2) critical current measurement methods under mechanical strain and
- 3) ac loss measurement methods.

In addition to these, we intend to establish a database system containing electromagnetic, thermal and mechanical property data of superconducting and other materials, which are necessary for designing superconducting and cryogenic devices.

In fiscal 1999, we summarized the results obtained before in the domestic round robin tests on the critical current measurement method of oxide superconductors. We drafted a measurement standard (guideline) and submitted it to the VAMAS. The draft was then discussed at the IEC/TC90 and published as an international standard.

In the same year, we developed a critical current measurement apparatus with a variable field-to-sample-angle mechanism and a variable temperature cryostat. Using this apparatus, we successfully measured the angular dependence of the critical current for a PAIR processed Bi-2212 tape conductor at 10-50 K and estimated the highest operating temperature of the conductor as a magnet

winding to be approximately 20 K.

As for the strain effect measurement methods, we made a literature survey and preliminary measurements on "uniaxial" and "bending" strain effect measurement methods. We established a simple and reliable bending method and proposed a round robin test based on this method.

As for the database system, we investigated the scope, data format, accessibility, etc. and constructed a small test system, in which we placed a stable and reliable workstation as a database server. We could access the database from most of popular web browsers via Internet. We confirmed that the system was workable from viewpoints of accessibility, search time and search-result and graphics presentations. In consultation with experts in the field of cryogenics we have been choosing materials and properties to be inputted to the data-base. So far we have inputted more than 3,000 data of thermal conductivities, thermal expansion coefficients, specific heats, resistivities, Young's moduli and Poisson ratios for copper, aluminum and stainless steels. We have also inputted more than 1,200 data of thermal conductivities, thermal expansion coefficients and specific heats for some other metallic elements and alloys.

**Keywords:** international standard, superconductor, measurement method, database

## 62 Measurement technologies and reference materials for low temperature thermophysical properties of solids

*A. Sato, T. Numazawa, F. Matsumoto and H. Nagai, High Magnetic Field Station*

[April 1997 to March 2002]

A national project has been started in 1997 to establish measurement technologies and reference materials for thermophysical properties of solids. We have joined the project for low temperature properties of solids on heat capacity and thermal conductivity. Since it is required to clarify the uncertainty in measurements and the characters of materials for reliable thermophysical property of data, we started to develop the both measurement systems by using the latest technologies. For heat capacity system, we have developed a heat relaxation method in the temperatures between 0.3 K and 200 K and the magnetic field up to 12 T. By using newly developed dilution refrigerator, the temperature region will be extended down to 0.1 K. A new chip with RuO<sub>2</sub> sensor has been developed to measure 0.1 K region. For thermal conductivity

system, a steady heat flow method was used and it covered the temperatures from 2 K to 200 K with the magnetic field of 5 T. The measurement range has been extended from 0.5 K to 300 K with magnetic field of 8 T. Several candidates of reference materials have been measured. Some garnet, ortho-aluminate and vanadate oxide crystals including rare-earth elements have been chosen and measured from the view point on the sharp magnetic transition peaks in the heat capacity and on the large magnetic field dependence of the thermal conductivity. Polycrystal of transparent YAG has been measured on thermal transportation properties. There was a clear relation between the deflection of the crystal and the thermal conductivity.

**Keywords:** measurement technology, reference materials, low temperature thermophysical properties

### Recent Publications

Magnetic Regenerator Materials for Sub-2K Refrigerator, T. Numazawa, O. Arai, A. Sato and M. Okamoto, *Advances in Cryogenic Engineering*, vol.46 (2000):421.

Thermal Conductivity of Isotropically Enriched Beta Rhombohedral Boron Crystal, N. Nogi, T. Numazawa, S. Tanaka and T. Noda, *Trans. JIM* (2000)

### 63 Measurement technologies and reference materials for low temperature thermal expansion of solids

*A. Sato, T. Numazawa, F. Matsumoto and H. Nagai, High Magnetic Field Station*  
[April 1997 to March 2002]

A national project has been started in 1997 to establish measurement technologies and reference materials for thermophysical properties of solids. We have joined the project to study low temperature thermal expansion property of solids. We have developed a thermal expansion measurement system between 5 K and 300 K. Strain gage sensors were used with a clip which was consisted of Ti-6Al-4V. This clip can be easily set to samples. The cold stage, which controls the sample temperature between 5 K and 300 K has been built by using a helium 4 refrigerator. The temperature controller could set the sample temperature within 0.1 K error above 20 K. The thermal expansion clip has been calibrated by using several reference materials such as Cu or Ti. The total error from 300 K to 10 K was estimated within 10 %. We have established most simple method to measure

the thermal expansion and sample preparation. Several materials have been listed to measure the thermal expansion below 300 K. Since most materials show very small amount of thermal expansion change below 20 K, the selected materials are considered from some unique magnetic properties such as a sharp lambda magnetic transition in RSm system (R=Ho, Dy, Gd) or Yahn-Teller effect in DyVO<sub>4</sub>. In particular, DyVO<sub>4</sub> showed clear anomaly on thermal expansion at 14 K where its crystal structure changes.

**Keywords:** measurement technology, reference materials, low temperature thermal expansion

### Recent Publications

Magnetic Regenerator Materials for Sub-2K Refrigerator, T. Numazawa, O. Arai, A. Sato and M. Okamoto, *Advances in Cryogenic Engineering*, vol.46 (2000):421.

Thermal Conductivity of Isotropically Enriched Beta Rhombohedral Boron Crystal, N. Nogi, T. Numazawa, S. Tanaka and T. Noda, *Trans. JIM* (2000)

### 64 Development of superconductors for ultrahigh field uses

*T. Takeuchi, High Magnetic Field Station*  
[April 1999 to March 2002]

Recently, the so-called 'Rapid-Heating, Quenching and Transformation' (RHQT) method has been developed to obtain long and ductile supersaturated-solid solution Nb(Al)<sub>ss</sub>, which is subsequently transformed to stoichiometric Nb<sub>3</sub>Al with fine grain structures. The achieved high stoichiometry accounts for the substantially improved high-field performance and is compatible with the excellent strain tolerance that makes Nb<sub>3</sub>Al superior to Nb<sub>3</sub>Sn conductors. Thus, the RHQT Nb<sub>3</sub>Al conductors are promising as a candidate for large-scale applications such as fusion magnets, accelerator magnets and GHz class NMR magnets.

$J_c$ - $B$ - $T$  characteristics which are important for the magnet design, were measured for RHQT JR and RIT Nb<sub>3</sub>Al conductors in this work. Further, a critical surface of the  $J_c$ - $B$ - $T$  characteristics are given by a temperature scaling law, which agrees well with the experimental results in wide temperature and field ranges. The critical surface enables us to evaluate  $J_c$  in low magnetic fields and low temperatures, where the current capacity is too large to measure it. Fig. 1 shows the critical sur-

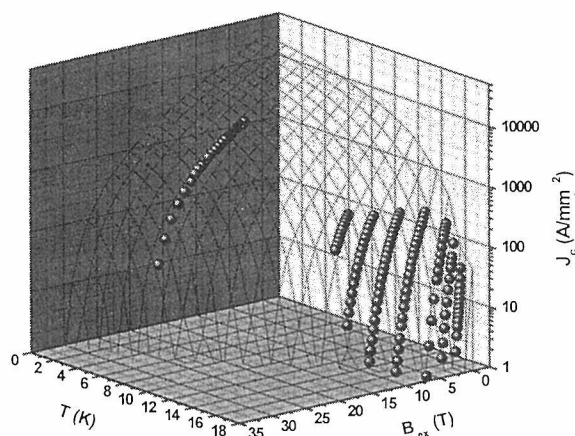


Fig. 1. 3D critical surface for RHQT JR Nb<sub>3</sub>Al wire and experimental results.

face of the  $J_c$ - $B$ - $T$  estimated for the measured RHQT JR Nb<sub>3</sub>Al wire. The  $J_c$  at 10 T, 4.2 K is estimated as 3400 A/mm<sup>2</sup> from the scaling law, which is important for design of superconducting accelerator magnets. Besides, the results of the scaling law suggests that  $J_c$  at 1.8 K, 23.5 T which is the field desired for the 1 GHz NMR magnets, may be estimated from  $J_c$  at 4.2 K, 21.0 T for convenience.

**Keywords:** transformed Nb<sub>3</sub>Al superconductors, high field, temperature scaling

## 65 Development of Fundamental Technologies for Excited Neutral Beams

*Y. Yamauchi, Neutral Beam Unit, High Resolution Beam Research Station*

[April 1997 to March 2002]

The electronic states of surfaces play significant roles in chemical reactions and crystal growths on surfaces of materials. The excited neutral beams are promising probes to get information from exactly outmost surfaces rather than electron or photon beams. Fundamental technologies to generate excited neutral beams are being developed.

In spite of the fact that photoelectron spectra or electron-excited secondary electron spectra include the information on the outermost layer, photons and electrons penetrate through the outermost layer and reach to more deeper layers. Those spectra contain the information on deeper layers where the ejected electrons are generated. Thus some ambiguity remains whether any features of spectra are originated from the outermost layer or the deeper layers. On the other hand excited neutrals also may release their internal energy to the surface electrons. The slow neutrals with a kinetic energy

of several tens meV are reflected by the potential which comes from the surface atoms and never reach to the deeper layers. The ejected electrons pick up only the information on the electronic state outside of the top-most layer. Therefore slow excited neutrals are essentially sensitive to the electronic state of adsorbed molecules or states spatially extended wave function from the surface to the vacuum. Further the spin selected neutral beams enable us to understand surfaces more precisely.

The present project includes two kinds of technologies, i. e., generating techniques for excited neutral beams and detecting techniques for secondary particles ejected from irradiated surfaces. As regarding to the beam forming, a beam system creating high density neutral beams under a clean vacuum environment, exciting atoms by electron impacts, removing ions and high Rydberg atoms, selecting the velocities, and polarizing the electron spins of atoms will be developed. Means to measure the energy angular distribution and the spin polarization of ejected low energy electrons will also be investigated.

Based on the fundamental technologies developed during the course of the present project, we have constructed an SPMDS apparatus. The apparatus is a scanning Auger electron microscope (cylindrical mirror analyzer (CMA), PHI 590A) combined with a metastable helium atom beam source and a Stern-Gerlach analyzer. The pulsed discharge version of a nozzle-skimmer discharge source simultaneously produces a metastable helium atom beam pulse and He I photon pulse but they reach the sample at different times. Both the MDS and UPS spectra are obtained in the same sample configuration by switching the time window of the signal acquisition from the CMA. Radiation of 1083nm from a laser diode (SDL 6702) is circularly polarized by a 1/4 plate then pumps He(2<sup>3</sup>S) of the incident beam up to He(2<sup>3</sup>P) with an increased or decreased spin quantum number under a magnetic field of 0.3 Gauss parallel to the radiation path. The polarization degree of the incident He(2<sup>3</sup>S) examined by the Stern-Gerlach experiment is nearly unity except that the incident beam contains about 10% He(2<sup>1</sup>S). The polarization of He(2<sup>3</sup>S) is able to be reversed by simply rotating the 1/4 plate. MDS is so surface sensitive that a slight contamination from residual gases even under the UHV environment of 5 × 10<sup>-11</sup> Torr causes a detectable deviation in their spectra. Therefore, the SPMDS spectra for the two opposite polarizations of M<sub>S</sub> = +1 and M<sub>S</sub> = -1 are alternately measured 100 times in 5 minutes to eliminate the contamination effect. For this rather rapid alterna-

tion of energy scanning, a data acquisition system is developed by integrating two multi-channel scalers and a computer controlled 1/4 plate rotator with interface electronics.

The apparatus has been successfully employed for the measurement of the spin dependence for SPMDS spectra of iron films deposited onto MgO(100) substrates in two opposite spin polarizations. Iron films were grown on MgO(100) single crystal substrates in the measurement chamber by the vapor deposition of 99.99% iron using an electron bombardment evaporator (Omicron EFM3). The pole figure of the x-ray diffraction of the iron film indicated that the structure was bcc Fe and that Fe(100) was parallel to MgO(100) but the [010] direction of Fe was parallel to the [011] direction of MgO. The remanence of the iron film was checked by the simple ex-situ magneto optical Kerr effect experiment. The iron films were magnetized in plane and transverse to the primary beam. At the analyzing spot of the CMA, the magnetic field was adjusted to 0.1 Gauss in the parallel or antiparallel direction to the remanence of the iron films. The spin dependence of SPMDS spectra was clearly observed for the magnetized iron film. The capability of the SPMDS apparatus in the investigation of the magnetism of outermost surfaces has been confirmed.

**Keywords:** neutral beam, metastable atom, excited neutral, surface

#### Recent Publications

Electron Spin Detection of Magnetic Surfaces by Means of Metastable Atom beams, Proc. 10th Sympo. Beam Engineering of Advanced Material Syntheses (1999): 9-12.

Metastable Helium Atom Stimulated Desorption of H<sup>+</sup> Ion, Phys. Rev. Lett. 84 (2000): 4725-4728.

66 Advanced characterization of micro and nano meter scale structure of materials by brilliant synchrotron x-rays at the SPring-8

*K. Sakurai and H. Eba, High Resolution Beam Research Station*  
[April 1997 to March 2002]

The present research program aims to establish new techniques for analysis with super precision and high resolution to evaluate micro and nano meter scale structure of materials. So far, micro X-ray fluorescence (XRF) imaging has been performed by a 2D positional scan of a sample

against a collimated beam. Although a synchrotron microbeam can enhance the spatial resolution down to 1~0.1  $\mu\text{m}$ , the total measuring time becomes quite long (a few hours to a half day), since one needs a number of scanning points in order to obtain a high-quality image. In this report, the performance of alternative technique based on completely different concept is demonstrated.

In the present experiment, a grazing-incidence arrangement is employed to make primary X-rays illuminate the whole sample surface. Parallel-beam optics and extremely-close-geometry are adopted in order to detect XRF with a CCD camera. Since scanning of the sample and/or incident beam is not necessary, the measuring time is reasonably short, typically 20sec.~3min. The spatial resolution is given as a product of the collimation (i.e., angular divergence),  $\phi$  and distance from the sample surface to the CCD device,  $d$ . Therefore it is extremely important to shorten the distance  $d$ . Details of the present XRF microscope are described elsewhere.

Figure 1 shows an X-ray image for a patterned chromium thin film (~1000Å) evaporated on the glass substrate (commercially available, for checking resolution). The image is in very good agreement with the optical image, and that X-ray fluorescence can give information on specific elements. The estimated spatial resolution is around

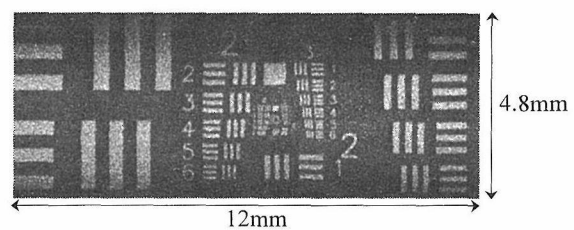


Fig.1 Metallic Cr thin film on glass substrate Incident X-ray Energy 7.2keV / Exposure Time 50sec

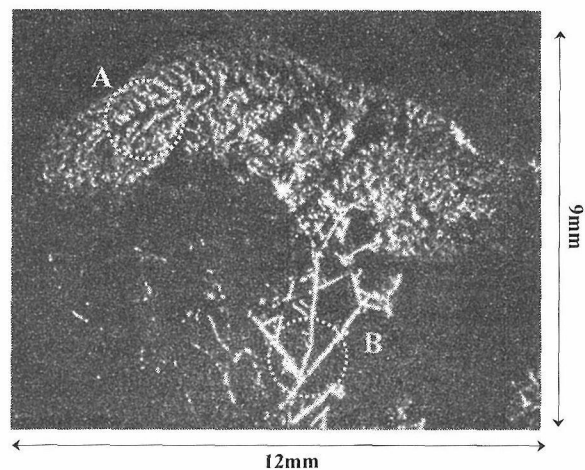


Fig.2 Ag dendrites precipitated from solution Incident X-ray Energy 7.2keV / Exposure Time 2min  $\times$  4

20  $\mu\text{m}$ . It should be noted that the exposure time required is only 50 sec.

Another example is shown in Fig.2. This is an image for silver dendrites grown from solution dropped on a silicon wafer. Different patterns are observed, for example, in the area A and B. This is because of different reaction rate due to concentration fluctuation and other conditions for diffusion. The image is obtained by 4 shots to the different part of the sample, because the synchrotron beam is vertically small. Although a CCD camera is not used as an energy-dispersive detector in this case, the use of tunable monochromatic synchrotron radiation can identify the kind of elements by differentiating the images obtained at the incident X-ray energy below and above the absorption edge of the element of interest. In the same way, chemical-state imaging can be also performed by using chemical shifts of absorption edges. The authors would like to thank Prof. A. Iida for his valuable discussion.

**Keywords:** synchrotron radiation, materials characterization, spectrometer, X-ray fluorescence

#### Recent Publications

Total-reflection X-ray Fluorescence Imaging: K. Sakurai, *Spectrochim. Acta B54*, 1497 (1999).

#### 67 Surface Chemical Analysis

*K. Yoshihara, The Center for Advanced Physical Fields*

*M. Yoshitake, Extreme High Vacuum Station*  
[April 1998 to March 2000]

Surface chemical analysis is a relatively new field, starting embryonically in 1968 in a few University departments. The major growth in applications of the techniques occurred in the last decade as the instrumentation developed. During this period the field of applications of surface analysis, both in academic research and in industry, grew widely to range from failure processes in advanced materials to the development of catalysts and microelectronics.

This project is closely related to the VAMAS activity. Within the VAMAS research project three main objectives were defined. (i) to provide the measurement infrastructure required for setting standard methods of specifying surface chemical analysis. (ii) to develop an agreed base for principles, definitions and equations for relevant aspects of surface analysis techniques and (iii) to identify ref-

erence procedures for materials, data, instrumentation and measurement methods. To meet these objectives, 31 sub-projects have now been established in VAMAS community. It is easier to understand the structure of this program if we note that the work naturally falls into one or more of five distinct areas. (i) the development or validation of the basic theory for the physical process involved in the techniques. (ii) the understanding and calibration of the measuring instruments. (iii) the development or calibration of software for data reduction and for communication. (iv) the development of reference materials and (v) the determination of reference data. Below we describe, briefly, developments in these areas.

In 1992, ISO/TC201 committee has been established, the objective of which is the standardization of surface chemical analysis. This committee has liaison with VAMAS Surface Chemical Analysis group and the fruits of VAMAS activities are transferred to ISO/TC201 as the ISO standards.

Since the VAMAS project has started in 1982, we have investigated the reliability of the quantification with AES and XPS with round robin, and proposed calibration procedures for the energy and intensity scales. Since 1989, we have also been constructing the spectral data processing system. This system is called Common Data Processing System (COMPRO). COMPRO is designed to be a program to convert an original spectral data file structure to common one (VAMAS standard data transfer format), to assess the data processing procedures proposed by scientists, to calibrate energy and intensity scales, to check a spectrum, and to build both spectra and correction factor database. In this system, the spectral data acquired on different instruments and/or computers can be compared to one another. By using this software, users of surface analytical machines can easily use the calibration process proposed by the VAMAS community.

Nowadays, it becomes very important to analyze the small area of surfaces, so that primary beam current density increases and may deteriorate the surface structure, and gives wrong information on surfaces. So it becomes important to estimate the degradation and to find the procedure to minimize the damage of surfaces. Since 1997, we have started a new research project on the damage induced by the primary beam.

In XPS, it is often observed that the X-ray flux may cause changes in the surface structure and chemistry in the surface region of organic materials. R.G. Copperthwaite summarized the radiation-induced chemical damage. (SIA 17, 2(1980)) G. Beamson and D. Briggs published the handbook

of X-ray spectra of organic materials and reported the degradation rates by X-ray flux in 1992. (High Resolution XPS of Organic Polymers, John Wiley & Sons, Chichester(1992)) Recently, Organic Materials Group of Surface Analysis Society of Japan reported the degradation rates of nitrocellulose by X-ray radiation, and concluded that peak intensity change of N is the indicator of the degradation if it is normalized by the X-ray source intensity. (J. Surf. Anal. 5(2), 220 (1999), J. Surf. Anal. 5(2), 224 (1999)). However, there is no standard guide to estimate the relation between the degradation rate and X-ray source strength.

The objectives of this project are: (1) to develop a procedure to estimate the degree and possible the nature of the degradation caused by X-ray irradiation during analysis, and (2) to evaluate the possibility of using the degradation behavior to estimate a relative X-ray source flux, density. To achieve these objectives, the Surface Analysis Society of Japan (SASJ) has prepared 3 kinds of organic materials [i.e. nitrocellulose + cellulose acetate (NC+CA), poly(vinylchloride) (PVC), and poly(tetrafluoroethylene) (PTFE)] which are attached to a thin aluminum sheet. These specimens were distributed to the participants and 40 institutes from 7 countries returned the results.

From this round robin, we can get the following conclusions: (1) it is rather difficult to find the correlation between silver intensities and the degradation rates of polymers in the interlaboratory test using various instruments, (2) there exists the fairly good correlation between the degradation rate of PVC and that of NC+CA, if the analysis is carried out using achromatic X-ray sources, (3) the degradation behavior of PTFE is so complicated, and it is hardly possible to get the correct degradation rate, (4) PVC and NC+CA will be good indicators to determine X-ray source strength in common.

**Keywords:** VAMAS, XPS, Degradation, Organic films

#### Recent publications

H. Tokutaka, K. Yoshihara, K. Fujimura, K. Iwamoto and K. Obu-Cann, Application of Self-organizing Maps (SOM) to Auger Electron Spectroscopy (AES), Surf. Interface Anal., 27, 783-788(1999)

A. Rar, S. Hofmann, K. Yoshihara and K. Kajiwara, Optimaization of depth resolution parameters in AES sputter profiling of GaAs/AlAs multilayers structures, J. Appl. Surf. Sci., 310, 144-145(1999)

S. Hofamm and K. Yoshihara, The MRI-model in COMPRO5:A new Data Processing Software

for the Quantitative Evaluation of Sputter Depth Profiles, J. Surf. Anal., 5, 40(1999)

#### 68 Development of Low Frictional Vacuum Materials with Strain Energy by Supersaturation as Trigger for Self-organization

*M. Tosa and A. Kasahara, Extreme High Vacuum Station*

*K. Yoshihara, Center for Advanced Physical Fields*

[April 1999 to March 2001]

Hexagonal boron nitride (h-BN) segregated on the surfaces of metals or alloys doped with boron and nitrogen can form the preferred (0001) crystal basal plane parallel to the base substrate material surface by self-organization. The binding force between c planes is much smaller than those of other planes and the friction force on the plane will be small in case of the horizontal force due to easy slide of the plane. The property of the small adsorption force of segregated h-BN layer will be applied to the vacuum micro scanning probe system without large sliding friction which leads to the development of the advanced memory media disc system with a huge amount of memory volume. This study therefore aimed the fabrication of h-BN layer with preferred (0001) crystal plane parallel to the base substrate by means of the control of surface segregation using strain energy.

The co-sputtering deposition process and the following vacuum annealing can prepare the h-BN compound layer on the surface of the sputtered film substrate with BN and alloy targets. Segregated BN can cover the film substrate prepared by the co-sputtering copper and BN. Tribological property of prepared BN film is evaluated with sliding friction force. We developed the vacuum micro-friction measuring device which can measure sliding friction force in range of from an atmospheric pressure down to ultra high vacuum pressure of  $10^{-8}$  Pa by a tandem turbo molecular pumping system. The range of loading weight can be also changed from about several 10 N down to less than  $100\mu$  N in the same range of vacuum pressure. The friction coefficient ( $\mu$ ) of the substrate of mixture of BN and copper partially covered with h-BN keeps less than 0.1 and the value can be less than one-third compare with no BN covered substrate at an atmospheric pressure of  $10^5$  Pa and in the ultra high vacuum of  $10^{-8}$  Pa. Decrease in loading weight from 1N to below 1mN increases the friction coefficient of no BN covered substrate by several ten while that of BN partially covered

substrate can keep almost constant (between 0.1 and 0.2) without large increase.

This shows therefore that the BN surface segregation can well improve vacuum micro-tribological property of the material and can be a good candidate for vacuum mechanical material and micro-gap scanning system in a vacuum.

**Keywords:** self-organization, surface segregation, co-sputtered film, vacuum tribology, hexagonal boron nitride

#### Recent Publication

Effect of Surface Properties on the Vacuum Friction Characteristics of the Stainless Steel, M. Tosa, A. Kasahara and K. Yoshihara, J. Surface Science Soc. Japan 21(1999): 434-437 (in Japanese)

#### 69 The Chamber Material for Standard Vacuum Pressure Measurement

*M. Tosa and A. Kasahara, Extreme High Vacuum Station*

*K. Yoshihara, Center for Advanced Physical Fields*

[April 1997 to March 2002]

Calibration of standard vacuum pressure gauge requires the surface modification method to generate the standard pressure field with accurately controlled constant pressure and the study of the interaction among the chamber wall material surface and the hydrogen behavior of deposition and permeation and residual gas molecules. The main residual gas in the vacuum chamber mainly contains hydrogen molecules in the ultra high vacuum. The reduction of the hydrogen behavior is therefore inevitable for the generation of standard stable vacuum field for the calibration of standard vacuum pressure gauge and the project aims the development of advanced surface modification of the vacuum chamber wall material which can reduce the hydrogen behavior to disturb the steady standard vacuum field.

The improvement of surface modification is studied by the application of surface segregation of hexagonal boron nitride (h-BN) on the copper surfaces. Copper metal is excellent in low hydrogen solution, high thermal and electric current conductivity and high vacuum packing but suffers from easy oxidation which becomes large outgassing source. The surface of h-BN is excellent in low gas adsorption but is brittle and the preparation of BN layer on the substrate is not so easy. Co-sput-

tering deposition technology using helicon radio frequency wave with a sintered disc of BN and Cu disc deposited the mixture of Cu and BN (Cu/B/N) on the Cu substrate. Helicon radio frequency sputtering deposition method can separate BN and Cu targets and can control wide range sputtering plasma yield with little damage on the substrate surface by plasma. Annealing the Cu/B/N film removed all three main copper Auger spectra peaks observed with Auger electron spectroscopy (AES), decreased carbon and oxygen peaks largely, then boron and nitrogen peaks increased much higher. Scanning AES image shows the perfect uniformity of the surface coverage by BN and little gas adsorption on the surface after an atmospheric exposure. X-ray photoelectron spectroscopy (XPS) measurement shows that  $\pi$  bond shake-up satellite of boron peak peculiar to h-BN. It is concluded that h-BN segregated uniformly on the all surface of the deposited film. The diffraction image revealed that segregated BN layers had the preferred orientation and tended to cover the segregated surface with the basal c plane (0001). Atomic force microscope (AFM) measurement shows that the surface of the segregated h-BN layer has same value of van der Waals' force as that of a sintered h-BN disc ( $\sim 1$ nN). Lateral friction force on the surface of Cu/B/N film after annealing is kept nearly constant 0.03nN as the load increases. The friction coefficient on the surface of as deposited film increases from 0.03 to 0.26 as the load increase, which also increases from 0.01 to 0.17 on the surface of the segregated h-BN layer. The distribution of the lateral friction force and coefficient on the surface of the h-BN layer of Cu/B/N films shows much more homogeneity than that of as deposited film.

This concludes therefore that the BN surface segregation layer on the substrate mixed with BN and copper can weaken surface interaction with atmospheric gas molecules in the vacuum chamber and can much lower gas adsorption on the surface of the chamber wall for the steady standard vacuum field.

**Keywords:** gas adsorption, gas permeation, gas desorption, standard pressure gauge, surface segregation, co-sputtered film, hexagonal boron nitride

#### Recent Publication

Enhancement of h-BN Surface Segregation, Y.S. Kim, Tosa, A. Kasahara and K. Yoshihara, J. Vacuum Soc. Japan 43(2000): 234-246(in Japanese)

## 70 Combinatorial Study on Interface and Surface of Functional Materials

*Toyohiro Chikyow, Extreme High Vacuum Research Station*

[June 1999 to March 2004]

For the future Large Scale Intergrated Curcuit (LSI), functional oxide materials, which is composed of several elements, are required to realize a better performance with more high density packing, higher processing speed and more power saving. For this purpose, some of the candidates are already on naminated. However, it is difficult to find optimum stoichiometry for several elements in a short term. Also, growth of oxide requires oxygen atmosphere; surfaces of semiconductor materials must be exposed in an oxygen free atmosphere in their growth to avoid their surface oxidation. To avoid the surface oxidation, some surface passivations or protection layers must be deposited on the surface before oxide growth. But this process also provides us a developing term problem to choice best termination or passivation method. In both case, a lot of elements and parameters must be handled. To solve the problem of handling, in this research program, a combinatorial methodology is employed to find best stoichiometry or best termination. Also it is used to find an answer to compromise the contradictory growth conditions of oxide and semiconductors. The combinatorial methodology was proposed from a hint and an analogy of the Combinatorial Chemistry.

### 1) Combinatorial methodology for material science and sythesis

In this method, lots of combinations of materials are formed on a substrate using masks or composition gradient system in one experiments. In some case, a combination of materials is formed with a temperature gradient heating system. Using these equipments, a set of samples are made in a short term, providing an efficient material synthesis. Another advantage of this method is that only one experiment can bring an accurate date because except variations, other parameters are commonly fixed. This factor also gives another efficiency in understanding phenomena in material synthesis.

### 2) High Throughput interface structure characterization

In the combinatorial oxides growth, a large numbers of sample are made with a number of variations in one experiment. For investigating these interfaces, position specified sampling and quick fabrication for the high resokution transmission electron microscopy (HRTEM) are required. For this purpose, a micro sampling method was em-

ployed. The micro sampling method is a combination of the focused ion beam system and small chip manipulation. At the beginning, a specimen, 2micron  $\times$  15 micron in size was cut from the interested region on the combinatorial samples. The specimen was picked up by manipulator and fixed on the edge of TEM sample mesh. Thin foils are fabricated from the specimen by FIB to characterize the interface structure. It was only required for several hours from the beginning to the end. TEM apparatus is equipped with the electron energy loss spectroscopy and imaging system. Elemental information and mapping is possible. The obtained images and chemical information are also delivered using Internet.

### 3) New idea for abrupt oxide/Si interface formation

An As-terminated Si (100) surface shows a chemically stable surface because whole dangling bonds at the surface are filled with electrons. Actually this surface showed durability in an oxygen atmosphere for more than 30 min at 400 C. On this surface, oxide materials are expected to grow with a sharp interface. Actually on the As-terminated Si surface, an abrupt interface of CeO<sub>2</sub>/Si was observed by high resolution transmission electron microscopy (HRTEM). On the conventionally processed Si surface, however, SiO<sub>2</sub> and additional amorphous CeO<sub>2</sub> regions were observed as ever reported. Apparently, From the results, surface passivation including the As-termination was found to play a crucial role for the abrupt oxide/Si interface formation.

In the successive research, another interfacial layers and oxides materials which have higher dielectric properties are investigated by combinatorial synthesis and high throughput charaterization including micro sampling method.

**Keywords:** Combinatorial, oxide, semiconductor, interface, HRTEM

## 71 Study on Strengthening of Ferrite Matrix Steels for Welded Structures

*K. Nagai, S. Torizuka, H. Nakajima, T. Hayashi, T. Hanamura, T. Mitsui, J. Takahashi, N. Sakuma, T. Saito, T. Shimizu, S. Wanikawa, M. Otaguchi, H. Shinohara, T. Inoue, N. Tsuchida and I. Salvatori, Materials Creation Research Station*

*S. Tsukamoto, G. Asai, I. Kawaguchi, S. Kuroda, K. Hiraoka, T. Nakamura, R. Itoh, Y. Kawaguchi, K. Sasabe, S. Meguro, T. Ohtani, Y. Muramatsu, H. Yamawaki, I. Uetake and C. Shiga, Joining and Interface Research Sta-*

tion

A. Ota, N. Suzuki, Y. Maeda and N. Nguyen,  
*Strength and Life Evaluation Research Station*  
H. Irie, *Mechanical Properties Division*  
[April 1997 to March 2002]

Building steel is one of major mass-produced items in the steel market. Easier recyclability, more efficient and less skilled welding and enhanced mechanical properties will be required for the building steels in the next century to construct sustainable infrastructure. However, present high strength steels of 600-800 MPa in tensile strength contain the alloying elements undesirable for recycle, and their welded joints show very poor fatigue strength, i.e. only one-tenth of tensile strength.

Low strength C-Si-Mn ferritic steels are potential alternatives, since they are easy to recycle and weld. To overcome the low strength, in the present study, the ultrafine grain structure has been aimed to create the ferrite grain size under 1 micron and double the strength for a 0.15wt%C steel (SM490 grade). An ultra-fine grain ferrite-cementite structure was produced with a ferrite grain size less than 1 micron. Based upon the preliminary accomplishments, the 18 mm square rods were manufactured. They showed tensile strength of 680MPa and ductile-to-brittle transition temperature of 77K.

High speed and no defect welding has to be developed coincident with preserving the ultra-fine grained microstructure from its heat in the heat-affected-zone (HAZ). In arc welding, an ultra-narrow gap arc welding processing was developed with an idea of simultaneous control of low heat distribution and large electricity input to make the HAZ as narrow as possible. Nineteen mm-thick steel plates joined by 2-pass processing showed a 2mm-wide HAZ. And further, a high-power CO<sub>2</sub> laser one-pass welding has been elucidated. A main problem is that plasma generation due to metal evaporation deteriorates the efficiency of laser beam heat. A high-power machine has been successfully introduced for further studies.

The samples having the ultrafine grain microstructure were subjected to various welding processing. The arc-welded samples showed 'softening' at the HAZ according to input heat. The spot-welded sample revealed almost ideal hardness distribution without any specific hardened region at the whole joint. The hardness variation was characterized in terms of microstructural evolution on welding.

Welded specimen large enough to simulate the conditions for service was subjected to mechanical tests with a large capacity of power to evaluate

the fatigue property. The lower fatigue strength of welded joints has been tried to basically increase by using a newly designed welding rod with a lower transformation temperature. With introducing compressive residual stress at the welded joints, the fatigue strength of high tensile steel's joint was successfully improved by a factor of three. The fatigue strength of structure member of box section 3.5 m long beams was also improved by inducing compressive residual stress on longitudinal corner weld. Reliable data have been accumulated for the full S-N curves.

Defects might be introduced into the materials and their joints through welding process. Tolerable size of the defects becomes smaller under higher stress conditions expected. Hence, more reliable inspection techniques have been developed like supersonic CT scanning of defects in a welded joint and magnetic flux leak detection by DTF for surface flaws. Laser speckle technique was advanced to follow the strain change at a bead both on heating and on cooling during welding process. The transformation in steels was monitored by chasing the strain deflection.

Finite Element Method was successfully applied to clarify the relationship between strain given in the thermo-mechanical processing and evolved ferrite grain size. And a simulation system to predict the deformation and fracture behavior of welded points has been also developed by combining calculation of stress and strain distribution and experimental tensile tests.

**Keywords:** ferritic steels for welded structures, grain refinement, welding process, heat-affected-zone, residual stress, welded joint, tensile strength, fatigue strength, simulation

## 72 Advanced Ultra-High-Strength Steels (1500-MPa-plus class)

S. Matsuoka, *Frontier Research Center for Structural Materials Strength and Life Evaluation Research Station*  
[April 1997 to March 2001]

There is an increasing demand for ultra-high-strength steel that has a tensile strength exceeding 1500 MPa, for example in the use of higher-strength bolts in the construction industry and in the weight reduction of automobile parts and main cables of long-span suspension bridges. The key to practical implementation does not lie in the achievement of the high strengths but rather in preserving the necessary reliability in the delayed frac-

ture and giga-cycle fatigue properties of the steel.

In the search for advanced ultra-high-strength steels, the center is trying to develop new martensitic steels that contain carbide-free boundaries and hydrogen trap sites to give high delayed fracture resistance. Other martensitic steels containing a large amount of nitrogen is also developed in order to attain a high fatigue resistance. Studies of the mechanisms of delayed fracture and fatigue will reveal new concepts for material design. Such studies require atomic-scale analysis of fine precipitates and interphase boundaries by AP-FIM and nanoscopic analysis of deformation and fracture structures by AFM and nano-hardness tester. Other works will include standardizing the evaluation of delayed fracture and constructing a database that contains fatigue property data for  $10^{10}$  cycle tests.

In the recent year, the activities are summarized in the following.

1. The delayed fracture test and thermal desorption analysis of diffusible hydrogen have been conducted for quenched-and-tempered SCM440 (0.4C-0.24Si-0.81Mn-1.03Cr-0.16Mo) low alloy steel with the tensile strength of 1400 MPa, changing the diameter and notch geometry of specimens. In order to examine the influence of applied stress and specimen geometry on critical diffusible hydrogen, the stress-strain state at the notch root was analyzed by the finite element method.
2. The high resistance to delayed fracture was realized for ausformed SCM440 steel with the tensile strength of 1450 MPa. The critical diffusible hydrogen was 4 times higher for ausformed SCM440 steel than for quenched-and-tempered one.
3. Based on the idea that the mechanical properties of inclusions were important to eliminate the fish-eye-type fracture on the giga-cycle fatigue of high strength steels, fatigue tests were carried out for quenched-and-tempered SUP12 spring steel with the tensile strength of 1800 MPa where the mechanical properties of inclusions were controlled. The inclusion-type origin disappeared, while the facet-type origin newly appeared. It was apparent that strengthening the base metal as well as controlling the inclusion was necessary to improve the giga-cycle fatigue properties.
4. Developing the nano-indentation and nano-fractography, the new analytical method of microstructures in nano-, mezo- and macro-scale was established. It was discovered that the nano-hardness was half of macro-hardness for SCM440 steel with the tensile strength of 1400 MPa and that the steel was strengthened

mainly by block boundaries.

**Keywords:** martensitic steel, delayed fracture, giga-cycle fatigue, AP-FIM, SPM, nanohardness tester

### 73 Strategic Research on Advanced Ferritic Steels for 650 °C USC Boilers (R&D of Structural Materials for 21<sup>st</sup> Century)

*Fujio Abe, Strength and Life Evaluation Research Station*

[April 1997 to March 2002]

The creep rupture strength has been improved to develop advanced 9Cr steels for application to large diameter and thick section boiler components such as main steam pipe and header of ultra-supercritical (USC) plant which will be operated at 650 °C and 350 atmospheric pressure. The resistance to Type IV cracking strength loss in welded joints is also serious for construction of thick section boiler components. The further improvement of creep rupture strength of 9Cr-3W base steel has been obtained by the fine precipitates of FePd base L<sub>10</sub> type ordered phase and by the small amount of boron through stabilizing tempered martensitic microstructure. Figure 1 summarizes schematically the effect of MX carbonitrides, FePd-L<sub>10</sub> ordered phase, Fe<sub>2</sub>W Laves phase and boron on the creep rate versus time curves. The fine precipitates of MX carbonitrides and FePd L<sub>10</sub> ordered phase decreases the creep rate from the initial stage of creep, because they present after tempering before creep test. Boron extends the transient region to longer times, resulting in a decrease in minimum creep rate. The precipitation of Fe<sub>2</sub>W occurs during creep and the decrease in creep rate with time becomes more significant with increasing time in the transient region. But the large coarsening of the Fe<sub>2</sub>W promotes the acceleration of creep rate after reaching a minimum creep rate. Full annealed high Cr ferritic steel is another candidate from a viewpoint of minimized degradation in creep strength due to microstructural evolution at long times.

**Keywords:** ferritic heat resistant steel, ultra-supercritical power plant, alloy designing, creep, steam oxidation, fatigue, welded joint

### Recent Publications

Degradation of Mod.9Cr-1Mo Steel during Long-term Creep Deformation, H. Kushima, K. Kimura and F. Abe, *Tetsu-To-Hagane*, 85 (1999): 841- 847.

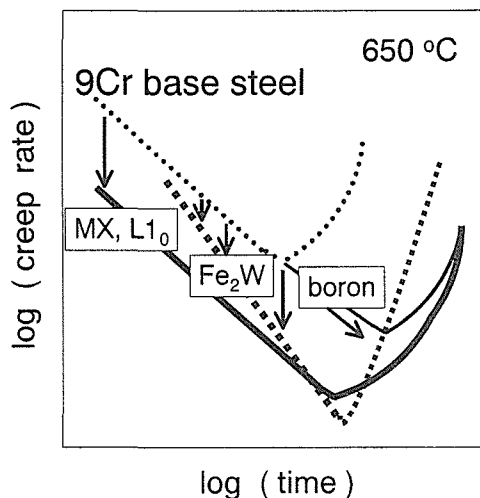


Figure 1 Effect of MX, FePd-L1<sub>0</sub>, Fe<sub>2</sub>W and boron on creep rate of 9Cr steel at 650 °C.

Effect of Thermomechanical Heat Treatment on Creep Characteristics of High Cr Heat Resistant Ferritic Steels, S. Muneki, M. Igarashi and F. Abe, Proc. of Case Histories on Integrity and Failures in Industry, Milan, Italy (1999): 361 - 370.

R & D of Advanced Ferritic Steels for 650 °C USC Boilers, F. Abe, M. Igarashi, S. Wanikawa, M. Tabuchi, T. Itagaki, K. Kimura and K. Yamaguchi, PARSONS 2000 Advanced Materials for 21<sup>st</sup> Century Turbines and Power Plant, The Institute of Materials, (2000): 129 -142.

A New Concept for Strengthening of Advance Ferritic Steels for USC Power Plant, M. Igarashi, S. Muneki, H. Kutsumi, T. Itagaki, N. Fujitsuna and F. Abe, PARSONS 2000 Advanced Materials for 21<sup>st</sup> Century Turbines and Power Plant, The Institute of Materials, (2000): 334 - 347.

Microstructural Change and Degradation Behaviour of 9Cr-1MoV Nb Steel in the Long Term, K. Kimura, H. Kushima, F. Abe, K. Suzuki, S. Kumai and A. Satoh, PARSONS 2000 Advanced Materials for 21<sup>st</sup> Century Turbines and Power Plant, The Institute of Materials, (2000): 590 - 602.

## 74 Enhanced Durability of Structural Steels in Marine Environment

*T. Kodama*

[FY 1997 to 2001]

Among structural steels for the use in marine and coastal environments we have concentrated our effort on the development of stainless steels and coatings that show corrosion resistance in splash zone, and low alloy weathering steels for coastal atmosphere. In the case of stainless steels, its performance in seawater should be evaluated

by the resistance to localized corrosion since it poses a more serious problem than general corrosion. For low-alloy steels that are used in atmosphere, on the contrary its performance is evaluated by the mass loss resulted from general corrosion. Low-alloy steels with different alloying elements were tested for coastal atmosphere using a new acceleration test developed in our laboratory.

### Materials Creation Studies

In the creation of new stainless steels highly resistant to marine corrosion, we have focused on cleanliness and nitrogen addition. The nitrogen addition was motivated by the preservation of less common metals such as Ni, Cr or Mo and the development of fully austenitic, resource-saving steels with the minimum addition of Ni. In this case as a reference material type 316L steel was used. For attaining high content of N in steels, we have developed a system of pressurized electroslag remelting (PESR), in which a stainless-steel rod (primary electrode) was melted by Ohmic heating through the slag layer under pressurized N<sub>2</sub> atmosphere of 1 to 4 MPa to form a 20kg ingot. By PESR a primary electrode of type 316L stainless steel was converted into 1.2% N bearing steels. Cross-sectional analyses of the ingot showed uniform distribution of N both in radial and coaxial directions. The N-bearing 316L SS, however, showed sensitization due to Cr nitride precipitation when it was quenched from 1200 °C. By thermodynamical analyses it was revealed that single austenitic phase becomes stable under the condition of minimum Ni or Mn addition and sufficiently high Cr and N contents. Proposed optimal composition ranged 23Cr-(0 to 2)Mo-(0 to 4)Ni-(1 to 1.5)N. The high-N and low-Ni austenitic stainless steel showed high strength ( $\sigma_B$ ) of 1300 MPa and very high resistance to localized corrosion in seawater. Figure 1 shows the crevice corrosion potential in artificial seawater plotted as a function of chromium equivalence to crevice corrosion ( $Cr+3Mo+10N$ ). New high-N stainless steels are immune to crevice corrosion at 35 °C and at very noble potential as high as that of oxygen evolution in artificial seawater.

### Joining and Surface Coating Study

High-N steels suffer from damages and degradation following melting and heat cycles during welding such as blowhole formation at the joints and sensitization at heat affected zone (HAS). The blowhole formation is associated with the release of dissolved nitrogen from substrate metal when it is melted. Actually blowholes were observed at the joints of 18Cr-14Ni-2.5Mo-0.8N when it was arc-welded using a filler of 20Cr-12Ni-4Mo steel. A proposed compromise to the blowhole formation

is the use of high-alloy filler such as 30Cr-20Ni-5Mo-Fe that shows higher N solubility than that of substrate metal. The higher solubility of the filler prevents the formation of N<sub>2</sub> bubbles at the joints by absorbing the released nitrogen. The welded part was cut into small test specimens to serve for localized electrochemical measurements. Figure 2 shows localized pitting potential of welded portion of 18Cr-14Ni-2.5Mo-0.8N measured electrochemically for specimens cut from weldments. Degradation in pitting resistance occurs when ordinary weld metal is used. The welded part showed a pitting potential as high as that of substrate metal when high alloy filler was employed. The sensitization of HAS occurs similarly to the case of carbide formation in stainless steels. The formation of Cr-nitride and related Cr-depletion zone was analyzed both experimentally and theoretically.

Spray coating gives a promising technique for the production of corrosion-resistant materials, where our goal is to develop a spray coating method that may substitute the titanium cladding. We employed high velocity oxy-fuel (HVOF) spray method in which high velocity particles are sprayed at relatively low temperature resulting in the formation of a pore-free film with improved adherence. Particles of stainless steels and nickel base alloys were sprayed on carbon steels to form corrosion resistant coatings by means of HVOF. Samples coated with pore-free films retain higher potential after prolonged immersion in seawater. For samples with higher porosity the potential drops to a value close to that of carbon steel when penetrated seawater reaches the coating/substrate interface. The penetrated seawater induces galvanic corrosion to substrate metal, which leads to the peeling of the coating. The combination of HVOF and Hastelloy C as a coating metal gives good corrosion performance. Basic studies have been conducted for the elucidation of improved galvanic behavior of nickel-base alloys.

#### Evaluation of Atmospheric Corrosion and Development of Low-Alloy Steels

The development of acceleration tests was initiated from a very basic standpoint; phenomenological but nanoscale analyses of water condensation on metal surfaces and rust nucleation on metal surface. The instrumental techniques included atom-force microscopy (AFM) and Kelvin force microscopy (KFM), which are applied to in-situ corrosion measurements under wet/dry conditions. Conventional scanning probe microscopes (SPM) such as atomic force microscope (AFM) and Kelvin force microscope (KFM) allowed the scanning of limited area of approximately 100 μm. We

have developed a new technique of super Kelvin force microscope (SKFM) which allowed us to measure profile and potential of wider area ranging nm to cm. By SKFM, it is demonstrated that corrosion proceeds by the repetition of the transfer of chloride ion to form FeCl<sub>2</sub> at corrosion front and the subsequent absorption of water owing to its deliquescence property.

Alloyed elements in steels dissolve either in cationic or anionic state in aqueous media followed by the precipitation in the form of rust. Since rusting is the process of colloidal coagulation of iron (oxy)hydroxides, the protective nature of rust is influenced by anions and cations coexistent in water phase because they affect the coagulation process either by sorption or by forming double oxides with iron. Detailed analyses of alloyed elements have been carried out from the viewpoint of ther-

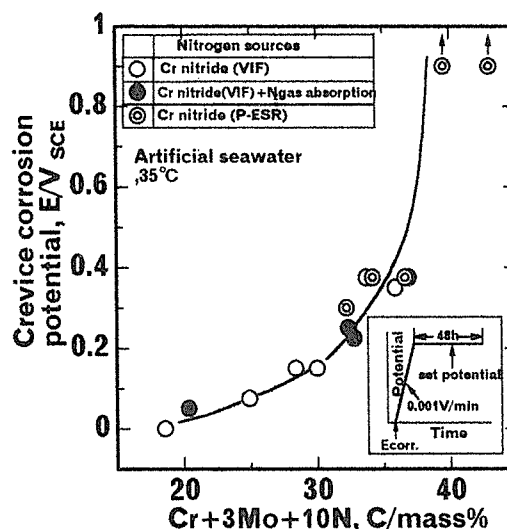


Fig.1 Crevice corrosion potential of 17/25Cr-0/14Ni- and 2/6Mo-0.2/1.3N stainless steels in artificial seawater as a function of chromium equivalence(Cr+3Mo+10N)

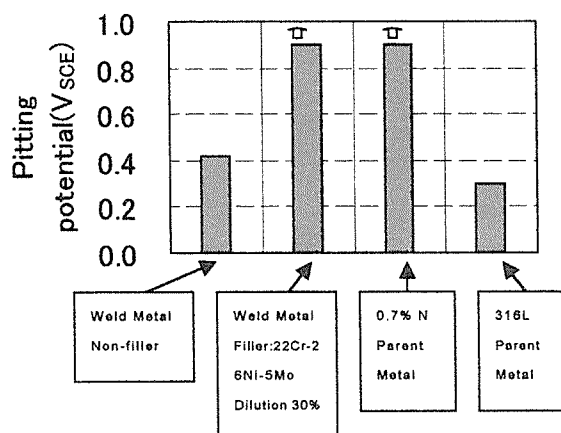


Fig.2. The effect of high-alloy filler on the degraded pitting resistance after welding. The pitting resistance is expressed by localized pitting potential. The use of high-alloy filler prevents the degradation following the welding to a high-N stainless steel (18Cr-14Ni-2.5Mo-0.7N).

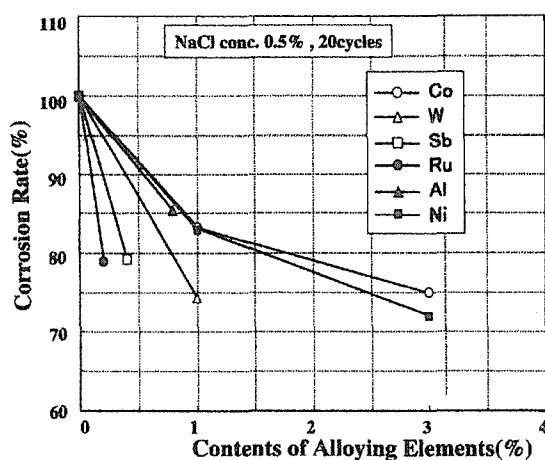


Fig.3 Effect of the content of alloying elements on the relative corrosion resistance of low alloy steels in the dry/wet/rinse cycle.

modynamics of double oxide formation, and the characterization, electrochemistry and material transport of rust. The roles of alloyed elements are classified into 1) double-oxide formation in the form of spinels, etc. 2) incorporation of oxyanions and noble elements into the rust. The incorporated anions change the structure and transport mechanism of rust. Figure 3 shows the relative corrosion loss of low alloy steels determined in wet/dry/rinse cycles simulating coastal atmosphere. Based on the fundamental data alloy design and actual exposure tests are in progress.

For macroscopic evaluation of atmospheric corrosion, a high-accuracy testing facility for atmospheric test was installed within NRIM. Other than NIRM site atmospheric exposure tests are in progress at marine and subtropical sites of Japan Weathering Test Center (JWTC). Test specimens include both standard low alloys and developed alloys. The former consists of steels with basic and simple composition and is to be served for database which is to be accessed by internet.

### Conclusion

A pressure electroslag remelting (PESR) system allowed to create innovative austenitic stainless steels with high nitrogen content. The new steels showed excellent resistance to seawater corrosion and high strength. A new method of welding is also demonstrated for the high-N stainless steels. In the field of low-alloy steels guiding principles for alloy designing have been shown based on thermodynamics and electrochemistry.

## 75 Manufacture Processing of Recyclable Simple-System Alloys

A. Sato, Frontier Research Center for Structural Materials

K. Minagawa and K. Halada, Ecomaterials Research Team

F. Yin, Y. Osawa and S. Takamori, Materials Creation Research Station

G. Arakane, Joining and Interface Research Station

S. Yamamoto, Materials Processing Division

K. Kawahara and O. Ohashi, Guest Researcher

[April 1996 to March 2001]

Because of various additives, the recycling of metallic materials used for automobile parts and other aspects should be solved. Nowadays, the recyclability of materials should be fulfilled in developing new structural materials. In the present research, 3 kind of metallic materials and processing methods for improving recyclability are concerned.

The damping performance of the M2052 alloy was evaluated in the conditions that were close to those in the practical use in 1999. The damping behavior of the M2052 alloy was clarified, including the strain amplitude dependence in the range of  $1 \times 10^{-5}$ ~ $1 \times 10^{-3}$ , and the frequency dependence in the range of 0.01~5000Hz. In the present research, the strain amplitudes in the high order resonant peaks of a beam sample were obtained by measuring the single amplitude of the force sensor in the first vibration mode and the strain amplitude on the beam surface, effective loss factors were then calculated for the high-frequency vibrations. It enabled us to discuss the difference in the logarithmic decrement with the reverse Q value in the strain-amplitude dependent damping alloy. It became clear that a large damping capacity could be expected for the low-frequency vibrations in the low temperatures with the present research. The centrally exciting measurement revealed that M2052 alloy sustained quite a large damping capacity even for the vibrations of more than 3000Hz, and this result was confirmed with the application as the damping rings in engine cylinders.

In order to develop the high-strength sintered iron alloy which is suitable for recycling, the fabrication process for the active fine powder which has the excellent sinterability was researched. We succeeded in developing the hybrid atomizing method in 1998. In this year, deposition was tried to make fine powder by this method. As the result, it became clear that the fine powder piled up in the positions along the flow of inert gas in the high-strength sintered iron alloy deposition equipment chamber. It was also confirmed that the consolidation of the powder particles occurred during the pile up of the powder, since fine powder parti-

cle were in the highly active condition.

From the viewpoint of the steel recycle, the development of the alternate material of free-cutting steels is one of the urgent problems. The effect of boron nitride (hBN) dispersed in the steel on the high-temperature lubrication during machining was examined. As the result, the decrease in the cutting resistance, improvement of chip disposability, and the lubricating effect of hBN were confirmed in deformation flow layer in the back surface of chip. Furthermore, the improvement of the tool wear resistance was also expected.

**Keywords:** Damping alloys, Ultrafine steel particles, Ultrasonic vibration, Casting, Chip-disposability, Martensite

### Paper list

1. X-Ray Diffraction Characterization of the Decomposition Behavior of  $\gamma_{Mn}$  Phase in a Mn-30 at %Cu Alloy, F. Yin, Y. Osawa, A. Sato and K. Kawahara, *Scripta Materialia*, 40(9), (1999): 992-998
2. Modulated Microstructure Observation in a Slowly Cooled Mn-19.7Cu-7.9Ni-2Fe (at.%) Alloy, F. Yin, Y. Osawa, A. Sato and K. Kawahara, *Zeitschrift für Metallkunde* 90(6) (1999)
3. Decomposition Behavior of the  $\gamma_{Mn}$  Solid Solution in a Mn-19.7Cu-7.9Ni-2Fe (at.%) Alloy Studied by Magnetic Measurement, F. Yin, Y. Osawa, A. Sato and K. Kawahara, *Materials Transactions JIM*, 40(5), (1999): 451-454
4. A New-type Damping Materials M2052 Alloy, K. Kawahara and F. Yin, *J. Vac. Soc. Jpn.* 42(1), (1999): 11-17
5. Decomposition Behavior of the  $\gamma_{Mn}$  Phase in Mn-Cu and MnCuNiFe alloys during Aging within the Miscibility Gap, F. Yin, Y. Osawa, A. Sato and K. Kawahara, *Proc. of Solid-Solid Phase Transformation Conference*, Kyoto, Japan, Japan Institute of Metals (1999): 148
6. Problems and Possibilities of Iron Powder Metallurgy from the Environmental View, K. Halada, K. Minagawa and K. Ijima, *Recent Progress in Iron Powder Metallurgy* (1996)
7. Porous Fe-Fe Composite as an Environment Conscious Materials (Ecomaterial), K. Halada, K. Minagawa, H. Okuyama, S. Ohno and N. Itsubo, *Advances in Powder Metallurgy and Particulate Materials* 16 (1996): 73
8. Ecobalance consideration on a recyclable Fe-Fe composite, K. Minagawa, K. Halada, S. Ohno and H. Okuyama, *2nd International Conference on Ecobalance* (1996): 568
9. Production of Recyclable Fe-Fe Composite Materials, K. Minagawa, K. Halada, H. Okuyama, S. Ohno and N. Itsubo, *The Third International Conference on Eco-materials* (Tsukuba, Japan) (1997.9)
10. Refining of Graphite Particles in Cast Iron by Applying Ultrasonic Vibration to Their Melts, Processing and Fabrication of Advanced Materials, Y. Osawa, G. Arakane, S. Takamori and A. Sato, *The Institute of Materials* (1998): 15-22
11. Effects of Ultrasonic Vibration on Refining of Crystal Structures of Al-Si Alloys During Solidification, Y. Osawa, G. Arakane, S. Takamori, A. Sato and O. Ohashi, *J. Jpn. Found. Soc.* 71 (1999): 98-103 (in Japanese)
12. Phase decomposition of the  $\gamma$  phase during aging in a Mn-30Cu at.% alloy, F. Yin, Y. Osawa, A. Sato and K. Kawahara, *Acta materialia*, 48-6 (2000): 1273-1282
13. The damping properties and practical application of M2052 damping alloy, K. Kawahara and F. Yin, *Proceedings of the 2nd High Damping Materials Forum*, Makuhari, Chiba, (2000,9)
14. Tetragonal distortion induced {101} twinning and structural modulation of  $\gamma$  Mn phase in a Mn-20%Cu alloy, F. Yin, Y. Osawa, A. Sato and K. Kawahara, *Zeitschrift für Metallkunde*, 91 (9) (2000)

### 76 Regenerative manufacturing process by utilizing impurities in materials

*Y. Osawa, S. Takamori and F. Yin, Materials Creation Research Station  
K. Minagawa, H. Kakisawa and K. Halada, Ecomaterials Research Team  
T. Kimura, Material Physics Division  
[April 1999 to March 2002]*

Zero-emission is the keyword for sustainable society. Materials nowadays must give high performance, then materials are becoming complicated and difficult to be recycled. Finally those materials are disposed as wastes. It is an urgent problem in materials engineering to reduce these wastes. Therefore it is important to develop new processes which enable us to utilize the material which has been disposed.

In this research, we focused on copper rich iron scrap and steel cans. Hot rolling process induces crack forming on the steel with high copper during steel making process. Then the steel with high copper is now abandoned. The end material of

steel can is an aluminum alloy. Steel cans are used as scrap in steel making process but the end material is removed as alumina.

In the case of copper rich iron scrap, we adopted a powder processing, together with cold forming process, to utilize copper rich iron scrap.

Until now, it is known that the tensile strength of iron alloys can be increased by precipitating fine  $\epsilon$ Cu. In the field of powder metallurgy Fe-Cu-C alloy is often used, but liquid Cu appears during liquid sintering and deteriorate the sinterability.

In this experiment, Fe-Cu alloy melt was rapidly solidified by atomizing to obtain Cu super saturated iron powder. V-groove cold rolling make it possible to obtain high tensile strength from these powders. We establish an method which eliminate the bad effect of copper.

In the case of steel cans, the end material is finally oxidized. The energy loss in this process is significant. We must find another process to utilize steel cans, then we tried to use these as the raw material of iron castings. Small amount of aluminum has been used to control the matrix structure until now, but significant amount of aluminum was not used in iron castings. Therefore we investigated the structure change and mechanical properties of iron castings which contain 0~20% aluminum.

It is found that aluminum modify the structure of cast iron and improve the abrasion resistance. And aluminum content is easily controllable because the yield rate is high and concentration change during melting is small. We found steel cans are suitable to use as a raw material for iron castings.

**Keywords:** Eco-material, Recycle, Powder Metallurgy, Copper, Cast Iron, Aluminum

#### 77 Effect of Aging Degradation on Localized Corrosion of Structural Materials for Light Water Reactors

*Y. Katada, S. Ohashi, K. Kurosawa, J. Kinugawa, Y. Muramatsu and Y. Asai, Joining and Interface Research Station*

*H. Irie, Mechanical Properties Division*

*T. Kasugai and K. Ei, Materials Processing Division*

[April 1996 to March 2000]

Life management of Nuclear Power Plant (NPP) for the acquisition of renewal license is one of the worldwide primary concerns. From the viewpoint of the integrity evaluation of structural materials,

therefore, the interaction between aging degradation of the materials and environmentally assisted cracking (EAC) is one of the important issues to be investigated.

The objectives of this research are to investigate the interaction between aged structural materials and EAC such as stress corrosion cracking, corrosion fatigue in high temperature water, and to mitigate the enlargement of local damage in weld joints by using a laser beam technique.

#### 1. Material degradation

In this year, microscopic observations by means of SEM, AFM, KFM were conducted in order to investigate the initiation of localized corrosion of nitrogen bearing stainless steels with and without manganese in saline solution. As a result, the higher the nitrogen content, the better the localized corrosive property for both series of materials. It was also found that the materials with manganese showed poor corrosion property compared to that without manganese due to MnS inclusions. It was interesting to know that the difference between surface potentials of both  $Al_2O_3$  and  $SiO_2$  inclusions could be successfully detected by KFM. This means that the microscopic approach by probe microscope can be promising techniques to reveal the mechanism of localized corrosion.

#### 2. Mitigation for the enlargement of local damage by laser beam technique

As one of the evaluations for corrosion behavior of weld metal of SUS304 stainless steel which was treated by  $CO_2$  laser beam after welding, electrochemical approach was conducted by using a micro-vibration-electrode in 8N-  $HNO_3$  solution. It was found that the post-treatment by laser beam technique for the HAZ was able to suppress the initiation of corrosion pits. Further investigation for the effect of laser beam will be carried out using thermally aged materials, which simulate sensitized welded region.

In-situ observation by a laser speckle method has been applied in order to measure the local strain behavior of weld metal in laser processing. A two-dimensional in-situ high temperature strain measurement system was newly developed. After optimization of measurement conditions such as the location and the sensitivity of sensor, intensity of laser light, selection of proper band-pass filters and so on, in-situ high-speed measurement of high temperature local strain by laser-speckle method was successfully made.

**Keywords:** aging degradation, localized corrosion, light water reactor, weld joints, laser beam

## 78 Computational Simulation of Mechanical Properties and Behavior of Materials for Atomic Power Plants by Taking Microstructures into Account

*M. Tabuchi, K. Kusunoki and N. Akaiwa, Strength and Life Evaluation Research Station, Computational Materials Science Division*  
[April 1999 to March 2004]

The materials used in atomic power plants degrade due to the initiation and growth of various kinds of damages induced by neutron irradiation, creep and so on. The present study aims to develop the programs to simulate the initiation and growth behavior of damages and mechanical properties of damaged materials by using micro, meso, and macroscopic computational method. The material designing method to prevent the embrittlement and the evaluation method of material reliability will be discussed.

### 1. Dynamical process of irradiation-induced defects and their effects on materials properties.

With use of computer simulations, this study aims to elucidate how the atomistic defects such as vacancies and interstitials in irradiated materials develop into microscopic and mesoscopic ones such as clusters of vacancies and interstitials and their complexes. Also we study how these defects affect the mechanical properties of the materials. For these purposes, we perform calculations based on atomistic models such as molecular-dynamics and the Monte Carlo simulations. Recently, we carried out the calculations of phonon density of states of alpha iron crystals with a point defect such as a vacancy or an interstitial atom. All the atoms surrounding the point defect are relaxed through molecular-dynamics. The results for a crystal with an interstitial atom show that, compared to cases for a perfect crystal and a crystal with a vacancy, several peaks appear at rather high vibrational frequency of about 13THz. The migration process of the interstitial atoms in the alpha iron crystal is also investigated.

### 2. Computational analysis for deformation and fracture of damaged materials at high temperatures.

The prediction method for degradation of tensile ductility of materials including He bubbles by using FEM analysis had been developed. In the present research, we are planning to conduct the computational simulation for creep and fatigue fracture properties of materials including damages such as He bubbles, creep voids and cracks. The 3D FEM codes, which can deal with creep, crack growth and fracture mechanics have been developed. The computational simulations of creep

crack initiation and growth from the He bubbles have been conducted. The creep fracture criteria have been investigated by comparing the computational analysis and experimental results of CT specimens. The simulation programs that take diffusive growth of He bubbles and creep voids into account are also being developed.

**Keywords:** computer simulation, irradiation damage, molecular-dynamics, phonon density of states, diffusion of point defects, helium embrittlement, FEM, creep fracture

### Recent Publications

Analysis of Stress-Strain Relationship in Materials Containing Voids by Means of Plastic Finite Element Method, H. Shiraishi and M. Tabuchi, *J. of Nuclear Science and Technology*, **37** (2000) p.288-299.

## 79 Mechanical Properties of Thin Films and Coatings

*S. Matsuoka, Frontier Research Center for Structural Materials, Strength and Life Evaluation Research Station*  
[April 1997 to March 2001]

Mechanical properties of thin films and coatings become a subject of much concern, because they are widely used in a large number of industrial fields. In this study, depth sensing indentation (DSI) technique is developed to measure hardness and elastic modulus of thin films and coatings. The study is closely related to the new technical working area TWA 22 "Mechanical properties of thin films and coatings" among VAMAS projects.

In this financial year, DSI was carried out for gold, platinum, silicon oxide and diamond like carbon thin films with thickness of 0.1, 0.3 and 1.0  $\mu\text{m}$  deposited on a sapphire substrate. The contact depths for the gold and platinum films increase with increasing the film thickness, corresponding to the decrease in the plastic deformation resistance. On the other hand, the DLC coatings show the same contact depth in the various film thicknesses. These results suggest that the constraint by the hard substrate is different for various film/substrate systems even under the same conditions of the film thickness and applied load. Measurements under various time-dependent conditions reveal that the hardness of the gold and platinum films depend on the loading rate ranges

from 0.01 to 1.0 mN/s. In particular, it is more dependent for the thicker films. This is considered that a time-dependent deformation mechanism such as creep deformation contributes to the plastic deformation resistance in the soft metals.

**Key Words:** Thin films, Coatings, Elastic modulus, Hardness, Depth sensing indentation

## 80 Toughness Evaluation of Structural Steels

*S. Matsuoka, Frontier Research Center for Structural Materials Strength and Life Evaluation Research Station*

[April 1999 to March 2001]

Many steel structures were damaged on Hanshin-Awaji great earthquake of January 17, 1995. The drastic example was the brittle fracture of steel box columns in high-rise buildings. This study aims at developing the toughness evaluation method useful for real-size components.

In the recent year, Charpy impact tests were carried out for two heats of SM490A steel with high and low toughness, using the specimens with the radius curvature of notch of 0.1, 0.25 (standard) and 0.5 mm. Test temperature was between -100 and 80°C. Fracture surfaces were observed by a scanning electron microscope SEM. The ductile fracture region was formed ahead of the cleavage fracture region. Similar appearance was observed in large-scale specimens fractured under the loading simulated Hanshin-Awaji earthquake. The relationship between Charpy impact energy and depth of ductile fracture region showed the unique curve, while the relationship between Charpy impact energy and test temperature was dependent on the toughness of the steel and the radius curvature of notch of the specimen. This suggests that the depth of ductile fracture region is the important factor when the toughness is evaluated for the real-size component.

**Keywords:** Hanshin-Awaji earthquake, structural steel, brittle fracture, toughness, fractography

## 81 Evaluation Method of High Temperature Fracture Property for Creep Brittle Materials

*M. Tabuchi, K. Kubo and T. Ohba, Strength and Life Evaluation Station*

[April 1997 to March 2002]

It is necessary to establish the test method of

creep crack growth in order to evaluate the reliability and residual life of high temperature components. The standard method of creep crack growth test for advanced heat resisting materials was proposed based on the results of VAMAS collaborative work; Technical Working Area (TWA) 19 for "High temperature fracture of creep brittle materials". This methodology was extended to the new VAMAS TWA25 for "Creep/fatigue crack growth in components", which has started in 1999. The objectives of TWA25 is to establish the accurate and reliable procedures for monitoring and assessing time dependent crack growth at elevated temperatures in components which contain defects.

The effect of mechanical constraint on creep crack initiation and growth under multi-axial stress condition is an important factor for evaluating fracture life of components. For this purpose, Japanese group: Tohoku University, IHI and NRIM that participates in VAMAS TWA25 is conducting the following research program. The effect of notch configuration on crack initiation and growth is investigated by using circular notched specimens. Creep crack growth in fine-grained heat affected zone of weldment is a serious problem. The test and evaluation method of crack initiation, growth and life for welded joint is investigated on advanced heat-resisting steels. The round robin tests have started in 1999.

We are also investigating the evaluation method of crack initiation and growth for creep brittle advanced heat resisting materials. The round robin tests on 2 types of TiAl intermetallic compound, which have full lamellar and duplex structures have been conducted. The effect of microstructures and fracture mode on creep crack growth properties was clarified and the life evaluation equations for both TiAl were derived.

**Keywords:** creep crack growth, component, mechanical constraint, VAMAS project, TiAl intermetallic compound

## Recent Publications

Creep Crack Growth Test Method and Creep Crack Growth Properties for TiAl Intermetallic Compound, M. Tabuchi, A.T. Yokobori, A. Fuji, K. Kubo, K. Yagi and T. Yokobori, J. of The Society of Materials Science Japan **49** (2000) p.80-85 (in Japanese).

82 Development of analysis method for dynamic dislocation motion at high temperature and study on controlling process of high temperature deformation

*F. Abe and K. Sawada, Strength and Life Evaluation Research Station*

*K. Kimura and M. Igarashi, Materials Creation Research Station*

[April 1999 to March 2001]

It is very important to make clear the creep mechanism controlled by dislocation glide and climb in order to improve high temperature strength of structural materials. Many phenomenological understandings of creep mechanism have been well done so far. However, the creep mechanism is not understood in terms of dislocation motion because the dislocation motion is not directly observed at high temperature. The purpose of this study is to establish analysis method for dynamic dislocation motion at high temperature under stress and to make clear factors controlling creep deformation in high chromium ferritic steels.

1. Development of analysis method for dynamic dislocation motion at high temperature

The high resolution CCD camera was introduced to FE-TEM and suitable temperature for in-situ observation of dislocation motion in TEM was examined for high chromium ferritic steel.

2. Study of controlling process of high temperature deformation

High chromium ferritic steels have tempered martensitic lath structure and is strengthened by  $M_{23}C_6$ , MX carbonitrides, Laves phase and solute atoms. These strengthening factors are very compli-

cated and change during creep deformation. We have to investigate individually the effects of the strengthening factors on dislocation glide and climb in order to make clear controlling process of creep. The coarsening process of the MX carbonitrides has not well understood because the MX particles are too small to measure the change of particle size during creep. In this study, we observed the coarsening of MX carbonitrides during aging and creep at 650, 700 and 750°C in ASME-P92 steel. The coarsening of MX carbonitrides during aging can be controlled by Ostwald ripening mechanism. It is concluded that creep deformation accelerates the MX coarsening by pipe diffusion of dislocation contacting with the MX carbonitrides during creep. The stress dependence of minimum creep rate decreases with increasing testing temperature. The value of stress exponent is 5.7 at 750°C. At higher temperature, the decrease of coherent strain between the MX carbonitrides and matrix by coarsening of the MX decreases the strengthening effect of the MX. The decrease of the strengthening effect can be related to low stress dependence of minimum creep rate at higher temperature.

**Keywords:** dislocation motion, creep, microstructural change, high chromium ferritic steel

#### Recent Publication

Creep behavior and stability of MX precipitates at high temperature in 9Cr-0.5Mo-1.8W-VNb steel, K.Sawada, K.Kubo and F.Abe, to be published in Mater. Sci. Eng. A

## Publications

### □ Papers published in 1999

#### Characterization/Properties

1. N. Yokoyama, O. Umezawa, K. Nagai, T. Suzuki and K. Kokubo, Cyclic Deformation Structure and Internal Fatigue Crack Generation in Ti-Fe-O Alloy at Liquid Nitrogen Temperature, *Matallurgical and Materials Transaction A*, 31A(2000) : 2793-2804.
2. T. Saito, Computational Materials Design, *Spuringe-Verlag*,
3. H. Miyazaki, N. Shinya, Y. Tomizawa, K. Koyano and Y. Sato, A system for measuring the adhesion forces of micro-objects under a scanning electron microscope, *Review of Scientific Instruments*, 71-8(2000) : 3123-3131.
4. H. Miyazaki, Y. Tomizawa, S. Saito, T. Sato and U. Shinya, Adhesion of micrometer-sized polymer particles under a scanning electron microscope, *Journal of Applied Physics*, 88-6(2000) : 3330-3340.
5. H. Fudouji, M. Kobayashi, N. Shinya, Arrangement of micro-scale particles by electrification, *KONA*, 17(1999) : 55-63.
6. T. Terashima, Y. Aoki, Y. Haga, A. Kuzawa, T. Suzuki, J.S. Qualls, T.F. Stalcup and J.S. Brooks, Low-field low-temperature magnetotransport studies of Cep, *Phys Rev B*, 60-22(1999) : 285-289.
7. M. Hase, M. Egashira and N. Shinya, Development of Novel Method to Create Three-Dimensional Arrangements of Particles Using Dielectrophoresis in Artificially Nanuniform Electric Field, *Journal of Intelligent Material Systems and Structures*, 10(1999) : 508-513.
8. A. Nakamura, M. Tosa, K. Yoshihara and S. Ikeda, Hydrogen Permeation properties & Surface Structure of BN coating Layer, *The proceedings of Icwes-11*,
9. A. Nakamura, T. Narushima and M. Kitajima, Surface Stress in Silicon Oxide Layer, *Trans MRS-3*,
10. D. Fujita, H.Y. Sheng, H.Okamoto, H. Nejyoh and T. Ohgi, Submicrometer transmission mask fabricated by low-temperature SF6 10 2 reactive ion, *Journal of Vacuum Science and Technology B*, (1998).
11. M. Harada, K. Sakurai, H. Eba and S. Kishimoto (KEK), Performance of the YAP:Ce scintillation detector, *Photon Factory Activity Report 1998*,
12. S. Arisawa, Hanping MIAO, H. Fujii, A. Ishii, Y. Takano, Stephane HABAT, T. Hatano and K. Togano, New method for preparing extremely thin Bi<sub>2</sub>Sr<sub>2</sub>Ca<sub>1</sub>Cu<sub>2</sub>O<sub>x</sub> ribbon like thin films and their superconducting Properties, *Physica C*,
13. D. Rogers and H. Nejoh, Fabrication of a Metal Nanostructure on the Si(111) surface, *The Journal of Vacuum Science and Technology (JVSTB)*,
14. Alok. Singh, E. Abe, H. Takakura and A.P. Tsai, An electron microscopic study of hexagonal phases in Zu-Mg-Re alloys, *MICRON*,
15. K. Hono and Ping De hai, Atomprobe Studies of nanocrystallization of amorphous alloys, *Materials Characterization*,
16. T. Sasaki, T. Sisido, M. Oku, S. Okada, K. Kudou, J. Ye, Y. Watanabe, N. Toyota, H. Horiuchi and T. Fukuda, Chemical State and Properties of the Nb<sub>5</sub> Sn<sub>2</sub> Ga Grown by the self-component Flux Metroce uscting tir as a sdvent, *Journal of Alloys and Compounds*,
17. H. Moriya, K. Nagai and O. Umezawa, Fracture Characteristics and Deformation Behavior of Solution-treated Ti-15V-3G-3Sn-3Ae Alloy, *Int. J. Materials and Product Technology*,
18. Fuxing Yin, Y. Ohsawa, A. Sato and K. Kawahara, X-Ray Diffraction Characterization of the Decomposition Behavior of Rmn phase in a Mn-30at%Alloy, *Scripta Materialia*, (1999).
19. T. Herrmannsdorfer (ETH/PSI), A. Donni (Niigata Univ.), P. Fischer (ETH/PSI), L. Keller (ETH/PSI), G. Bottager (ETH/PSI), M. Gutmann (ETH/PSI), H. Kitazawa and Jie Tang, Successive Magnetic Ordering of the Tb Sublattices in Tb<sub>3</sub>Pd<sub>20</sub>Si<sub>6</sub>, *Journal of Physics: Condensed Matter (J.Phys.:Condens.Matter)*,
20. Xie Huimin, S. Kishimoto, N. Shinya, Dai. Fulong, Zou. Dazing and Liu. Sheng, Thermal Deformation Analysis of Electronic Packaging Components Using Electron Moire Method, *Journal α Strain*,
21. T. Hashimoto, K. Yamamoto, T. Kimura and M. Nobuki, Effect of Vanadium on Residua Strain in Li<sub>2</sub>-type(AlMn)<sub>3</sub>Ti(V) Alloy Pouders and Bond Ductility of Pre-milling Alloys, *"Material Transitions, JIM"*,
22. Hu Xiao, M. Tachiki and T. Koyama, Phase diagram of a superconducting and artiferromagnetic system with So(5)symetry, *Physical Review Letters*,
23. S. Tsukamoto, A. Shida, T. Wakasa and K. Hiraoka,

- Measurement of Beam Energy Absorption in CO<sub>2</sub> Laser Beam Welding, *Journal of the Japan Welding Society*,
24. H. Isago, N. Kobayashi, H. Miwa and T. Tomura, An Adjacent Dibenzotetraazaporphyrin Intermediate Between Tetraazaporphyrin and Phthalocyanine, *Inorganic Chemistry*,
  25. K. Furuya, N. Ishikawa and C.W. Allew (Argonne National Institute), In-Situ observation of shape and atomic structure of Xe nanocrystals embedded in Aluminium, *Journal of Microscopy*,
  26. T. Ohashi, T. Inoue, S. Toritsuka, K. Tsuzaki and K. Nagai, Plastic strain and ferrite grain size after thermo-mechanical treatment of Si-Mu Steel blocks, *Acta Materialia*,
  27. N. Ezaki and T. Ohno, The Investigations of Adsorption of Fluorine Atoms on the Si(001) Surface, *Surface Science*,
  28. T. Ohno, Q.K. Xue, Q.Z. Xue, R.Z. Bakhitizin, Y. Hasegawa, I.S.T. Tsong and T. Sakurai, Structures of GaN(0001)2x2,4x4 and 5x5 surface reconstructions, *Physical Review Letters(PRL)*,
  29. Y. Ogawa, H. Nakamura, A. Kasahara and T. Kodama, Ionic Conductivity of CaS-Na<sub>2</sub>S Solid Solution, *Mater. Trans. JIM*, 40-6(1999) : 479-484.
  30. D.H. Ping, K. Hono, H. Kanekiyo and S. Hirose, Evolution of hard Magnetic (Fe<sub>3</sub>B,Fe<sub>23</sub>B<sub>6</sub>)/Nd<sub>2</sub>Fe<sub>14</sub>B nanocomposite microstructure by additions of Nb and Cu to a Nd<sub>4.5</sub>Fe<sub>77</sub>B<sub>18.5</sub> alloy, *Applied Physics Letter*,
  31. Y. Hishinuma, H. Kitaguchi, MIAO Hanping, H. Kumakura and K. Ito, Critical Current Density Distribution in Superconducting Oxide Layer of PAIR Processed Bi-2212/Ag Composite Tapes, *Superconducting Science and Technology*,
  32. A.P. Tsai, Metallurgy of Quasicrystals, *Physical properties of Quasicrystals, solid-state Science 126 (Springer-Verlag Berlin Heidelberg)*, (1999).
  33. K. Hono, Atom probe microanalysis and nanoscale microstructures in metallic materials(Overview), *Acta Materialia*,
  34. K. Mitsuishi, M. Kawasaki, M. Kakeguchi and K. Furuya, Determination of atomic positions in a solid Xe precipitate embedded in Al matrix, *Physical Review Letters*,
  35. H. Kitaguchi, Hanping MIAO, H. Kumakura and K. Togano, Relationship between Bi-2212 layer thickness and J<sub>c</sub> enhancement by PAIR Process, *Physica C*,
  36. L.Y. Xiao, T. Kiyoshi, O. Ozaki and H. Wada, Case Study on Quench Evolution and Passive Protection of High Tc Superconducting Pancake Coil, *Cryogenics*,
  37. S. Kuroda and P. Blazdell, Plasma Spraying of sub-micron Ceramic Suspensions Using a continuous Jet Printer, *Materials Science and Engineering, A*,
  38. T. Mochiku, M. Nakahara (Tsukuba Univ.), T. Kamiyama (Tsukuba Univ.), H. Asano (Tsukuba Univ.) and K. Hirata, Neutron Powder Diffraction of Sr<sub>1.9</sub>Nd<sub>1.1</sub>Cu<sub>2.1</sub>Nb<sub>0.08</sub> and Sr<sub>2</sub>(Nd<sub>0.75</sub>Ce<sub>0.25</sub>)<sub>2</sub>Cu<sub>2</sub>NbO<sub>10</sub>, *KENS REPORT-XII*,
  39. Y.C. Guo, Y. Tanaka, T. Kuroda, S.X. Dou and Z.Q. Yang, Addition of nanometer SiC in the silver-sheathed Bi2223 superconducting tapes, *Physica C*,
  40. Jinhua. Ye and Zhigang. Zou, Single crystal growth and Characterization of a new bismuth indium niobate compound, Bi<sub>5</sub>In<sub>2</sub>Nb<sub>3</sub>O<sub>18-x</sub>, *Journal of Alloys and compounds*,
  41. H. Takeya, Moshe KUZNIETZ, "Formation and characterization of (Pr,Dy)Ni<sub>2</sub>B<sub>2</sub>C samples", *PhysicaB*,
  42. S.K. Maloney, K. Hono, I.J. Polmear and S.P. Ringer, The chemistry of precipitates in an aged Al-2.1Zn-1.7Mg at% Alloy, *Scripta.mater*,
  43. N. Yanagihara (Teikyo Univ.), K. Uchida (Teikyo Univ.) , M. Wakabayashi (Teikyo Univ.), Y. Uetake (Teikyo Univ.) and T. Hara, Effect of Radical Initiators on the Size and the Formation of Silver Nanocluster in Poly (Methyl Methacrylate), *Langmuir*,
  44. Zhiung. Zou, Jinhua. Ye and Y. Nishizawa (Ibaraki Univ.), Preparation and Magnetic Properties of In<sub>2-x</sub>Zn<sub>x</sub>Cu<sub>2</sub>O<sub>5</sub>(x=0 ~ 1.4) Solid Solution, *Journal of Materials Science Letters*,
  45. M. Murayama, K. Hono, K. Hirukawa, T. Ohmura and S. Matsuoka, The combined effect of molybdenum and nitrogen on the fatigued microstructure of 316 type austenitic stainless steel, *Scripta mater(Scripta materialia)*,
  46. Y. Takano, Y. Kimishima (Yokohama National Univ.), H. Taketomi (Tokyo Denki Univ.), S. Ogawa (Tokyo Denki Univ.), S. Takayanagi (Hokkaido Kyokai Univ.) and N. Mouri (Institute for Solid state Physics, Univ. of Tokyo), New Copper-Free Layered PEROVSKITE Superconductors: KCa<sub>2</sub>Nb<sub>3</sub>O<sub>10</sub> and Related Compounds, *Journal of Superconductivity*,
  47. Moshe KUZNIETZ and H. Takeya, Two-step magnetic ordering in polycrystalline DyNi<sub>2</sub>B<sub>2</sub>C samples, *Journal of Physics*,
  48. H. Takeya and MosheKUZNIETZ, Magnetic Properties of the (Pr,Dy)Ni<sub>2</sub>B<sub>2</sub>C solid solutions, *Journal of Magnetism and Magnetic Materials (J.M.M.)*,

49. MIAO Hanping, H. Kitaguchi, H. Kumakura, K. Togano, T. Hasegawa and T. Koizumi, Optimization of melt-processing temperature and period to improve critical current density of Bi-2212/Ag multilayer tapes, *Physica C*,
50. H. Kitaguchi, K. Ito, T. Takeuchi, H. Wada, H. Kumakura, H. Miao, K. Togano, T. Hasegawa and T. Koizumi, Performance at 10 ~ 50K of Bi-2212/Ag multilayer tape fabricated using PAIR Process, *Physica C*,
51. F. Dugain (ILL), M. de Boissieu (INPG), K. Shibata (Tohoku Univ.), R. Currat (ILL), T.J. Sato, A.R. Kortan, J.B. Suck (Ger. Chemnitz Zwickau Univ.), K. Hradil (Ger LMU), F. Frey (Ger LMU) and A.P. Tsai, Inelastic neutron scattering study of the dynamics of the AlNiCo decagonal phase, *Eur.Phys.J.B.* 7, 513-516, (1999).
52. S. Kishimoto and N. Shinya, New Fabrication Method for Metallic Colloid Cellular Materials Containing Polymers,
53. D.G. Kim, M.J. Shin, K.H. Kim and T. Hanawa, Surface treatments of titanium in aqueous solutions containing calcium and phosphate ions, *Bio-Medical Materials and Engineering*,
54. YU Xihong, Y. Mitarai and H. Harada, Phase separation in Two kinds of  $L_{12}$ -Ni<sub>3</sub>Al and Ir<sub>3</sub>Nb of Refractory superalloys, *Scripta Materialia*,
55. Ying Mu, T. Kobayashi, H. Sumita, K. Tsuji and T. Hanawa, Titanium release from plate and screws implanted in the rabbit, *Journal of Biomedical Materials Research*,
56. Ying Mu, T. Kobayashi, H. Sumita, R. Yamamoto and T. Hanawa, Metal ion release from titanium with active oxygen species generated by rat macrophages in vitro, *Journal of Biomedical Materials Research*,
57. T. Hanawa, K. Asami, H. Uga (IHI) and K. Murakami (IHI), Surface modification of titanium utilizing repassivation reaction in aqueous solutions, *Biomaterials*,
58. Liu Yufu and Y. Kagawa, Energy release rate for interface debond crack in a fiber pullocet model, *Composites science and Technology*,
59. Ping De hai, K. Hono, H. Kanekiyo and S. Hiro-sawa, Microstructural evolution of Fe<sub>3</sub>B/Nd<sub>2</sub>Fe<sub>14</sub>B nanocomposite magnets microalloyed with W and N, *Acta materialia*,
60. M. Kitajima, K. Ishioka, H. Nakanotani, S. Tateishi, T. Mori, N. Fukada, K. Murakami and S. Hishita, Three different forms of hydrogen molecules in silicon, *Jpn.J.Appl.Phys.Express Letters*,
61. E. Abe and A.P. Tsai, Quasicrystal-Crystal Transformation in Zn-Mg-Rare-Earth Alloys, *Physical Review Letters.(Phys.Rev.Lett.)*, 83(1999) : 753.
62. Ping De hai, K. Hiraga, Y. Sakka and Ahn Byung-Wook, A Grain Boundary Diffusion Model of Dynamic Grain Growth during Superplastic Deformation, *Acta Materialia*,
63. A. Ichinose, C-Y. Yang, D.C. Larbalestier, S.E. Babcock, A. Kikuchi, K. Tachikawa and S. Akita, Growth Conditions and Microstructure of Y<sub>2</sub>O<sub>3</sub> Buffer Layers on Cube-Textured Ni, *PHYSICA,C*,
64. A.P. Tsai, Y. Murakami and A. Niikura, The Zn-Mg-Y phase diagram involving quasicrystals, *Philosophical Magazine A*,
65. A.P. Tsai, N. Chandrasekhar and K. Chattopadhyay, Size Effect on the Superconducting Transition of Embedded Lead Particles in Al-Cu-V Amorphous Matrix, *Applied Physics Letters*,
66. Toetsu Shishido, Jinhua Ye, K. Kudo, S. Okada, K. Obara, T. Sugawara, M. Oku, K. Wagatsuma, H. Horiuchi and T. Fukuda, Solid Solution range of born microhardness and oxidation resistance of the perovskite type RERh<sub>3</sub>Bx(RE=Gd,Y,Sc)compounds, *Journal of Alloys and Compounds*,
67. M. Shimoda, S. Tsukamoto, Y. Watanabe (NTT), M. Sugiyama (NTT), S. Maeyama (NTT), T. Ohno and N. Koguchi, Surface Stoichiometry of S-terminated GaAs(001)(2×6)-S studied by Synchrotron Radiation Photoelectron Spectroscopy, *Photon Factory Activity Report 1998 (PF Activity Report 1998)*,
68. S. Tsukamoto and N. Koguchi, Magic numbers in Ga clusters on GaAs(001) surface, *Journal of Crystal Growth*,
69. Y.Q. Wu, Ping De hai, K. Hono and A. Inoue, Microstructural characterization of an  $\alpha$ -Fe/Nd<sub>2</sub>Fe<sub>14</sub>B nanocomposite magnet with a remaining amorphous phase, *Journal of Applied Physics*,
70. A. Miyazaki, H. Kimura, Xiaopeng JIA, K. Shimamura and T. Fukuda, Comparison of Ba(B<sub>1-x</sub>Al<sub>x</sub>)<sub>2</sub>O<sub>4</sub> Single Crystals on their Diameters, *Crystal Research and Technology (Cryst.Res.Technol)*, 34-7(1999) : 817-820.
71. M. Ohnuma, K. Hono, H. Onodera, J.S. Pedersen, S. Mitani and H. Fujimori, Distribution of Co Particles in Co-Al-O Granular Thin Films, *Materials Science Forum vol.307(1999) Journal of Metastable and Nanocrystalline Materials vol.1(1999)*,

72. R. Sugano, T. Onogi, K. Hirata and M. Tachiki, Current-Drier Vortex State in Bi-2212 with Columnar Defects, *Phys.Rev.B to be published in October Issue*, (1999).
73. O. Vasyukiv and Y. Sakka, Preparation of nano-size zirconia powder with narrow particles and aggregates size distribution through, *Nanostructured Materials (Nanostruct. Mater)*,
74. Junqing Guo, S. Tsukamoto, T. Kimura and H. Nakae, Nucleation process control of undercooled stainless steel by external nucleation seed, *Acta Materialia*,
75. S. Ito, R. Hasegawa and M. Amano, Ions formation during glow discharge mass spectrometry, *Mater. Trans. JIM*,
76. K. Sakurai, H. Eba, S. Numako and J. Iihara, X-ray fluorescence spectrometer for trace chemical characterization, *Spring 8 Annual Report 1999*,
77. K. Sakurai, S. Numako and H. Eba, Detection of 10-14g order trace metals in a droplet, *Spring 8 Annual Report 1999*,
78. S. Arisawa, Hanping MIAO, H. Fujii, A. Ishii, Y. Takano, T. Hatano and K. Togano, In-situ observation of the growth of ribbon-like thin films of Bi-2212 on Ag substrate, *Journal of Low Temperature Physics*,
79. S. Ooi, T. Shibauchi and T. Tamegai, Vortex Avalanches in Vortex Lattice Phase in  $\text{Bi}_2\text{Sr}_2\text{CaCu}_2\text{O}_{8+y}$ , *Physica B: Condensed Matter*,
80. H. Kumakura, H. Kitaguchi, T. Mochiku, K. Togano and S. Okayasu, Magnetically investigated E-J characteristics of Bi-2212/Ag tape conductors, *Physica C*,
81. T. Mano, K. Watanabe, S. Tsukamoto, M. Oshima, H. Fujioka and N. Koguchi, New self-Organized Growth method for  $\text{LaGaAs}$  Quantum Dots on  $\text{GaAs}(001)$  Using Droplet Epitaxy, *Japanese Journal of Applied Physics Part 2 (JJAP)*,
82. Z.-C. DONG, D. Fujita, T. Ohgi, T. Yakabe and H. Nejoh, STM Induced Photon Emission from Single Molecules on  $\text{Cu}(100)$ , *Japanese Journal of Applied Physics*, (1999).
83. S. Ito, H. Yamaguchi, T. Kimura, R. Hasegawa and T. Kobayashi, Determination of carbon and nitrogen in iron and steel by glow discharge mass spectrometry, *ISIJ International*,
84. Hideki. Miyazaki, Hiroshi. Miyazaki, K. Ohtaka and T. Sato, Photonic band in two-dimensional lattices of micrometer-sized spheres mechanically arranged under a scanning electron microscope, *Journal of Applied Physics (J.Appl.Phys)*,
85. H. Sakata, M. Oosawa, K. Matsuba, N. Nishida, H. Takeya and K. Hirata, Imaging of a Vortex Lattice Transition in  $\text{YNi}_2\text{B}_2\text{C}$  by Scanning Tunneling Spectroscopy, *"Phys.Rev,Left(PRL)"*,
86. M. Murayama, K. Hono, W.F. Miao and D.E. Laughlin, The Effect of Cu Additions on the Precipitation Kinetics in Al-Mg-Si Alloy with Excess Si, *Metallurgical and Materials Transactions A*,
87. Y. Kimura, H. Hidaka and S. Takagi, Work-Hardening Mechanism during Super-Heavy Plastic Deformation in Mechanically Milled Iron Powder, *Journal of Materials Japan*,
88. T. Terashima, S. Uji, H. Aoki, M. Takashita, T. Matsumoto, K. Maesawa, R. Settai and Y. Ohnuki, dHvA Effect Study of the Metamagnetic Transition in  $\text{CeRu}_2\text{Si}_2$ -Transition Behavior of the dHvA Oscillations, *Physics of Strongly Correlated Electron Systems JJAP Series 11*, pp.3-5,
89. M. Oshikiri and Ferudy. Ariasethyawan, Band gaps and quasi particle Energy calculations on  $\text{ZnO.Zns}$  and  $\text{Znse}$  in Zinc-Blende structure by GW Approximation, *Physical Review B*,
90. Y. Takano, I. Umehara, M. Endo, F. Ishikawa, M. Yamaguchi and K. Sato, Pressure Effect in  $\text{ErAg}_2$ , *Physica B*,
91. M. Hase, N. Nakajima, K. Mizoguchi, H. Harima and K. Sakai, Ultrafast decay of coherent plasmon-phonon coupled modes in highly doped  $\text{GaAs}$ , *Physical Review B*,
92. A. Nakamura, T. Narushima, M. Kitazima, T. Kurashina and T. Kawabe, Effect of Surface Disorder on the Surface Stress of  $\text{Si}(100)$ , *Applied Surface Science*,
93. Y. Mitarai, H. Harada, Y. Ro and M-H Hong, Temperature dependence of the flow in  $\text{Ir}_3\text{Nb}$  with the  $\text{L}_2$  structure, *Phil Mag Letter*,
94. M. Imai, R.R. Hudgings, M.F. Jarrold, P. Dugourd, High-resolution ion mobility measurements for silicon cluster anions and cations, *Journal of Chemical Physics, J.Chem.Phys.*,
95. Y. Mitarai, Y. Ro, S. Nakazawa, H. Harada and Yuefeng Gu, Effect of Precipitate morphology on strength of Ir-Nb alloys with Two-phase coherent structures, *Scripta Materialia*,
96. GU. Yuefeng, Y. Mitarai and H. Harada, Compression Properties of B-doped Ir-15Nb Two-phase Refractory Superalloys, *Scripta Materialia*,
97. K. Morita and K. Hiraga, High Temperature Deformation Behavior of a Fine-Grained Tetragonal Zirconia, *Scripta Materialia*,

98. J. Ye, S. Sadewasser, J.S. Schilling, Z. Zou, A. Matsushita and T. Matsumoto, Evidence from High-Pressure Experiments that  $\text{PrBa}_2\text{Cu}_3\text{O}_x$  is a Normal  $\text{YBa}_2\text{Cu}_3\text{O}_x$ -like Oxide Superconductor, *Physica C*,
99. Ping De hai, K. Hono, A. Inoue, Y.Q. Wu and M. Hamano, Microstructural characterization of an  $\alpha$ - $\text{Fe}/\text{Nd}_2\text{Fe}_{14}\text{B}$  nanocomposite magnet with a remaining amorphous phase, *F.Appl.Phys*,
100. H. Kimura, Xiaopeng JIA and A. Miyazaki, Stability of  $\text{Ba}(\text{B}_{0.9}\text{Al}_{0.1})_2\text{O}_4$  molten zone by floating zone technique on the ground, *J. Crystal Growth*,
101. T. Mano, K. Watanabe, S. Tsukamoto, H. Fujioka, M. Oshima and N. Koguchi, Fabrication of InGaAs Quantum Dots on GaAs(001) by Droplet Epitaxy, *Journal of Crystal Growth*,
102. T. Mano, K. Watanabe, S. Tsukamoto, Y. Imanaka, T. Takamasu, H. Fujioka, G. Kido, M. Oshima and N. Koguchi, Magnet-photoluminescence study of InGaAs quantum dots fabricated by droplet epitaxy, *Physica E*,
103. T. Hbihara, K. Koizumi, S. Uji, T. Terakura, H. Suzuki, H. Kitazawa and G. Kido, Ferromagnetic surface properties of  $\text{CePb}_3$ , *Physical Review B*,
104. T. Ohki, Sheng. Dong and H. Nezyou, Observation of Au deposited self-assembled monolayers of octanethiol by scanning tunneling microscopy, *Surface Science*,
105. YU Xihong, Y. Mitarai and H. Harada, The formation of an fcc/ $L_{12}$  lamella structure in Ni-12.6Al-20Ir-5Nb refractory superalloys, *Scripta Materialia*,
106. K. Hata, S. Shimizu, T. Suzuki, A. Goto, G. Kido and H. Kitazawa, Experimental aspects of an NMR quantum computer with CeP, *Applied Physics A*,
107. Kim. Byung-Nam, Two-Dimensional Simulation of Grain Growth Based on an Atomic Jump Model for Grain Boundary Migration, *Materials Science and Engineering A*,
108. Kim. Byung-Nam and K. Hiraga, Contribution of Grain Boundary Sliding in Diffusional Creep, *Scripta Materialia*,
109. T. Matsumoto, Jie Tang and N. Mouri, High Pressure Apparatus for in situ X-ray Diffraction and Electrical Resistance Measurement at Low Temperature, *The Rigaku Journal*,
110. Philip BLAZDELLO and S. Kuroda, Thermal Spraying for the New Millennium, *Materials World*,
111. S. Ranganathan, K. Chattopadhyay, O.A. Sigh and K.F. Keitoh, Decagonal Quasicrystals, *Progress in Materials Science*,
112. T. Takeuchi, The compound  $\text{Nb}_3\text{Al}$ , *Handbook of Superconducting Materials (Institute of Physics Publishing)*,
113. H. Kumakura, Development of Bi-2212 conductors and magnets for high magnetic-field generation, *Superconductor Science and Technology Japan Special Issue*,
114. M. Nishida (Kumamoto Univ.), S. Ij (Kumamoto Univ.), K. Kitamura (Kumamoto Univ.), T. Furukawa (Kumamoto Univ.), A. Chiba (Kumamoto Univ.), T. Hara and K. Hiraga, New Deformation twinning mode of B19' martensite in Ti-Ni shape memory alloy, *Scripta Materialia*, 39-12(1998) : 1749-1754.
115. Y. Hata (Tsukuba Univ.), Y. Sugaie (NIRIM), H. Tita (Tsukuba Univ.), H. Suzuki, G. Kido, Crystal structure and magnetism of  $\text{SrV}_6\text{O}_{11}$  single crystals, *J.Applied.Physics*, 85-8(1999) : 4768-4770.
116. T. Noda, M. Fujita and M. Okada, Transmutation and induced radioactivity of W in the armor and first wall of fusion reactors, *J-Nucl. Materials*, 258(1998) : 934-939.
117. H. Araki, H. Suzuki, S. Sato, T. Noda and Yang Wen, Effect of high temperature heat treatment in vacuum on microstructure and pending properties of SiCf/SiC composites prepared by CVI, "*J. Nucl. Mater*", 258(1998) : 263.
118. M. Yata and K. Nakamura, An interpretation on the temperature dependent mode of Cu on Cu(001)- $(2\sqrt{2} \times \sqrt{2})R45^\circ -0$  surfaces, *Surface Science*, 417(1998) : 267-280.
119. T. Suzuki, M. Shimono and S. Takeno, Vortex on the Surface of a Very Small Crystal during Martensitic Transformation, *Physical Review Letters*, 82-7(1999) : 1474-1477.
120. Fuxing Yin, Y. Ohsawa, A. Sato and K. Kawahara, Magnetic Measurement Determination of the Deposition Behavior of the  $\gamma$  Mn Solid Solution in Mn-Cu-NiFe Alloy, *Material Transactions, JIM*, 40-5(1999).
121. S. Tsukamoto, M. Shimoda, M. Sugiyama, Y. Watanabe, S. Maeyama, T. Ohno and N. Koguchi, Transition from GaAs(001)( $2 \times 6$ )-S to ( $2 \times 3$ )-S surface observed by synchrotron radiation photoelectron spectroscopy, X-ray absorption near edge structure, and X-ray standing waves, *IOP Conference Series (Institute of Physics)*, 162(1999) : 604-608.
122. D.N. Perera and A.P. Tsai, Dynamics tensile measurements of  $\text{Pt}_{60}\text{Ni}_{15}\text{P}_{25}$  below the calorimetric glass transition temperature, *J.of Physics: condensed Matter*, (1999) : 3029-3042.
123. T. Nonomura, Hu Xiao and M. Tachiki, Flux-line

- entanglement as the mechanism of melting transition in High-temperature superconductors in a magnetic field, *Physical Review(PR)*, 59-18(1999).
124. Y. Kakeda, T. Umezawa, I. Chiba, H. Syouji and K. Takahashi, Magneto-optical recording on CoPtRe alloy films as a novel material, *IEEE Transactions on Magnetics*, 35-4(1999) : 1-6.
  125. A. Matsumoto, H. Kumakura and K. Togano, Hg doping effects on synthesis, microstructure and superconducting properties of the Bi-2212 phase, *Physica C*, (1999) : 34-40.
  126. K. Yagi and F. Abe, Long-Term creep and Rupture Properties of Heat Resisting steels and Alloys, *Acta Metallurgica Sinica*, 11-6(1998) : 391-396.
  127. T. Ogitsu (Univ.of Tokyo), T.M. Briere (Univ.of Tokyo), K. Kusakabe (Univ.of Tokyo), S. Tsuneyuki (Univ.of Tokyo) and Y. Tateyama, First-principles study of the ortho-KC60 polymer, *Physical Review B*, 58-20(1998) : 13925-13930.
  128. E. Abe, K. Hiraga and Y. Matsuo, The structure of an Al-Pb decagonal quasicrystal studied by HREM, *Philosophical Magazine Letters (Phil.Mag.Lett.)*, 70(1994) : 163-168.
  129. M. Watarai, T. Hanawa, K. Moriyama and K. Asaoka, Amount of metallic ions released from Ti-Ni Alloy by abrasion in simulated bioliquids, *BioMedical Materials and Engineering*, 9(1999).
  130. H. Kawano (RIKEN), H. Yoshizawa (Tokyo Univ.), H. Takeya and K. Kadowaki (Tsukuba Univ.), Anomalous Phonon properties in the intermetallic superconductor  $YNi_2B_2C$ , *Physica B*, 241(1998) : 874.
  131. H. Mamiya, I. Nakatani and T. Furubayashi, Slow Dynamics for Spin Glass-Like Phase of a Ferroagnetic Fine Particle System, *Physical Review Letter:(Phys.Rev.Lett)*, 82-21(1999) : 4332-4335.
  132. T. Yorozu and Hu. Xiao, Magnetization hystereses in trilayer systems with an in-plane component defect, *Journal of Applied Physics(J.Appl.Phys)*, 86-3(1999) : 1581-1595.
  133. Fuxing Yin, Y. Ohsawa, A. Sato and K. Kawahara, Modulated microstructure observed in a slowly cooled Mn-19.7Cu-7.9Ni-2Fe(at%) alloy, *Zeitschrift Fur Metallkunde*, 90-6(1999).
  134. M. Hase and K. Katsumata, Antiferromagnetic resonance in the spin-peierls compound  $CuGeO_3$  doped with Zn, *RIKEN review*, 24(1999) : 17-18.
  135. T. Katsumata, T. Sakai, Y. Oshiba, Y. Isoda, S. Komuro, T. Morikawa and H. Kimura, Growth and characteristics of long duration phosphor crystals, *Journal of Crystal Growth*, 198/199(1999) : 869-871.
  136. E. Abe, T. Sato and A.P. Tsai, Structure of a quasicrystal without atomic clusters, *Physical Review Letters(Phys.Rev.Lett.)*, (1999) : 5269-5272.
  137. A. Yamada (Tohoku Univ.), M. Kitajima, A. Endou, H. Takaba, K. Traishi, S. Salai Cheettu Ammal, M. Kubo, G. Nakamura and A. Miyamoto, Tight-binding Molecular Dynamics Simulation of Desordered SiO Molecule during the Oxidation of Si(111)Surface, *Jpn.J.Appl.Phys*, 38-4(1999) : 2434-2437.
  138. Y. Fukuda, Shuu Ei, K. Furuya and H. Suzuki, Photoluminescence Change of As-prepared and Aged Porous Silicon with NaOH Treatment, *Journal of the Electrochemical Society*, 146-7(1999).
  139. K. Mizoguchi, M. Nakayama, M. Hase and S. Nakajima, Observation of Coherent Folded Acoustic Phonons Propagating in GaAs/AlAs Superlattice by Two-color Pump-probe Spectroscopy, *Physical Review B*, 60(1999).
  140. M. Yethiraj (Oak Ridge N.L.), H. Kawano (Oak Ridge N.L.), K.Mck. Paul (U of Warwick), C.V. Tomy (U of Warwick), H. Takeya and H. Yoshizawa (U of Tokyo), Nonlocal Effects in the Superconductor  $YNi_2B_2C$ , *Journal of Physics and Chemistry of Solids*, 60(1999) : 1059-1062.
  141. H. Kawano (Oak Ridge National Lab), H. Takeya, H. Yoshizawa (Univ.of Tokyo) and K. Kadowaki (Univ.of Tsukuba), Ferromagnetic ordering in superconducting state of  $ErNi_2B_2C$ , *Journal of Physics and Chemistry of Solids(J.Phys.Chem.Solids)*, 60(1999) : 1053-1057.
  142. D.T. Adroja, B.D. Rainford, S.K. Malik, K.A. Gschneidner Jr, V.K. Pecharsky and H. Takeya, Neutron scattering studies on CeRhSb and PrTsb(T=Rh and Pd) compounds, *Journal of Alloys and Compounds(JALCOM)*, 288(1999) : 7-12.
  143. T. Hanamura, H. Shibata, Y. Waseda, H. Nakajima, S. Toritsuka, T. Takahashi and K. Nagai, In-situ observation of Intragranular Ferrite Nucleation at Oxide Particles, *ISIJ International*, 39-11(1999).
  144. H. Suzuki, T. Furubayashi, Guanghan Cao, H. Kitazawa, A. Uemura, K. Hirata and T. Matsumoto, Metal-Insulator Transition and Superconductivity in Spinel-Type System  $Cu_{1-x}Zn_xIr_2S_4$ , *Journal of the Physical Society of Japan (J.Phys.Soc.Jpn)*, 68-8(1999).
  145. J. Nagakawa, Y. Murase, N. Yamamoto and Y. Fukuzawa, Theoretical and Experimental Study on the Significant Creep Deformation of SUS 316 Induced

- by Irradiation at 60 °C , *Kei Engineering Materials*, 171 ~ 174(2000) : 313-320.
146. D. Fujita, H.Y. Sheng, Z.C. Dong, H. Okamoto, T. Ohgi and H. Nejoh, Microstructure of Concentric Ring Patterns on Ta/Si(100), *Journal of Vacuum Science and Technology B*, Nov/Dec(1999).
  147. T. Furubayashi, N. Matsumoto, R. Endo, S. Nagata and T. Matsumoto, Metal-Insulator transition and superconductivity in  $\text{Cu}(\text{Ir}_{1-x}\text{Rh}_x)_2\text{S}_4$  System, *Physical Review B*, 60-8(1999) : 5258-5265.
  148. J. Nagakawa, Radiation Damage in Fusion Reactor Materials, *Computational Materials Design*, 34 (1999) : 164-178.
  149. H. Kitazawa, Andreas. Donni, Peter. Fischer and F. Fauth, Evidence for an isostructural phase transition in the metastable high-temperature modification of  $\text{TbPdAl}$ , *Journal of Alloys and Compounds*, 289(1999) : 11-17.
  150. K. Ishioka, M. Kitajima, K. Murakami, S. Hishita, S. Tateishi, K. Nakanoya, N. Fukata and T. Mori, Hydrogen molecules trapped by multivacancies in silicon, *Phys.Rev.B*, 60-15(1999) : 10852-10854.
  151. M. Shimono, H. Onodera and T. Suzuki, FCC-BCC phase transition in iron under a periodic boundary condition, *Materials Transactions, JIM*, 40-11(1999) : 1306-1313.
  152. Fuxing Yin, K. Ohsawa, A. Sato and K. Kawahara, Phase decomposition of the phase during aging in a Mn-30at. % Cu alloy, *Acta Materialia*, 48.
  153. H. Mamiya and I. Nakatani, Phase Transition of an Iron-Nitride Magnetic fluid: Effects of Temperature and Weak Magnetic Field, *IEEE TRANSACTIONS ON MAGNETICS*, 35-5(1999) : 4061-4063.
  154. H. Eba, N. Ishizawa, F. Marushige and Y. Noda, Synchrotron X-ray study of the monoclinic high-pressure structure of  $\text{AgGaS}_2$ , *Physical Review B (Phys.Rev.B)*, 61(2000).
  155. T. Hanawa, Behavior of titanium in biological systems, *Bulletin of Kanagawa Dental College*, 26-2(1998) : 121-127.
  156. K. Hono, L. Reich and S.P. Ringer, Origin of the initial rapid age-hardening in an Al-d1.7Mg-1.1Cu alloy, *Philosophical Magazine Letters*,
  157. Xu YA, H. Ohtsuka, K. Anak, S. Miyazaki, K. Ito and H. Wada, Effects of High Magnetic Field on Recrystallization Texture in Silicon Steels, *Proc. of The Second Symposium on New Magneto-Science*, (1998).
  158. K. Takazawa and H. Abe, Landau Level of Gaseous Nitric Oxide studied by Two-Color Multiphoton Ionization Spectroscopy, *The Journal of Chemical Physics*,
  159. M. Murayama, Y. Horita and K. Hono, Microstructural Evolution in an Al-Cu Alloy Deformed Channel Angular Pressing, *Mater.Trans.JIM(Materials Transactions JIM)*,
  160. S.E. Donnelly, K. Furuya, Meiki Sou, R.C. Bircher and C.W. Allew, 1.MeV Electron Irradiation of Solid Xe Nanoclusters in Al-an in-situ HRTEM Study,
  161. GU Yuefeng, Y. Mitarai, Y. Ro and H. Harada, Microstructures and Mechanical Properties of Ir-Nb-Ni fcc-L1<sub>2</sub> Two-phase Refractory Superalloy,
  162. GU Yuefeng, Y. Mitarai, Y. Ro and H. Harada, Microstructures and Fracture Behavior of Ir-Nb Two-phase Refractory Superalloys containing Various Amounts of Nb, Ni, Mo, C and B,
  163. GU Yuefeng, Y. Mitarai, Y. Ro, T. Yokokawa, T. Maruko and H. Harada, Microstructures and Deformation Behaviors of Ir-15Nb-XNi and Ph-15Nb-XNi Two-phase Refractory superalloys,
  164. B.S. Murty, D.H. Ping, K. Hono and A. Inoue, Direct evidence for oxygen stabilization of icosahedral phase during crystallization of  $\text{Zr}_{65}\text{Cu}_{27.5}\text{Al}_{7.5}$  metallic glass, *Applied Physics Letters*,
  165. N. Nagashima, S. Matsuoka and K. Miyahara, Nanoindentation tests for Inclusions in High Strength Steels,
  166. Y. Sakka, K. Sodeyama and T. Furubayashi, Whiteness of fine hollow microspheres prepared from vitric volcanic materials, *Journal of Ceramic Society of Japan*,
  167. K. Sakurai and Xiaomei Guo, Crystallization of yttrium aluminum perovskite at around room temperature, *Journal of Materials Science Letters*,
  168. H. Katayama, K. Noda, M. Yamamoto and T. Kodama, Difference in Corrosion Behavior between Pure Iron and Carbon Steel after Short-time exposure test, *Symposium Proceedings Volume (The Electrochemical Society)*,
  169. I. Nishida, M. Hashimoto, O. Oohashi and K. Shioda, Thermoelectric Properties of  $\text{Pb}_{1-x}\text{Sn}_x\text{Te}$  Compounds and FGM,
  170. H. Kimura, A. Miyazaki and Xiaopeng JIA, Crystal properties of  $\text{Li}(\text{B}_{1-x}\text{Al}_x)_2\text{O}_7$  grown by Czochralski method, *Journal of Materials Science Letters*,
  171. M. Yoshitake, Y. Aparna and K. Yoshihara, Realization of self-restorative surface with low and stable work function, *Proceedings of the 5th Interna-*

- tional Symposium on Advanced Physical Fields,*
172. M. Yoshitake and K. Yoshihara, Kinetics of surface composition recovery in self-composition-controlling films, *Proceedings of the 5th International Symposium on Advanced Physical Fields,*
173. M. Yoshitake, Y. Aparna and K. Yoshihara, Stability of work function under gas exposure and gas getting on the ternary self-composition controlling-film, *Proceedings of the 5th International Symposium on Advanced Physical Fields,*
174. M. Yoshitake and K. Yoshihara, Self-control property of surface composition on films, *Proceedings of the 5th International Symposium on Advanced Physical Fields,*
175. J. Alkemper, V. Snyder, N. Akaiwa and P.W. Voorhees, Dynamics of Late-Stage Phase Separation : A Test of Theory, *Physical Review Letters*, 82-13(1999) : 2725-2728.
176. A. Gotou, S. Shimizu, P.V.P.S.S. Sastry and J. Schwartz, Magnetic Scaling in the underdoped superconductor  $Hg_{0.8}Re_{0.2}Ba_2Ca_2Cu_3O_8$  studied by  $^{63}Cu$ NMR, *Physical Review B rapid communication*, 59-22(1999) : 169-172.
177. Y. Yoshida, H. Ohta, M. Aono, Y. Uchikawa, K. Narasaki, Y. Kamekawa, J. Koike, K. Shinada, K. Kamijo, Neutronagnetic SQUID Measurement in a Superconducting Magnetic Shield, *IEEE Transactions on Applied Superconductivity*, 8(1998).
178. N. Yamamoto, J. Nagakawa, K. Shiba, An Evaluation on Helium Embrittlement Resistance of Low Activation Ferritic/Martensitic Steel F<sub>82</sub>H, *Journal of Nuclear Science and Technology*, 36-8(1999) : 713-715.
179. I. Nishida, S. Yoneda (Keiou Univ.), E. Ohta (Keiou Univ.), H. Kaihu (Toritsu Univ.), I. Ohsugi (Ikuei Kousen), K. Miyamoto (Kougakuin Univ.), Crystal Growth of PbTe doped with Pb<sub>12</sub> by the Physical Transport Method, *Journal of Crystal Growth*,

## International Cooperation

Apr. 1999 to Mar. 2000  
International Collaboration Research

### Australia

1. Studies on conductor fabrication Processes of high-Tc BiSrCaCuO super-conductors (University of Wollongong)
2. A comparison of high energy density beam and arc welding technique for joining advanced materials of both the metal-matrix composite and inter-metallic compound types (CSIRO)
3. Development of Novel Rare Earth Permanent Magnets and Their High Magnetic Field Study (University of South Wales)

### China

1. Environmental life cycle analysis of materials (Beijing University of Aeronautics)
2. Enhancement of Superconducting Properties in Bi<sub>2</sub>Sr<sub>2</sub>Ca<sub>2</sub>Cu<sub>3</sub>Ox/Ag Wires and Tapes (Northwest Institute for Metal Research)
3. Comparison Researches of Materials Life Cycle Assessment (MCLA) Between Japan and China (Sichuan Union University)
4. Atomic-scale Structure Fabrication using Scanning Tunneling Microscope (STM) [Beijing Laboratory of Vacuum Physics]
5. Environmentally Assisted Cracking (EAC) of Structural Materials for Light Water Reactors (Shanghai Research Institute of Materials)
6. Joint Research on Synthesis and Analysis of Nano-structured Materials in an Atomic Scale (Tsinghua University)

### EU

1. Research on Materials for Nuclear Fusion Reactor (KFA-Julich etc.)
2. Evaluation Model of the Characterization Data of Materials (Institute for Advanced Materials, Joint Research Center, Petten Site)
3. Effects of Strain on Super-conducting Properties and Microstructure for High Tc Super-conducting Tapes and Wires (University of Twente)
4. Research on the Particle Assembling Process using Nanometer-sized Particles (Lund University)

### Finland

1. Assessment of Long-Term Creep Rupture Strength of Heat Resistant Steels (VTT Manufacturing Tech-

nology)

### France

1. Superconducting and cryogenic materials (Service National des Champus Intenses, CNRS)
2. Structural Study of Disordered Materials by Synchrotron Radiation X-rays (Centre de Recherches sur les Matériaux à Hautes Températures, CNRS)
3. Study on Microstructure and Super-conducting Properties of High Temperature Superconductors with High Critical Current Density (Laboratoire des Materiaux et du Genie Physique)
4. Atomic-scale Single Electron Transistor (CEA Saclay)
5. Materials Processing using High Magnetic Fields (CNRS/MATFORMAG)
6. Effects of Strain on Superconducting Properties and Microstructure for High Tc Superconductors (Laboratoire des Champs Magnetiques Intenses)

### Germany

1. High Performance Superconducting Materials (Forschungszentrum Karlsruhe)
2. Development of Documentation Panel, Numerical Data (Fachinformationszentrum Karlsruhe)
3. Designing of New Continuous Refining Process (Haus der Technik e.v. Essen)
4. Nanoscopic Evaluation of Material Properties (Max-Planck-Institut für Eisenforschung GmbH, Universität des Saarlandes)
5. In Vitro and In Vivo Biocompatibility of Biomaterials (Free University of Berlin)
6. Joint Research on the Structural Analysis of Clusters and Interfaces by Sub-Angstrom Electron Microscopy (Max-Planck-Institute für Metallforschung)
7. Study on the Electronic Band Structure using GW Method based on the Linear Muffin Tin Orbital Method (MAX-Planck-Institut FKF)
8. Development of Intelligent Life Assessment in Power and Process Plants (University of Stuttgart)
9. Characterization of High-field Performances for Oxide Superconductors (Georg-August-Universität Göttingen Institute für Metallphysik)

### Hungary

1. Noise Analysis of Single Electron Transister (Department of Physics, Jozses Attila University)

## India

1. Studies of quasi-crystalline based composites (Indian Institute of Science)

## Italy

1. Superconducting properties of advanced superconductors in time-varying magnetic fields (EDISON SPA, R & D)
2. Intercomparison of methods and materials for strain measurements at cryogenic temperatures (Istituto di Metrologia "G. Colonnetti" -C.N.R)
3. Mechanism of Deformation, Fracture and Corrosion in Ni-base Superalloys (Istituto Tecnologia Materiali e Processi Energetici)

## Korea

1. Performance characterization of materials at high temperature (Korea Research Institute of Standards and Science)
2. Evaluation of the high temperature properties for titanium-based particulate Composites (Korea Advanced Institute of Science and Technology)
3. Studies on the fabrication of Bi-2223 superconducting wire and its application (Korea Institute of Machinery and Metals)
4. Fabrication and characterization of semiconductor quantum dots (Korea Research Institute of Standards and Science)
5. Plasma assisted surface modification on metallic biomaterials (Korea Institute of Machinery and Metals)
6. Application of pulsed high magnetic fields for the measurement of high-performance permanent magnets (Korea Research Institute of Standards and Science)

## Netherlands

1. Studies for Measuring Technique of Quantum Effect and for Strongly Correlated Electron System (Amsterdam University)
2. Study on Magnetic Properties of Steels at High Temperature (Delft University of Technology)
3. Assessment of Environmental Loading of Materials (Center of Environmental Science Leiden University)
4. Interface Roughness and Thickness of Thin Film Multi-layer Structures (FOM Institute for Atomic and Molecular Physics)
5. Study on Electronic Instabilities in Magnetic Materials With F-electrons Under Multi-extreme Conditions (University of Amsterdam)
6. Design and Evaluation of Super-alloys for Gas Tur-

bine Applications (University of Twente)

7. Characterization of High-field and Strain-tolerance Performances for Super-conductors (University of Twente)

## Poland

1. Magnetization and Optical studies in Diluted Magnetic Semiconductors in High Magnetic Fields (Polish Academy of Science)

## Sweden

1. Fabrication and characterization of semiconductor quantum dots (Lund University)
2. Atomic-scale Single Electron Transistor (Chalmers University of Technology)

## Switzerland

1. Research and Development of High Performance Ceramic Super-conducting Wires (University of Geneva)
2. Characterization of Oxide Superconductors (University of Geneva)
3. Research on Fabrication of Highly-reliable Structural Ceramics through Advanced Powder Processing (Swiss Federal Institute of Technology)
4. Evaluation of High Temperature Properties for Titanium and Ceramic Matrix Composites (Swiss Federal Laboratory for Materials Testing Research)

## U.K.

1. Quantum Properties of Nanostructures of Compound Semiconductors (University of Nottingham)
2. Prediction Technology of Life and Remaining Life of Huge Structures under Service Condition and its Application to Design (The Welding Institute)
3. Assessment of Ultra-Long-Term Creep Rupture Strength of Heat Resisting Steels (GEC Alsthom Generators Ltd.)
4. Research of Methods for Large-scale Numerical Simulations (University College London)
5. Measurement and Evaluation Methods for Critical Current in High Temperature Superconductors (University of Cambridge)

## U.S.A.

1. Research and development on systems and materials for magnetic refrigeration (Francis Bitter National Magnet Laboratory, MIT)
2. Databases on high temperature superconducting materials (National Institute of Standards and Technology)

3. Studies of high-strength/high-conductive materials and their application to high-field magnets (Francis Bitter National Magnet Laboratory, MIT)
4. Fundamental studies on the conductor fabrication of high temperature oxide superconductors (National High Magnetic Field Laboratory)
5. Measurement and evaluation methods for superconducting properties (National Institute of Standards and Technology)
6. Developments and applications of extremely high-field magnets and magnet systems (National High Magnetic Field Laboratory)
7. Joint Research on the "in-situ" analysis/evaluation of atomic and micro-structural changes in materials (Argonne National Laboratory)
8. Study of nano-composites magnetic materials for cryogenics (National Institute of standards and Technology)
9. Fundamental study of vortex state in high Tc superconductors (Argonne National Laboratory)
10. High pressure research on strongly correlated electron systems (University of California)
11. Effect of high magnetic field on solid/solid phase transformations (North-western University)
12. Studies on mechanisms of nanoscale microstructural evolution in advance metallic materials (University of Virginia)
13. Study on the mechanical properties of directionally solidified intermetallic compounds (Oak Ridge National Laboratory)
14. Evaluation of thick coatings formed by advanced thermal spray processes (New York State University)
15. Photolysis of Silicon Compounds by Infrared Free Electron Laser (Los Alamos National Laboratory)
16. Basic Studies on Mechanisms of Micro-structural Evolution in Next Generation Steels (Virginia Polytechnic Institute and State University)
17. Study on the Flux-line States and Josephson Plasma in High-Tc Superconductors (Argonne National Laboratory)
18. Physical Properties of the Transition Metal Compounds under High Pressure (Carnegie Institution of Washington)
19. Development of Nb<sub>3</sub>Al Multi-filamentary Superconductor (Ohio State University)
20. Analysis and Numerical Modeling of High Energy Beam Welding Phenomena (Penn State University)
21. Joint Research on Materials and System for Adiabatic Demagnetization Refrigerator (NASA/Goddard Space Flight Center)
22. Superconductors for Large Scale Applications (University of Wisconsin)

□ List of Visiting Foreign Researchers who came to NRIM from Apr.1999 to Mar.2000

\*STA Fellows

Country and Name	Affiliation	Term	Research Subject
<b>Australia</b>			
Donna Nicole Perera*	University of Sydney	1999.4.1 ~ 2000.3.31	Experimental and Theoretical Characterization of Grass-forming Multi-component Metallic Alloys
Ninh the Nguyen*	University of Sydney	1999.4.1 ~ 1999.8.31	Evaluation for Fatigue Strength of Welded Joints in Residual Stress Field
Steve Hwang*	University of Western Australia	1999.9.11 ~ 2000.3.31	Improvement of Hydrogen Desorption of Mg-based Hydrogen Storage Alloys by Microstructure Control using Powder Processing
<b>Austria</b>			
Harald. W. Weber	Atominstiute der Oestereichschen Universitaet	1999.10.15 ~ 1999.10.19	Evaluation Methods and Standardization of Superconductors
<b>Belarus</b>			
Victor E. Borisenko	Belaruian State University of Informatics and Radioelectronics	1999.12.13 ~ 1999.12.18	Fabrication and Characterization of Compound Semiconductor Nanostructures
<b>Belgium</b>			
Alexandre Mayer	Universitaires Notre-Dame de la Paix	1999.8.20 ~ 1999.8.30	Simulation of the Tunneling Projection Microscopy
Johan Vanacken	Katholieke Universiteit Louven	2000.3.13 ~ 2000.3.17	Materials with Atomic-scale Structure
<b>China</b>			
Ya Xu	Japan Science and Technology Corporation (JST)	1999.4.1 ~ 2000.3.31	Effects of High Magnetic Field on Solid/Solid Phase Transformations and Structural Control of Materials by Magnetic Field
Feng Tang	JST	1999.4.1 ~ 2000.3.31	Evaluation of High Temperature Mechanical Properties for Ti <sub>2</sub> AlNb-based Intermetallic Alloys
Yuefeng Gu*	Shanghai Jiao Tong University	1999.4.1 ~ 1999.9.30	Grain Boundary Structures and Ductility Improvement of Platinum Group Metals based Refractory Superalloys
Hai Qiu	The University of Tokyo	1999.4.1 ~ 2000.3.31	Study on the Strength and Toughness of Ultra-fine Grained Steel and its Welded Joint
Guo Junqing	JST	1999.4.1 ~ 2000.3.31	Production of Single Quasicrystals
Yang Wen	China Institute of Atomic Energy	1999.4.1 ~ 2000.3.31	Interfacial Control and Evaluation of Properties of CVI SiC/SiC Composites

Country and Name	Affiliation	Term	Research Subject
Yaquiao Wu*	Institute of Materials Research, Chinese Academy of Science	1999.4.1 ~ 1999.9.30	Microstructures and Properties of Nd-Fe-B based Nanocomposite Magnets
Yuning Jiao*	Institute of Metals Research, Chinese Academy of Science	1999.4.1 ~ 2000.1.31	Research on Structure Formation by Solidification Processing
Jiang-Qing Su*	Institute of Metals Research, Chinese Academy of Science	1999.4.1 ~ 2000.3.31	Study on the Mechanical Proper- ties of Grain Boundaries in Ni <sub>3</sub> Al
Fuxing Yin	JST Domestic Research Fellow	1999.4.1 ~ 1999.9.30	The Development of High-strength Mn based Damping Alloys with the Introduction of Hard and Ferro- magnetic Particles
Xiaopeng Jiao	Institute of DEO	1999.4.1 ~ 2000.3.31	Investigation, Crystal Growth and Characterization of New Nonlinear Optical Crystals for Wavelength Modulation
Tu Geng	JST Domestic Research Fellow	1999.4.1 ~ 1999.9.30	Design of Heat Resistant Alloys based on Thermodynamic Calcula- tions
Daozhi Liu*	Faculty of Materials Science and Engineering, Tianjin Uni- versity	1999.4.1 ~ 2000.3.31	Development of Fe-based Shape Memory Alloys with Perfect Shape Recovery
Guanghan Cao*	Department of Physics, Zheji- ang University	1999.4.1 ~ 2000.3.31	Substitutional Effect on the Thio- spinel Compound CuM <sub>2</sub> S <sub>4</sub> (M=5d Transition Metal Elements)
Chu Feng Min	Chinese Institute of Atomic En- ergy	1999.9.1 ~ 2000.2.29	Fundamental Research of High Resolution Electron Microscopy
Kewei Gao*	University of Science and Tech- nology, Beijing	1999.9.14 ~ 2000.3.31	Hydrogen Embrittlement of TiAl based Alloys
Jian Xin Zhang*	Institute of Metal Research, Chinese Academy of Sciences	1999.9.30 ~ 2000.3.31	Development of Advanced Shape Memory Thin Films by Sputtering
Gu Hongwei*	Beijing General Research Insti- tute for Non-ferrous Metals	1999.12.9 ~ 2000.3.31	Study of Properties and Structural Changes in Superconducting Materi- als and Strong Correlation Materi- als under Pressure
Dong Jianxin*	Department of Materials Sci- ence and Engineering, Univer- sity of Science and Technology Beijing	2000.2.28 ~ 2000.3.31	Investigation on the Relationship between High-temperature Creep Properties and Microstructural Changes of Ni base Superalloys
Dong Junhua*	Institute of Corrosion and Pro- tection of Metals, Chinese Academy of Science	2000.1.10 ~ 2000.3.31	Mechanism of Rust Formation on Steel in Coastal Atmosphere
Chinese Taipei			
F.R.Chen	National Tsing Hua University	1999.11.14 ~ 1999.11.20	Application of Maximum Entropy Method toward High Resolution Electron Microscopy

Country and Name	Affiliation	Term	Research Subject
<b>Czech</b>			
Josef Nemeč*	Academy of Science of the Czech Republic	1999.4.1 ~ 2000.3.31	Changes in Creep Strength and Governing Factor of Inherent Creep Strength of 12Cr Ferritic Creep Resistant Steels
Vladimir Matolin	Charles University	1999.8.26 ~ 1999.9.1	Formation of Eitaxial Thin Aluminum Oxide Film on Niobium Single Crystal
<b>Egypt</b>			
Abdel-Monem Mohamed El-Batahgy*	Central Metallurgical Research and Development Institute	2000.1.30 ~ 2000.3.31	Study on Creep Strength Property of Welded Joint oh High Cr Ferritic Creep Resistant Steel
<b>France</b>			
Stephane Odasso*	Research Center on the Mechanism of Crystal Growth	1999.4.1 ~ 1999.4.30	Electron Transport Measurements in Lead Nanostructures Patterned onto Ideal Si(111)-(1x1):H Templates
Fabrice Dugain*	Institute Laur-Langevin	1999.4.1 ~ 2000.3.31	Neutron Scattering on Quasicrystals
Retal Christophe	Universite de Rouen, UFR Science	1999.4.1 ~ 1999.8.31	3 Dimension Atom Probe Analysis of Guinier Preston Zones in Al-Ag Alloy
Stephane Labat*	MATOP, URA CNRS, Faculte de St. Jerome	1999.4.1 ~ 1999.8.17	A Study of Inplane Stress on Superconducting Properties of High-Tc Superlattice Films
Peter Wyder	Grenoble High Magnetic Field Laboratory	1999.11.20 ~ 1999.11.27	Development of High Field Magnets
Ludvic Renaud	Laboratoire de Micro-scopie Ionique URA CNRS and Universite de Rouen	1999.11.28 ~ 1999.12.4	Development of an Energy Compensated Optical Tomographic Atom Probe
Xavier Sauvage	Universite de Rouen, UFR Sciences	1999.11.28 ~ 1999.12.4	HREM Observation of Cu-Nb in-situ Metal Matrix Composite
Marc de Boissieu	UMR/CNRS	2000.2.5 ~ 2000.2.10	Neutron Scattering on Quasicrystals
Jean-Claude Vallier	Centre de Recherches sur les Tres Basses Temperatures	2000.2.20 ~ 2000.2.24	Evaluation Methods and Standardization of Superconductors
Claude Landron	Centre de Recherche sur la Physique des Hautes Teparature	2000.2.22 ~ 2000.3.19	Structural Study of Disordered System by Synchrotron Radiation X-rays
Gastaldi Joseph	CRMC2/CNRS	2000.3.4 ~ 2000.3.14	Neutron Scattering on Quasicrystals
Oliver Portugal	Institut National des Science Appliqueesservice National Champs Magnetiqués Pulsé	2000.3.12 ~ 2000.3.18	Materials with Atomic-scale Structures
Gerald Da Costa	Laboratoire de Micro-scopie, Ionique URA CNRS and Universite de Rouen	2000.3.20 ~ 2000.3.29	Development of an Energy Compensated Optical Tomographic Atom Probe
<b>Germany</b>			
Gerd Kley	Federal Institute for Materials Research and Testing (BAM)	1999.11.5 ~ 1999.11.13	Investigation on Barrier-free Processing for Design for Environment

Country and Name	Affiliation	Term	Research Subject
Manfred Dauemling	NKT Research Center	2000.3.6 ~ 2000.3.10	Evaluation Methods and Standardization of Superconductors
Markus Pristovsek	Institut für Festkoer-perphysik, Technische Universität Berlin	2000.3.6 ~ 2000.3.18	Investigation on New Functional Materials by Atom-Sublime Process
Wolfgang J. Ossau	Wurtzburg University	2000.3.26 ~ 2000.3.31	Materials with Atomic-Scale Structures
<b>India</b>			
Budaraju Srinivasa Murty*	Indian Institute of Technology, Kharagpur	1999.4.1 ~ 2000.3.31	Nanocrystallization of Amorphous Alloys
Aparna Yarrama-Reddy*	National Physical Laboratory	1999.4.1 ~ 2000.3.31	Study on Surface Segregation in Films and Property of Surface with Segregation
Srinivasa Ranganathan*	Indian Institute of Science	1999.4.25 ~ 1999.5.24	The Role of Clusters in Quasicrystals
Jayavel Ramassamy*	Crystal Growth Centre, Anna University	1999.8.16 ~ 2000.3.31	High-Quality Single Crystal Growth of High-Tc Superconductors and their Properties
<b>Italy</b>			
Ilaria Salvatori*	Centro Sviluppo Materiali	1999.4.1 ~ 2000.3.31	The Basic Research for Controlling of Ausenite Grain Sizes of SUS304
<b>Korea</b>			
Iksu Chong	JST Domestic Research Fellow	1999.4.1 ~ 2000.3.31	Synthesis and Properties of High Tc Superconducting Materials
Yeon Soo Sung*	Argonne National Laboratory	1999.4.1 ~ 1999.10.29	Development of Large Current Carrying Bi-based Oxide Superconducting Tapes
Chang-Seok Oh*	Korea Electric Power Research Institute (KEPRI)	1999.4.1 ~ 2000.3.31	Thermodynamic Calculation for Ni-base Superalloys
Kim Kyung-cho	Korean Science and Engineering Foundation Post-doctoral Fellow	1999.4.20 ~ 2000.3.31	Development of Non-destructive Evaluation Techniques for Microstructure and Small Defects in Steel
Ji Yen Park	Korea Atomic Energy Research Institute	1999.9.1 ~ 2000.2.29	Synthesis and Irradiation Effects of SiC Composites
Soo Young Kang*	Seoul National University	1999.9.30 ~ 2000.3.31	Design of Heat Resistant Intermetallic Compound
Dong Woo Lim	Korean Industrial Property Office	1999.10.4 ~ 1999.10.10	Materials with Atomic-Scale Structures
Lim Cha-Yong	Korea Institute of Machinery and Materials	1999.10.12 ~ 1999.11.1	Electron Microscopy Study of Refined Microstructure in Aluminum Alloys
Kwang Soo Shin	Research Institute of Industrial Science and Technology (RIST)	1999.10.31 ~ 2000.2.29	Surface Characterization by Grazing-Incidence X-ray Techniques using Synchrotron Radiation
Yeon Soo Sung	JST	1999.11.1 ~ 2000.3.31	Formations of Large Supercooling State and New Functional Materials

Country and Name	Affiliation	Term	Research Subject
Song-yop Hahn	School of Electronical Engineering, Seoul National University	1999.11.10 ~ 1999.11.11	Evaluation Methods and Standardization of Superconductors
Kang-Sik Ryu	Korea Electrotechnology Research Institute	1999.11.10 ~ 1999.11.14	Materials with Atomic-Scale Structures
Jae-Young Leem	Korea Research Institute of Standards and Science (KRISS)	1999.11.28 ~ 1999.12.4	Fabrication and Characterization of Semiconductor Quantum Dots Lasers
Hong, Hyun UK	Korea Advanced Institute of Science and Technology	2000.1.17 ~ 2000.2.24	Study on the Fabrication of Ni <sub>3</sub> Al-based Intermetallic Compounds by Directional Solidification
Oh Jun Cheol	Pohang University of Science and Technology	2000.1.17 ~ 2000.2.25	APFIM and HREM Investigations of the Microstructures of Fe-Cr-Co-Mo Steel
Kim Shae-Kwang	Sung Kyun Kwan University	2000.1.18 ~ 2000.2.25	Cladding Process Combined Plastic Working with Semi-Molten Processing
Kyung Sub Lee	Institute of Science and Technology of Sungkyunkwan University	2000.3.7 ~ 2000.3.9	Fabrication of Monolayer Thin Films for Advanced Substrate Materials
Malaysia			
Md. Hasan Zahir*	University of Sains Malaysia	1999. 4.1 ~ 1999.10.29	Synthetic, Spectroscopic and Electrochemical Investigation of Metal-Phthalocyanine Complexes that Show Unusual Electronic Absorption Spectra
Myanmar			
Thi Thi Lay	JST Domestic Research Fellow	1999.4.1 ~ 2000.3.31	Photon Probe Measurement of Quantum Effects due to Nanostructures
New Zealand			
Shoujin Sun*	The University of Canterbury	1999.4.1 ~ 2000.3.31	The Development of High Strength High Conductive Copper Base in-situ Composites
Netherlands			
Jan-Kees Maan	University of Nijmegen	1999.11.21 ~ 1999.11.27	Development of High Field Magnets
Joseph Perenboom	High Field Magnet Laboratory, University of Nijmegen	2000.3.26 ~ 2000.3.31	Generation and Application of High Magnetic Fields
Nigeria			
Joseph Anireju Lori	Department of Chemistry, Ahmadu Bello University	2000.2.21 ~ 2000.3.31	Study on Elucidation of Reaction Mechanism between Biomaterial Surface or Metallic Ions and Biomolecules
Russia			
Viatcheslav E. Korsoukov*	Ioffe Physical Technical Institute, Russian Academy of Sciences	1999.9.30 ~ 1999.11.29	Surface Reactions induced by Surface Stress

Country and Name	Affiliation	Term	Research Subject
Victor L. Mironof	Institute for Physics of Micro-structutres, Nizhny Novgorod	1999.12.13 ~ 1999.12.18	Fabrication and Characterization of Compound Semiconductor Nano-structures
Alexei Grigorievich Vitukhnovsy	Lovedev Physical Institute, RAS (Russian Academy of Science)	2000.2.5 ~ 2000.2.20	Electronic States and Photon Emission from Dendrimer Molecules
Slovak			
Michael Rabara	University of Tokyo	1999.4.1 ~ 2000.3.31	Basic Research in the Development of Superconducting Magnets for Fusion Use
Spain			
Hang Ping Miao	JST	1999.4.1 ~ 2000.3.31	Formations of Large Supercooling State and New Functional Materials
Nicolas Garcia	Laboratorio de Nanotecnologia	2000.3.20 ~ 2000.3.31	Gigantec Magneto-Resistance at Nanometer-scale Contact
Sweden			
Peter Johansson	Division of Solid State Theory, Dept. of Physics, Univ. of Lund	2000.2.28 ~ 2000.3.4	Research on the Quantum Effect Growth using the Extreme High Vacuum Fields
Switzerland			
Rune Flükiger	University of Geneve	2000.2.13 ~ 2000.2.20	Studies on the High Temperature Superconductors
Turkey			
Coskun Isci	Dokuz Eylul University	1999.9.5 ~ 1999.9.13	Materials with Atomic-Scale Structure
Yusuf Hascicek	National High Magnetic Field Laboratory	1999.10.15 ~ 1999.10.19	Evaluation Methods and Standardization of Superconductors
U.K.			
Philip Blazdell*	Brunell University	1999.4.1 ~ 2000.3.31	Novel Forming of Ceramic Coatings
Timothy M. King	Kochi Univ. of Technology	1999.4.1 ~ 2000.3.31	Research Concerning Upgrade of the Materials by Atom-Sublime Process
Jeremy P. Weston*	University of Cambridge	1999.5.21 ~ 2000.3.31	Study on Brazing for the Construction of Rocket Engine
David Cardwell	University of Cambridge	1999.10.16 ~ 1999.10.20	Evaluation Methods and Standardization of Superconductors
Gavin R. Bell	Imperial College of London	2000.1.6 ~ 2000.1.22	Investigation on New Functional Materials by Atom-Sublime Process
John Gisby	National Physical Laboratory	2000.3.5 ~ 2000.3.18	Dispersion Properties of Inclusion in Molten Metal by the Cold Crucible Levitation Method
Robert F. Brooks	National Physical Laboratory	2000.3.5 ~ 2000.3.18	Dispersion Properties of Inclusion in Molten Metal by the Cold Crucible Levitation Method
Colin Walters	Rutherford Appleton Laboratory	2000.3.20 ~ 2000.3.24	Evaluation Methods and Standardization of Superconductors

Country and Name	Affiliation	Term	Research Subject
Mohamed Henini	University of Nottingham	2000.3.25 ~ 2000.3.30	Materials with Atomic-Scale Structures
Ukraine			
Oleg Orestovich Vasylykiv*	Institute of Materials Science Problems of the Ukrainian National Academy	1999.4.1 ~ 2000.3.31	Synthesis and Sintering of Nano-size Powders and Characterization of Nano-phase Materials
Alexander D. Pogrebnjak	Sumy Institute for Surface Modification, Sumy State University	1999.11.1 ~ 1999.11.18	Material Surface Modification by High-Current Ion Implantation
Lyudmyla A. Karachevtseva*	Institute of Semi-conductor Physics	2000.1.10 ~ 2000.3.9	Structural and Chemical Features of Microporous n-Si Photonic Materials
Hanna Borodidians'ka	Institute for Materials Science Problems of Ukrainian National Academy of Sciences	2000.1.18 ~ 2000.3.31	Study on the Fabrication of Ni <sub>3</sub> Al-based Intermetallic Compounds by Directional Solidification
Oleksandr Marchenko	Institute for Physics, Ukrainian National Academy of Sciences	2000.2.5 ~ 2000.3.31	Self-Assembly of Organic Molecules on Metal Surfaces
U.S.A.			
James Dintaman Martin	North Carolina Univ.	1999.7.27 ~ 1999.8.3	Open Framework Metal Halide Materials-Inorganic Liquid Crystals
Easo P. George	Oak Ridge National Laboratory	1999.9.16 ~ 1999.10.21	Study on the Hydrogen Induced Embrittlement in Intermetallic Compounds
Justin Schwartz	National High Magnetic Field Laboratory (NHMFL)	1999.10.11 ~ 1999.10.14	Development of High Temperature Superconductors
John Dudley Corbett	Ames Laboratory, Dept. of Chemistry, Iowa State University	1999.10.13 ~ 1999.10.19	Cluster Chemistry in Intermetallic Polar Salts
Dongle Shi	Dept. of Materials Science and Eng., Univ. of Cincinnati	1999.10.16 ~ 1999.10.20	Evaluation Methods and Standardization of Superconductors
O.L.Krivanek	University of Washington	1999.11.16 ~ 1999.11.19	Atomic Resolution Electron Energy Loss Spectroscopy
John L. Lyman	Los Alamos National Laboratory	1999.11.28 ~ 1999.12.11	Enrichment of Silicon Isotopes with Infrared Free-Electron Laser Irradiation
Vladimir V. Semak	Applied Research Laboratory, Pennsylvania State University	1999.11.28 ~ 1999.12.11	Analysis and Numerical Modelling of High Energy Beam Welding
James R. Anderson	University of Maryland	2000.1.11 ~ 2000.1.19	Materials with Atomic-Scale Structure
R. C. Bircher	Argonne National University	2000.1.16 ~ 2000.1.22	Observation of Nano-meter Sized Precipitates Inside Metals
C. W. Allen	Argonne National University	2000.1.16 ~ 2000.1.22	Observation of Nano-meter Sized Precipitates Inside Metals
Murray Gibson	Argonne National University	2000.1.22 ~ 2000.1.27	High Resolution Electron Microscopy Observation of Amorphous Structures
F. B. Dunning	Department of Physics, Rice University	2000.2.6 ~ 2000.2.12	Spin Polarimetry of Electrons

Country and Name	Affiliation	Term	Research Subject
J. W. Morris, Jr.	Univ. of California, Berkley	2000.2.21 ~ 2000.2.25	Analysis and Numerical Mopdelling of High Energy Beam Welding
Lee Heatherby	Metal and Ceramics Division, Oak Ridge National Laboratory	2000.3.1 ~ 2000.3.11	Thin-Film Fabrication and Surface Analysis of Nanostructures
Jack Crow	NHMFL	2000.3.4 ~ 2000.3.11	Development of High Field Magnets
John R. Miller	NHMFL	2000.3.5 ~ 2000.3.8	Research on the Basis Making for Promoting the Practical Application of International Advanced Materials
Areneil Reyes	NHMFL	2000.3.12 ~ 2000.3.18	NMR Research on Solid State Physics

## □ Brief Introduction of STA Fellowship Program

In response to growing calls from the international community for greater international cooperation, the STA Fellowship program was established to provide foreign researchers with opportunities to conduct research at Japanese national laboratories and public corporations which are not part of the university system.

The program is managed by the Japan Science and Technology Corporation (JST) Which is one of the key organizations for implementing policies of the Science and Technology Agency (STA) in cooperation with the Japan International Science and Technology Exchange Center (JISTEC). Fellowship qualifications are as follows:

1. Possession of Ph.D. or equivalent qualifications.
2. Long term fellowship is less than 35 years of age or have received his/her PhD within the last 6 years. Short term fellowship is no limitation of age.
3. Good health to do research-work and live in Ja-

pan.

4. Skillful language of Japanese or English words.

The tenure is from 6 months to 2 years (long term Fellowships), or 1 ~ 3 months (short term Fellowships).

JST provides fellowships with a round-trip airline ticket, a monthly living expenses, a family allowance, an initial international moving allowance, accommodations (long term fellowships), accommodations allowance (short term fellowships).

And to the long term fellowships it is paid the travel cost in Japan related to research activities but it is not applied to the short-term fellowships. Research expenses will be paid to the host institutes.

Further information can be obtained at JISTEC:  
2-20-5, Takezono, Tsukuba City, Ibaraki Pref. 305-0032, Japan.

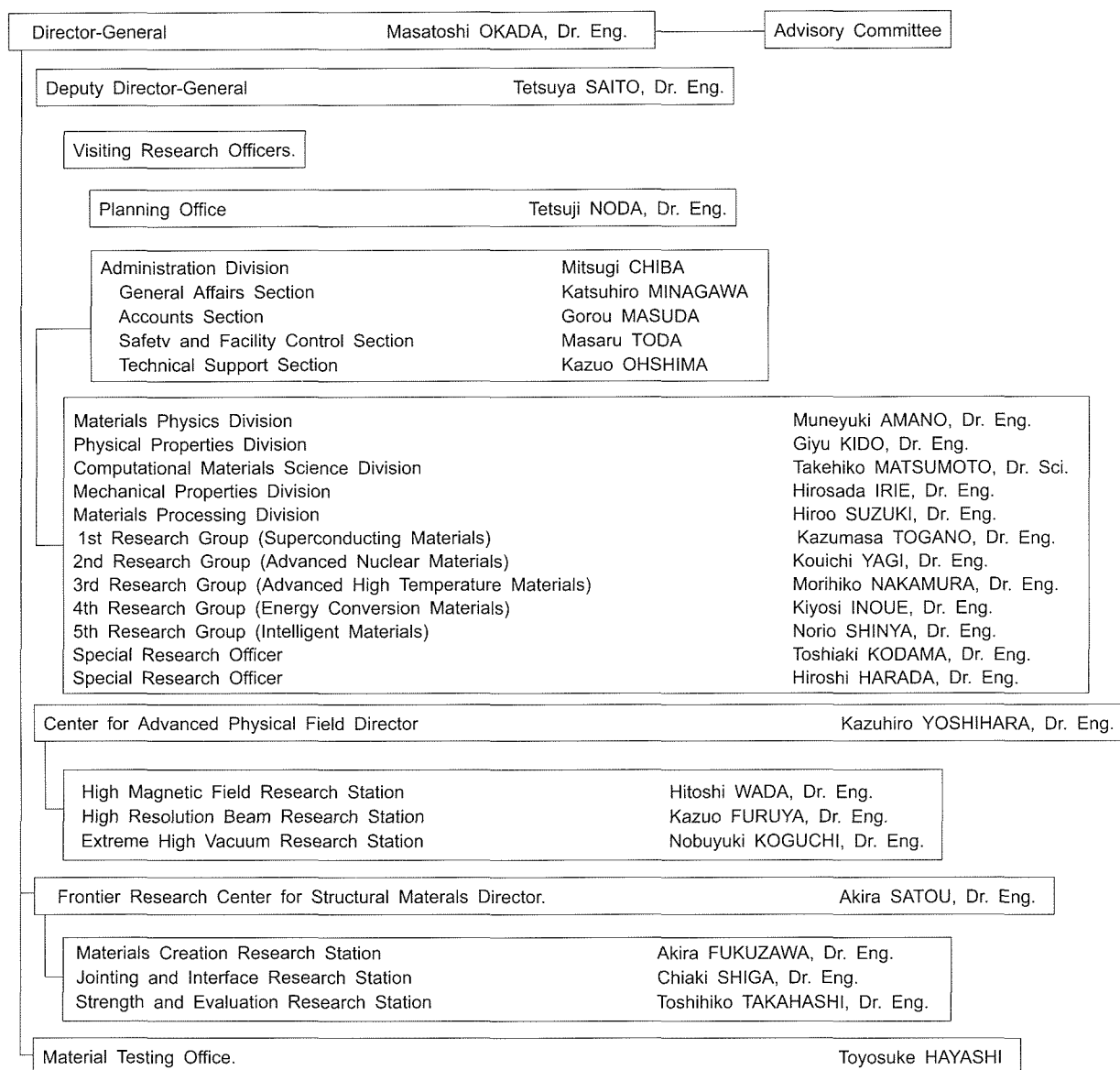
Phone +81-298-53-8250

Fax +81-298-53-8260

## □ Organization

### Organization of NRIM

#### Organization



## □ Budget and Personnel in Fiscal Year of 2000

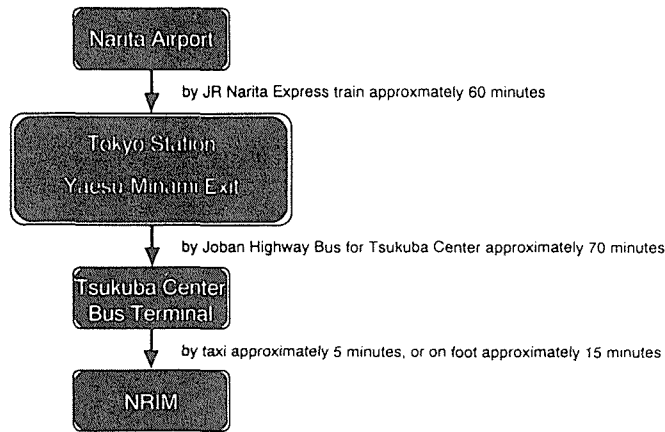
Budget		Personnel	
Research and Facilities	6,420	Administrative staffs	79 (8)
Personnel expenses	3,685	Researchers	322 (4)
Total	10,105	Total	401(12)

unit : million yen

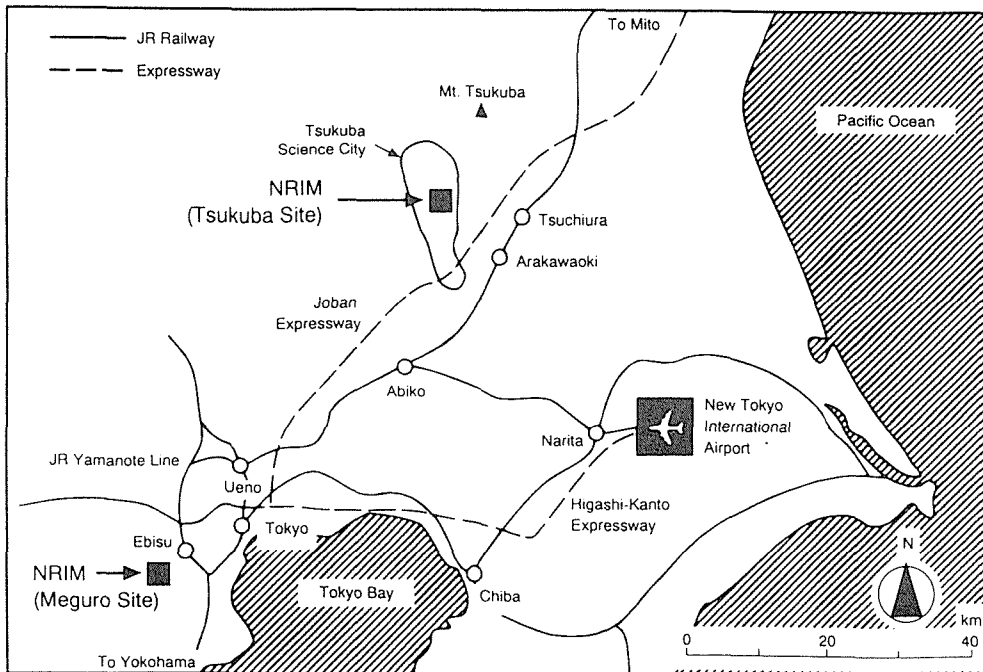
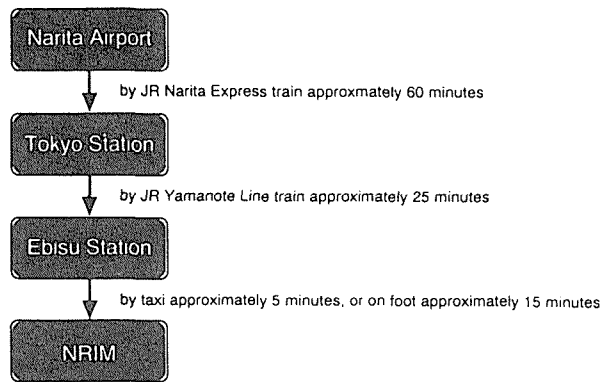
Number in parenthesis : Material Testing Office

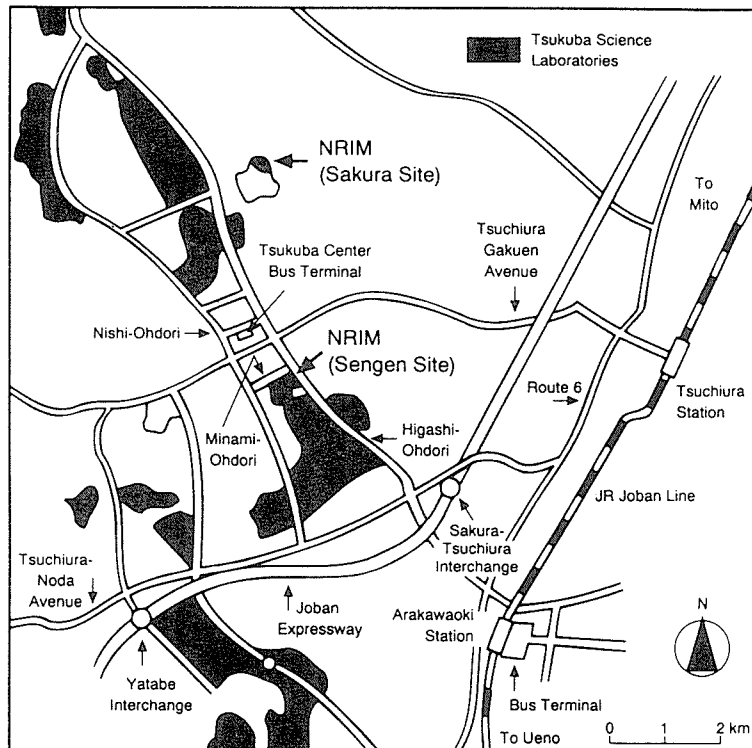
# How to get NRI

To NRI Tsukuba Site  
 1-2-1 Sengen, Tsukuba-shi, Ibaraki 305-0047  
 Phone +81-298-59-2000, Fax +81-298-59-2029

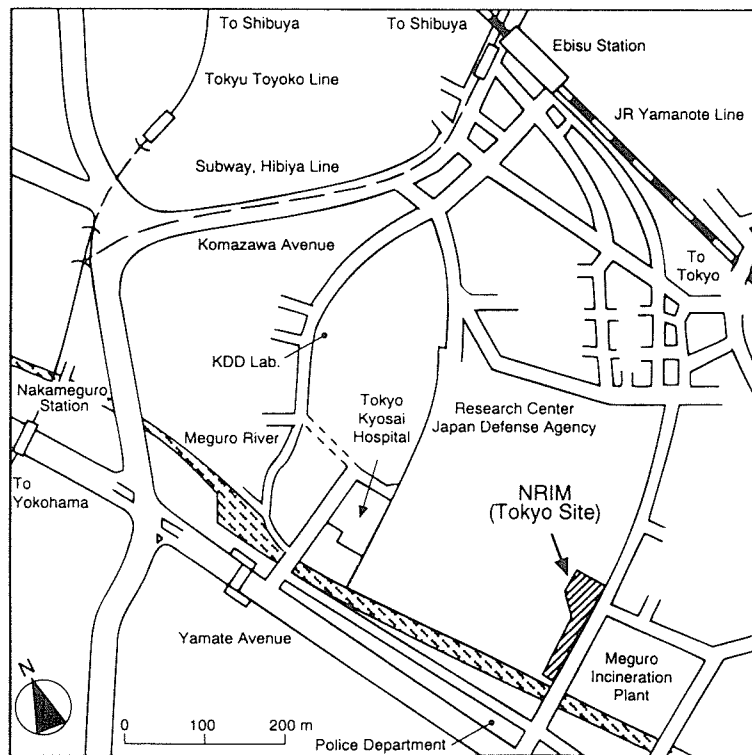


To NRI Meguro Site  
 2-2-54 Nakameguro, Meguro-ku, Tokyo 153-0061  
 Phone +81-3-3719-2271, Fax +81-3-3719-2177





Tsukuba Site



Tokyo Site

## List of Keywords

<b>A</b>			
aging degradation	64	computer simulation	47, 64
alignment	9	computerized materials data	42
alkaline-earth metals	16	cooling of laser illuminated photocathode	3
alloy designing	59	Copper	63
Aluminum	63	co-sputtered film	55, 56
aluminum alloy matrix composite	22	Cr	20
Aluminum-titanium-manganese ternary system	30	crack closure	20
Aluminum-titanium-manganese-vanadium quaternary system	30	creep	59, 66
anisotropy	9	creep crack growth	66
antiferromagnetism	10	creep fracture	64
antimonic acid	19, 22	creep rupture	13
APFIM	6	cryogenic temperature	15, 17
AP-FIM	58	crystal asymmetry	36
Argon ion laser	3	crystal growth	18
atom probe	6	Cu alloy	22
		current carrying capacity	45
		Current Lead	33
<b>B</b>		<b>D</b>	
B2 structure	37	Damping alloys	62
Bi-2223	33	database	49
Bi-2223magnet	47	DDTC	6
binary stable quasicrystal	43	defect	25
boron	27	deformation	25
brittle fracture	66	Degradation	54
buffer layer	24	delayed fracture	58
		Depth sensing indentation	66
		dielectric constant	36
		Diffusion bonding	20
		diffusion of point defects	64
		diffusional creep	15
		dislocation	12
		dislocation activity	15
		dislocation climbing velocity	11
		dislocation motion	66
		DNA	9
		<b>E</b>	
		Eco-material	63
		ecomaterials	42
		Elastic modulus	66
		electrical conductivity	22, 23
		electrical resistivity	16
		electron correlation	7
		electrophoretic deposition	22
		excited neutral	52
		extremely high vacuum	44
		<b>F</b>	
		fatigue	25, 59
<b>C</b>			
cadmium-magnesium-rare earth metals system	43		
cadmium-ytterbium	43		
Cast Iron	63		
Casting	62		
cavitation	15		
CFD	47		
chalcogenides	7		
charge carrier	23		
chemical vapor infiltration	27		
Chip-disposability	62		
cladding	20		
coating	20		
coating of Cs3Sb on cathod tip	3		
Coatings	66		
coherent phonons	25		
cold rolling	22		
collaborative study	44		
colloid	19		
colloidal processing	22		
Combinatorial	56		
combustion synthesis	44		
component	66		
composite	20, 22		

fatigue	59		
fatigue crack growth rate	20		
fatigue hardening	14		
fatigue properties	12, 15		
fatigue softening	14		
fatigue strength	57		
fatigue test	22		
Fe	20		
FEM	64		
ferrite	48		
ferritic heat resistant steel	59		
ferritic steel	26		
ferritic steels for welded structures	57		
fiber-reinforced Ti alloy matrix composite	20		
first-principles calculations	12		
flux-line lattice melting	10		
fractography	66		
fracture toughness test	17		
free electron laser	27		
frequency modulation	36		
<b>G</b>			
gas adsorption	56		
gas desorption	56		
gas permeation	56		
giga-cycle fatigue	58		
grain boundary sliding	15		
grain growth	15		
grain refinement	57		
<b>H</b>			
Hanshin-Awaji earthquake	66		
Hardness	65		
heat resistant ferritic steels	11		
heat-affected-zone	57		
helium embrittlement	26, 64		
hexagonal boron nitride	55, 56		
high brightness electron source	3		
high chromium ferritic steel	66		
high field	51		
high field magnet	47		
high gradient magnetic separation	47		
high magnetic field	22		
high magnetic field	44, 47		
high pressure	4		
high strength	22		
high-lying energy level	18		
high-purity iron	6		
high-resolution beam	44		
high- $T_c$ superconductivity	10		
HRTEM	56		
hydrogen	25		
hydrogen embrittlement	15, 26		
hydrogen storage	37		
<b>I</b>			
ID-MS	6		
incongruent melting	18		
infiltration	20		
infrared and Raman spectra	3		
inherent creep strength	11		
in-plane texture	24		
Intelligent materials	39		
interface	56		
interface wear	20		
Intermetallic compound	30		
intermetallic compound	44		
international standard	49		
ionic conductor	23		
Ir/Rh-base Refractory Superalloys	24		
irradiation damage	64		
isotope separation	27		
isotopically controlled materials	27		
<b>J</b>			
$J_c$			33, 38
<b>L</b>			
L12-type titanium trialuminide			30
laser beam			64
laser illumination			3
"laser,"			18
lattice distortion			3
light water reactor			64
localized corrosion			64
long-term creep			13
low temperature thermal expansion			51
low temperature thermophysical properties			50
<b>M</b>			
magnesium			37
magnetic field			15, 48
magnetic materials			4
Martensite			62
martensitic steel			58
materials characterization			53
Materials Design			24
materials efficiency			42
materials environmental life-cycle analysis			42
M-C atomic pairs			11
measurement method			49
measurement technology			50, 51
mechanical alloying			37
mechanical constraint			66
mechanical properties			29
metal matrix composites			22
metal-insulator transition			7

Metals of Group V	20	quasicrystal	3, 43
metastable atom	52	Quench	33, 38
microactuator	41		
microcrack	15	<b>R</b>	
microstructural change	66	radiation damage	25
microstructural control	18	Rapid-Heat	33, 38
microstructural evolution	13	rare-earth elements	18
microstructure	6, 29	recyclability	42
Microstructure Analysis	24	Recycle	63
microwave surface resistance	24	reference materials	50, 51
modeling	16	reflection high-energy electron diffraction	3
molecular-dynamics	64	refractive index	36
multiple functions	39	refractory metal	18
		residual stress	57
<b>N</b>		resonance photoionization	18
nanocomposite	19	Room temperature ductility	30
nanohardness tester	58		
nanoparticle	19	<b>S</b>	
nanostructure	6	Salmon	9
Nb <sub>3</sub> Al	33, 38	self-organization	55
Nb-matrix ratio	45	semiconductor	56
neutral beam	52	semi-solid processing	20
Ni	20	shape memory effect	41
Ni-base superalloy	24	shear test	17
NMR spectrometer	47	Si <sub>3</sub> N <sub>4</sub>	24
		silicides	16
<b>O</b>		silicon	27
optical measurements	7	"silicon carbide, transmutation"	27
Organic films	54	simulation	57
Oxidation resistance	30	sintering	19
oxide	56	solid phase extraction	6
oxide superconductor	47	solid state process	18
		solid-state electrolyte	23
<b>P</b>		spectrometer	53
particle assemblage	39	SPM	58
particulate composites	29	sputtering	41
pearlite	48	stainless steel	15
peritectic reaction	18	standard pressure gauge	56
phase transformation	48	standard reference data	12
phase transformations	6	standardization	17
phase transitions	3	standardization of test method	22
phonon density of states	64	steam oxidation	59
phonons	3	"steel, aluminum alloy"	12
photoelectron diffraction	3	stress concentration	15
plastic working	20	"stress ratio, microstructure"	14
point defects	25	stress relaxation	13
powder metallurgy	29	structural material	15, 17
Powder Metallurgy	63	structural steel	65
powder processing	42	structure	48
		substitution	36
<b>Q</b>		superconducting magnet	47
quantum efficiency for photoelectric effect	3	Superconducting Shield	33
		superconductor	49
		superplasticity	15



**NRIM Research Activities**

**2000**

Date of Issue : 15 March, 2001

**Editorial Committee :**

Chiaki SIGA

Toshio OGATA

Tetsuo UCHIKOSHI

Hiroaki KUMAKURA

Shirou TSUKAMOTO

Susumu TAKAMORI

**Publisher :**

Planning Office

National Research Institute for Metals

1-2-1, Sengen, Tsukuba-shi, Ibaraki 305-0047 Japan

Phone : + 81-298-59-2045, Fax : + 81-298-59-2049

Copyright©National Research Institute for Metals

Director-General : Dr. Masatoshi OKADA

Printed by ISEBU Corporation

# **NRIM Research Activities**

**2000**

